AD-A086 991 NEW UNIV OF ULSTER COLERAINE (NORTHERN IRELAND) SCH--ETC F/G 20/2
GROWTH AND APPLICATION OF CADMIUM TELLURIDE.(U)
JAN 80 R H WILLIAMS, M H PATTERSON DA-ERO-77-G-026

UNCLASSIFIED NL

1 - 2

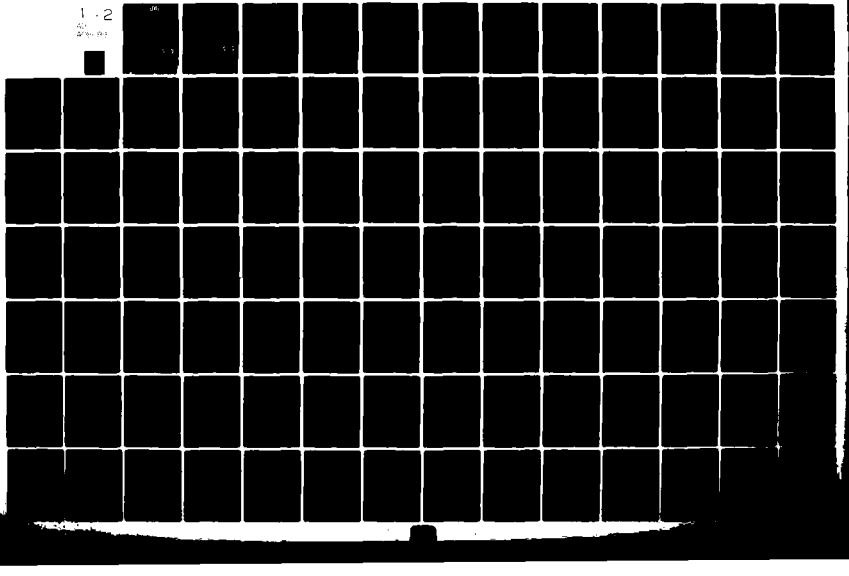

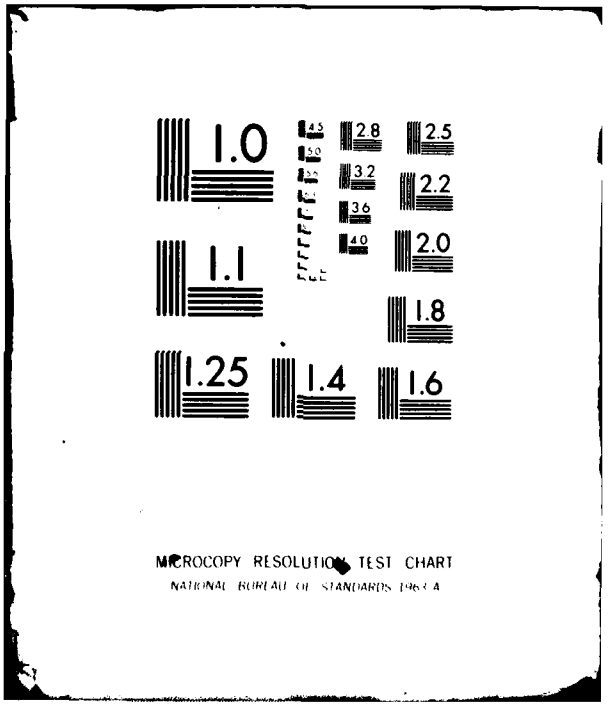
1.0
1.1
1.25
1.4
1.6
1.8
2.0
2.2
2.5
2.8
3.2
3.6
4.0
MICROCOPY RESOLUTION TEST CHART
NATIONAL BUREAU OF STANDARDS 1963-A

(1) LEVEL II

AD

ADA086991

GROWTH AND APPLICATION OF CADMIUM TELLURIDE

Final Technical Report

by

R.H. Williams and M.H. Patterson

January 1980

EUROPEAN RESEARCH OFFICE

United States Army

London England

DTIC
ELECTE
JUL 22 1980
S D
B

GRANT NUMBER DA-ERO 77-G026

R.H. Williams

Approved for Public Release; distribution unlimited

DTIC FILE COPY

80 7 22

AD

GROWTH AND APPLICATION OF CADMIUM TELLURIDE

Final Technical Report

by

R.H. Williams and M.H. Patterson

January 1980

EUROPEAN RESEARCH OFFICE

United States Army

London England

DTIC
ELECTE
JUL 22 1980
S D
B

GRANT NUMBER DA-ERO 77-G026

R.H. Williams

Approved for Public Release; distribution unlimited

SECURITY CLASSIFICATION OF THIS PAGE (When Data Entered)

REPORT DOCUMENTATION PAGE

READ INSTRUCTIONS BEFORE COMPLETING FORM

1. REPORT NUMBER	2. GOVT ACCESSION NO. AD-A086991
3. RECIPIENT'S CATALOG NUMBER	Final technical rept.
4. TITLE (and Subtitle) Growth and Application of Cadmium Telluride •	5. TYPE OF REPORT & PERIOD COVERED Feb 77 — Jan 80
	6. PERFORMING ORG. REPORT NUMBER
7. AUTHOR(s) R.H. Williams M.H. Patterson	8. CONTRACT OR GRANT NUMBER(s) DAERO-77-G-026
9. PERFORMING ORGANIZATION NAME AND ADDRESS The New University of Ulster, School of Physical Sciences, Coleraine, Co. Londonderry, N. Ireland.	10. PROGRAM ELEMENT, PROJECT, TASK AREA & WORK UNIT NUMBERS 6.11.02A 1T161102BH57-07
11. CONTROLLING OFFICE NAME AND ADDRESS USARSG(E) Box 65 FPO NY 09510	12. REPORT DATE Jan 80
	13. NUMBER OF PAGES 159
14. MONITORING AGENCY NAME & ADDRESS (if different from Controlling Office)	15. SECURITY CLASS. (of this report) UNCLASSIFIED
	15a. DECLASSIFICATION/DOWNGRADING SCHEDULE

16. DISTRIBUTION STATEMENT (of this Report)

Approved for Public Release, Distribution Unlimited

17. DISTRIBUTION STATEMENT (of the abstract entered in Block 20, if different from Report)

18. SUPPLEMENTARY NOTES

19. KEY WORDS (Continue on reverse side if necessary and identify by block number)

Bridgman	Photoemission	Schottky Barriers
Czochralski	Auger Spectroscopy	Ohmic Contacts
Surfaces	I-V	Defect Model
Etchants	C-V	

20. ABSTRACT (Continue on reverse side if necessary and identify by block number)

see over

DD FORM 1 JAN 73 1473 EDITION OF 1 NOV 65 IS OBSOLETE

UNCLASSIFIED

SECURITY CLASSIFICATION OF THIS PAGE (When Data Entered)

405988

20. ABSTRACT

Large Single Crystals of CdTe were grown by the methods of Liquid Encapsulated Czochralski, Fast Vertical Bridgman, Travelling Heater Method, Stockbarger method. Electrical characterisation was done by Seebeck, Hall Effect and Conductivity measurements. Surfaces were investigated using XPS, UPS, AES and LEED. Metal-CdTe contacts were fabricated. Formation of these was monitored using XPS, UPS, LEED, AES. Barrier Heights were established by I-V, C-V and UPS measurements. Results show that the effect of the CdTe surface on the type of contact formed is very marked.

ACCESSION for
NTIS White Section
DDC Buff Section
UNANNOUNCED
JUSTIFICATION
BY
DISTRIBUTION/AVAILABILITY CODES
Dist. AVAIL. and/or SPECIAL
A

Abstract

In this report we report on the growth of single crystal CdTe. Various aspects of clean and contaminated CdTe are considered along with the interfaces formed with metal electrodes. The II-VI compound has a large range of possible applications. In all of these applications some form of contact is required between the CdTe and a metal. As will be seen this is not a straightforward process. An understanding, then, of the nature of the contact between the metal and the semiconductor is of crucial importance. Large single crystals of CdTe were grown at our Laboratory by the methods of Fast Vertical Bridgman, Travelling Heater method and by Liquid Encapsulation. These were characterised electrically by the Hall effect, Seebeck effect and Conductivitity measurements. The CdTe surface left by various surface preparations was investigated using AES, XPS, UPS and LEED. Metal contacts were made to some of these CdTe surfaces. The formation of Schottky barriers was monitored using XPS, UPS, AES and LEED. The Thick film values of Schottky barrier heights were established by C-V and I-V methods. We have discussed the results of these observations in terms of various theories of Schottky barrier formation and in particular the 'defect' model. Our results show that the differences in the electronic nature seen in metal-CdTe contacts are more easily understood in terms of the chemical and metallurgical microstructure of the interface, than in terms of more conventional theories. Furthermore, thin surface layers have dramatic effects on the electronic nature of the metal-CdTe interface.

CONTENTS

LIST OF ILLUSTRATIONS

LIST OF TABLES

INTRODUCTION

Cadmium Telluride has been known as a compound for about 100 years. In 1879 it was prepared, along with other Tellurides, by the chemist Margottet in France. He reacted tellurium with various metals at 'red heat'. It was shown later, by Fabre in 1888, that this process led to well crystallised material. In 1909 Tibbals reported another investigation of tellurides, among them was CdTe.

Up until the 1940's the only apparent use of CdTe was as a pigment. In 1946, Frerichs and Warminsky and 1947, Frerichs reported that "Incomplete phosphors" such as chalcogenides of Cadmium in thin film form were highly photosensitive to a range of photon energies, including β and γ radiation. They offered the suggestion that this effect could be used for the fabrication of γ-ray image converter tubes, or, if combined with suitably efficient amplifiers, in γ quantum counters. By 1948 photocells using CdTe were being built (Schwarz, 1948) and it was noted that preparative and heat treatment conditions as well as stoichiometric excesses of either kind were of great influence in the functioning of these devices.

In the 1950's several detailed investigations of the behaviour of CdTe single crystals were made; Jenny and Bube 1954, Appel and Lautz 1954. In particular Kroeger and De Nobel, 1955 and Boltaks et al, 1955 carried out detailed doping studies which established the basis for various uses of the compound. In 1959 De Nobel published his Thesis. This not only described the behaviour of the compound in great detail but also explained the behaviour of dopants in terms of a coherent model. De Nobel and Kroeger in a patent filed in 1959 and published in 1962 said

> "As is well known CdTe is a semiconductor which has very advantageous properties as compared with the other chalcogenides of Cadmium, such as comparatively great mobility, a simple controllability of the conductivity from n to p type, and conversely, so that cadmium telluride may be used in semiconductor devices such as crystal diodes or transistors. It is also known that CdTe is photosensitive to many kinds of radiation, for example, Infra-red, visible and X-radiation, so that it may be used in photosensitive devices such as photodiodes, photoconductive bodies or infra-red telescopes, image intensifiers, camera tubes, photoelectric cells, X-ray dosimeters and the like."

So even by 1959 there was already a promising list of applications of CdTe, to which more were added year by year. All the desirable properties of CdTe, including easy fabrication in thin film form were well known. The major groups of applications are now considered.

1. Infra-Red Windows

The extremely flat transmission in the infra-red makes CdTe quite attractive for optical windows (Deutsch, 1975 and Kottke, 1971). It can be fabricated either in a fine grained hot pressed form marketed as Irtran 6 by Eastman Kodak Ltd., in polycrystalline slices or in single crystal form with very low optical absorption at wavelengths at long as 30 microns. It can be used for optical components such as lenses, Brauster Windows, partial reflectors and special filters, e.g., in the 5 to 25 micron range it is nearly ideal if the visible is to be excluded.

2. Electro-Optic Modulators and Non-Linear Optics

Because CdTe is a semiconductor with energy gap of ~1.5 eV it is opaque in the visible range of the spectrum. It does however have a low absorption coefficient from its band edge at ~9μm to ~30μm which is near the edge of the Reststrahl band. The fundamental lattice frequency is located at $141cm^{-1}$ (70μ). CdTe has a large electro-optic coefficient (Johnson et al 1969). CdTe has the zincblende ($\bar{4}3m$) structure, so it lacks a centre of symmetry. The maximum phase retardation will be for the light propagating along the (110) direction, polarised in the (100) with the electric field in the other (110) direction.

In order to be useful for any modulation CdTe must be of high optical quality with no inclusions, few impurities and very little strain so that no birefringence, scattering or absorption is introduced. Single crystals with dimensions of the order of centimeters, homogeneous and of high resistivity must be used. High resistivity eliminates ohmic losses and free carrier absorption. Low carrier concentrations are also desirable.

3. Gunn Effect

CdTe exhibits the Gunn effect i.e. above a certain threshold applied field, high frequency current

oscillations are produced (Foyt et al, 1966). In many ways CdTe is comparable to GaAs for use in Gunn effect devices. Maximum efficiency should be approximately the same for both materials as the spike amptitude for both is approximately 50% of the maximum current. There are however two areas where CdTe appears inferior to GaAs, i.e. Threshold voltage and carrier ionisation. For CdTe threshold voltage is ~15K.cm^{-1} as against 3KV.cm^{-7} for GaAs. As thermal conductivity is low then the implication is that continuous wave CdTe Gunn diodes are unlikely. However for short pulse operation where heat dissipation can occur in the diode then CdTe could be used.

4. Piezoelectric and Similar Devices

Although CdTe is a piezoelectric semiconductor and a variety of its basic constants have been determined (Berhncourt et al, 1963) it has not yet been applied in this area. Solid state travelling wave amplifiers and other delay line devices are important components in modern radar systems for example, and it is perhaps surprising that the use of CdTe in these applications has not been pursued.

5. Luminescence

CdTe has a significant history as a material for electroluminescent diodes (Mandel 1964; Morehead 1966; Morikawa 1968; Chapnin 1968; Gu 1973 and 1975). Because CdTe has a direct band gap it can have a strong luminescence emission. Stimulated emission has been excited by optical pumping (Basov 1966) by electron beam bombardment (Vavilov 1966), and by impact ionisation (Van Atta et al, 1964). It can be doped both n and p type, so the possibility of making lasers by minority carrier injection has been attempted (Mandel 1964) but as yet no success is reported. It appears then that CdTe could have significant application as an electroluminescent material in competition with GaAs and the other III-IV components, if the problems of "Killer" centres and the contact problem could be overcome.

6. Solar Cells

In 1957 Loferski published his paper on the optimum properties for a good solar cell material, which

clearly demonstrated that semiconductors with band gaps close to 1.5 or 1.6eV would have the highest solar conversion efficiencies. CdTe with a band gap of 1.44eV would therefore appear to be nearly ideal for the purpose. CdTe also has a high optical absorption coefficient, thus less than two microns of CdTe should be capable of absorbing all the usable energy from the solar spectrum. Coupled with the ease of production of CdTe films and crystals it is clear why such an interest is taken in CdTe as a solar cell material (Lomakina et al 1957; Cusano 1962; Bernard 1966; Lebrun 1970 etc.). A full review of the place of CdTe as a material for solar photocells is given by M. Rodot 1977.

7. Nuclear Detectors

The combination of high average atomic number, high bandgap and reasonable mobility-lifetime products for both electrons and holes give CdTe a quite unique combination of properties which make it a very promising material for use as a nuclear detector material. In 1964 Arkadeva et al published a paper on the subject and were followed shortly after by Mayer 1967. In 1968 Mayer produced a review paper which deals in detail with the use of CdTe as a nuclear detector. It is also dealt with in some detail in the proceedings of the 1st international conference on CdTe held in Strasbourg in 1971.

8. Photoconductivity

Like many of the II-VI compounds CdTe is a good photoconductor. Only a few practical applications have been suggested. The most direct has been of a photoconductive detector designed to operate between room temperature and 400°C. (Farrell et al 1974) CdTe used was high resistivity, both chlorine doped and undoped materials were used. A persistant photoconductivity or photo memory has been observed at low temperatures (Karpenko 1970, Strauss 1971) but as yet no applications of this have been made.

9. Medical Applications

CdTe sensors are now being used in several areas of nuclear medicine. CdTe probe techniques, originally developed to study dental pathology in dog models are being used clinically to diagnose venous thrombosis of the legs and to detect occult dental

infections in patients scheduled for prosthetic cardiovascular and orthopaedic surgery. Similar Instrumentation is in use in animal research of myocardial infarction and synthetic tooth substitutes. Transmission techniques have also been developed to diagnose pulmonary edema and to measure bone mineral changes in space flight. Investigations are also under way in the use of linear or two dimensional arrays of CdTe γ sensors for medical imaging Development of photoconductive CdTe X-ray detectors for C.T. scanners has also begun. A full review of the medical applications of CdTe is given by Entine et al 1977. The papers by Bojsen et al 1977, Allemand et al 1977, Kaufman et al 1977, Vogel et al 1977, are also recommended.

10. Miscellaneous Uses

CdTe has been employed in catalysis (Pamfilov 1967, Mazurkevich 1971) and in the photo decomposition of water (Calvert 1962).

As can be seen from the above CdTe has a range of possible applications in several areas of solid state electronics and optoelectronics. The starting materials Cd and Te are competitively priced when compared to other semiconductors. Hence all the conditions for widespread use are fulfilled. Nevertheless CdTe is not widely used in semiconductor electronics today.

One of the main reasons for this lack of use is the "Contact problem". This is a problem of long standing, remarked upon by Kroeger and De Nobel in 1954. It is hard to discuss as the definition of an "ohmic" contact in practice is a flexible one. Any contact which does not significantly perturb the characteristics of the desired devices in their range of operating temperatures is acceptable whether strictly ohmic in the physical sense or not. The practical principles of providing contacts to wide bandgap II-VI compounds have been described in some detail by Aven and Swank 1969 from which the above definition has been adapted. They also note the two main principles by which contacting may be achieved.

i) Establish a proper work function match on the surface so that a contact may provide a sufficient carrier supply under all conditions of operation.

ii) Lower the surface barrier and cause it to be as thin as possible by heavy doping of the region underlying the contact to provide a high tunnelling

probability for carriers from the semiconductor to avoid rectification.

In both cases one has to start by knowing the nature of the semiconductor surface. This determines its electron emission behaviour (work function). On a fundamental level this leads to a consideration of surface bonding which leads to the concept of surface states. These surface states can have an effect on the behaviour of the metal-conductor contact. The fundamental properties of CdTe, relevant to contacting, have been evaluated by Swank 1967, who evaporated gold onto an UHV cleaved (110) face of CdTe. They are presented below.

Electron Affinity	(χ)	= 4.28eV
Work Function	(ϕ_s)	= 4.67ev
Work Function of Au on CdTe	(ϕ_m)	= 5.08

The true surface state, obtained under UHV, will be immediately modified by absorption when exposed to real atmospheres eg. Air, O_2 etc. Since Oxygen is not easily desorbed even under vacuum one might suspect that noble metals such as Au, Pt ... would show barriers here, whereas metals such as Al, or even In, which can reduce the oxygen at the semiconductor surface could be expected to show different behaviour.

Etching and heat treatments are often employed before or during contact formation, causing further complications. Among these are loss of cadmium from the surface region, or hydrolysis of the Tellurium in the surface leaving non stoichiometric surfaces which may give rise to different results.

All these surface and sub-surface effects are undoubtedly responsible for a great deal of the confusion which exists regarding contacts to CdTe. However these effects, once understood can be controlled and device fabrication made consistently controllable.

It has been shown that CdTe could be a very versatile semiconductor. The main drawback to its application is in the region of understanding the processes involved in fabricating metal-Cadmium Telluride contacts. In the work reported herein, we have tried to elucidate the processes occurring and to explain the formation of Schottky Barriers to Cadmium Telluride in the light of the most recent theories.

Before one can fabricate Schottky barriers, one has to have Cadmium Telluride of the right physical dimensions, electrical behaviour etc. In Section 2 we report on the crystal growth and electrical characterisation of Cadmium

Telluride crystals. A review of the methodology used by previous workers is presented, followed by the methods used by us, their successes and failures etc.

In Section 3 we report on the characterisation of the Cadmium Telluride surface. A review of what little work has been published on the subject is presented. This is followed by a description of the surface sensitive techniques we have used to probe the surface. The results, conclusions and recommendations from our investigations of various CdTe surfaces are presented.

In Section 4 the metal-CdTe contact is considered. Techniques for evaluating the early formation of Schottky barriers, and the thick film values of Barrier height were employed for metals on clean and oxidised surfaces. The experiments indicate that in many cases the interfaces formed are not atomically abrupt and there is considerable inter mixing between the metals and the CdTe. The results of the experiments are compared to similar experiments on other metal-Semiconductor systems. The Observations are discussed in terms of various theories of schottky barrier formation and in particular we consider the defect model and its applicability to CdTe.

2. THE GROWTH AND CHARACTERISATION OF CADMIUM TELLURIDE CRYSTALS

2.1 Introduction

This section deals with the growth and characterisation of cadmium telluride crystals grown at our laboratory. Part two will give a brief account of the three main categories of crystal growth that have been applied to cadmium telluride in the past i.e. Vapour growth, melt growth and solution growth. The more successful methods of crystal growth, within these categories, will be discussed along with the results obtained by other workers. Part three details the methods used here to synthesise cadmium telluride, both in undoped and doped forms, and the methods of ampoule preparation used for the various techniques to be employed. Part four describes the techniques used to probe the nature, purity and electrical properties of the crystals grown. Part five will be an account of the different types of crystal growth employed in this work, their advantages, disadvantages, successes and failures and the results of characterisation of crystals grown by each technique will be discussed.

Finally Recommendations are presented of the most suitable methods to use for growth of crystals of desired electrical characteristics.

2.2 Methods and Results of CdTe Crystal Growth

2.2.1 Vapour Growth

As the first synthetic crystals of II-VI compounds were grown from the vapour phase it would seem appropriate to consider this method of crystal growth first.

The basic requirement for growth from the vapour phase is a continuous flow or supply of Cadmium and Tellurium elements through the gas phase. This requires a source of the elemental components, which may come either from the dissociation of CdTe itself or from the individual elements. These gaseous species diffuse or flow to a region where supersaturation occurs and crystal growth takes place. (For a description of the theory of vapour growth see Cabrera and Coleman, 1963).

The mode of transport subdivides vapour growth into dynamic and static techniques.

In the dynamic technique a carrier gas is used and the system is in a state of externally induced flow. The advantage of this system is that crystals can be grown without preforming the compound (Frerichs. R., 1946 and 1947).

In the static vapour growth method transport takes place by diffusion through a gas phase. In this set up the source material is generally CdTe powder kept in the high temperature region of the furnace. By dissociation to the vapour species and diffusion to a lower temperature region, crystal growth occurs.

The first synthetic crystals of CdTe were grown in 1947 by Frerichs using the dynamic vapour growth technique. He used hydrogen (H_2) as the inert carrier gas. An incoming flow of H_2Te was used to react with Cadmium to form CdTe, see fig. 2.1. However crystal size was small. Lynch, 1962 also used the Frerichs' method with modifications but still crystal size was small. In 1963 Teramoto studied the sublimation and recrystallisation of CdTe through a temperature gradient in a nitrogen (N_2) atmosphere. He achieved several crystal types ranging from dodecahedra with flat (110) surfaces of up to $5mm^2$ in area, to hexagonal plates and rods up to 2cm × 2mm in size. In 1971, Akutagawa and Zanio studied the sublimation and recrystallisation of CdTe through a temperature gradient in an evacuated ampoule. By control of thermal gradients crystals up to $3cm^3$ in volume were grown. They were able to produce high resistivity material by controlling the stoichiometry, using conditions of growth where $P_{Cd} = 2P_{Te_2}$. This was done by introducing a cadmium reservoir to the growth ampoule, which was kept at a predetermined temperature.

There is one other vapour growth technique which has been used by several workers to produce CdTe crystals. This method is based on the principle of chemical transport reactions. The underlying principle of this method is that of the equilibrium in a chemical reaction. A reaction is made to take place at a hot region in a furnace, then the gaseous products make their way by drift and diffusion to a cooler region where the equilibrium of the reaction is altered and the reverse reaction occurs, eg.

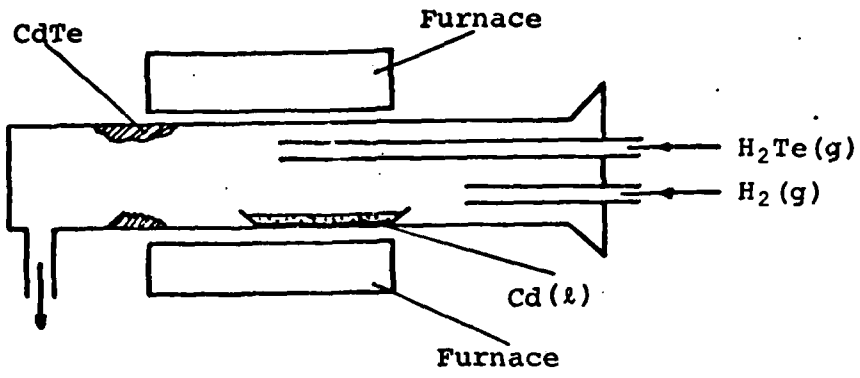

Fig. 2.1. Furnace Arrangement for Vapour Growth of CdTe, as used by Frerichs (1947).

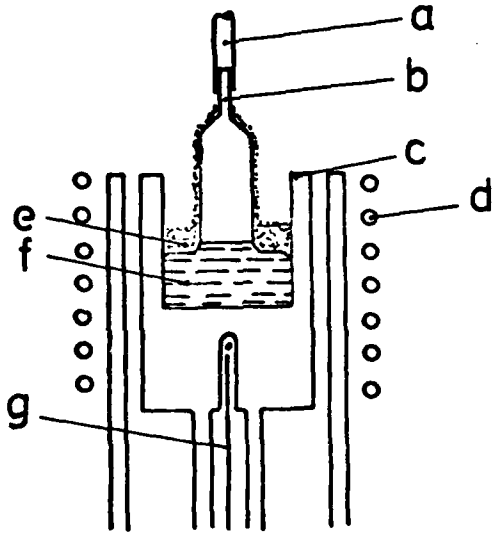

Fig. 2.2. Schematic Diagram of the Liquid Encapsulation Method of Crystal Growth.

a. seed holder: b. seed: c. carbon susceptor and quartz crucible: d. R.F. Coil: e. B_2O_3: f. CdTe: g. Thermocouple.

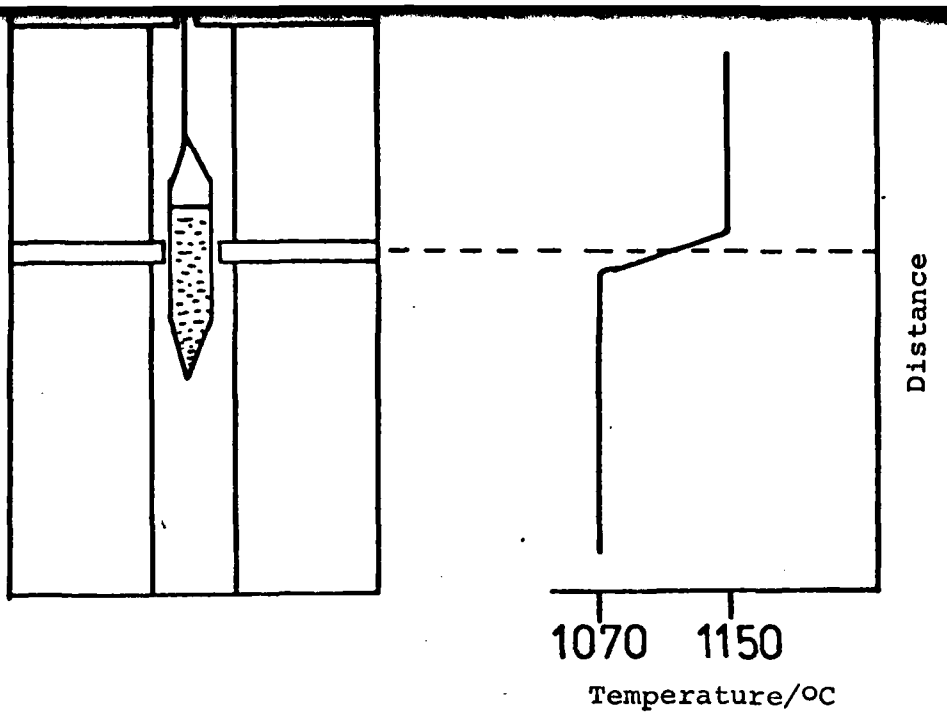

Fig. 2.3. Schematic Diagram of the Apparatus and Temperature Profile Commonly Used in the Stockbarger Growth of CdTe Crystals.

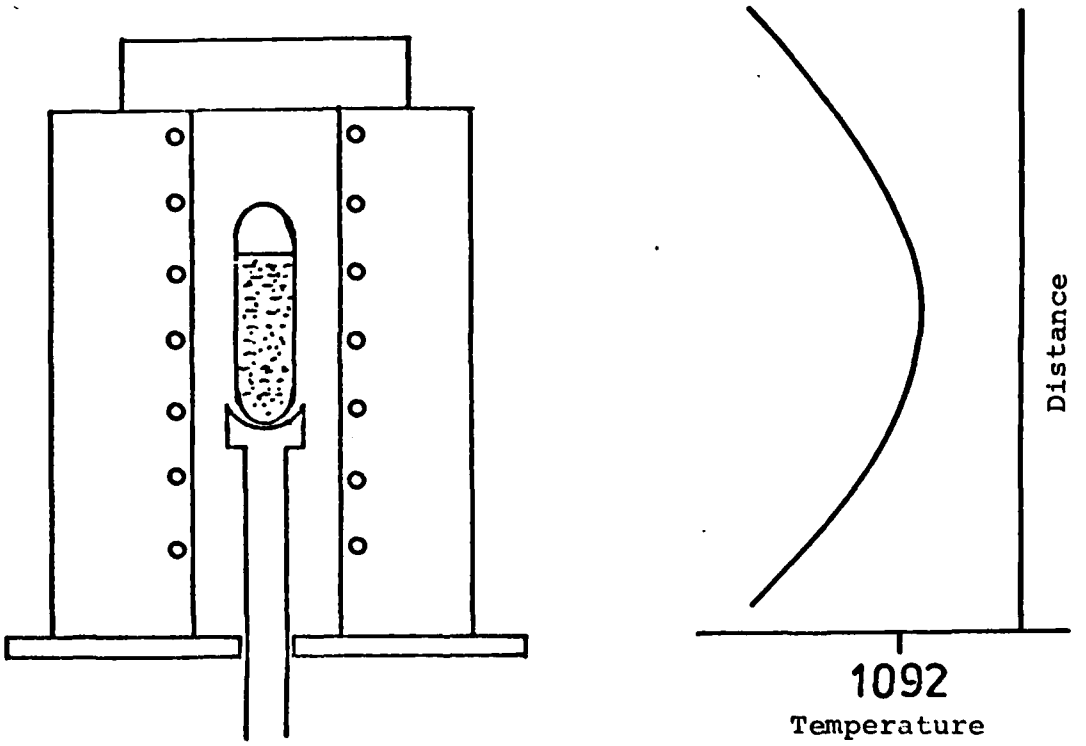

Fig. 2.4. Schematic Diagram of the Apparatus and Temperature Profile Commonly Used in the Bridgman Method of CdTe Crystal Growth.

In the hot zone: $CdTe(s) + I_2(g) \rightarrow CdI_2(g) + \frac{1}{2}Te_2(g)$

in the cool zone: $CdI_2(g) + \frac{1}{2}Te_2(g) \rightarrow CdTe(s) + I_2(g)$

The $I_2(g)$ produced in the cool zone reaction then diffuses back to the hot zone where the series of reactions repeats.

In general the reaction may be written:

$$CdTe(s) + 2HX(g) = CdX_2(g) + H_2(g) + \frac{1}{2}Te_2(g)$$

X = Cl, Br, I.

By a suitable choice of overall pressure P, temperature of hot and cold zones, and the hydrogen to halogen atomic density ratio (H/X) effective chemical transport can be maintained.

Paorici et al (Rev.Phys.Appl. 12 (1977) p.155) used I_2 only as transport agent (i.e. H/I=0). They obtained platelets with smooth mirror surfaces up to 15mm × 5mm in size. In 1973 they used HCl and in 1975 they used HBr as transport agents. and obtained platelets with maximum size 10mm × 15mm × 200μm. In 1974 they used mixtures of H_2 and I_2 as transport agents and obtained polyhedra shaped crystals of maximum size 12mm × 10mm × 5mm.

There is, therefore, an abundance of variations on the basic theory of vapour growth of CdTe crystals. However they all seem to exhibit the same major disadvantages. These are

1. Small crystal size
2. Lack of control of initial nucleation.
3. Lack of control over doping.
4. In the case of chemical transport techniques. incorporation of transport agent into the crystals produced (see. Nitsch et al, 1962).

2.2.2 Melt Growth

For the preparation of large single crystals of CdTe, growth from the melt has many advantages. Conditions, however, of high temperatures etc. lead to the dissociation and mass transport to lower temperature regions, of the volatile components, Cd and Te, hence care has to be taken

to overcome this. Several techniques have been used and they are discussed below.

Crystal Pulling and Liquid Encapsulation (LEC)

The principle of Liquid encapsulation was first used in the growth of the volatile compounds PbTe and PbSe. (Metz et al, 1962).

In the LEC technique an inert liquid is used which completely covers the melt. The loss of volatile components from the melt is prevented if an inert gas pressure is applied to the surface of the liquid encapsulant and is in excess of the equilibrium vapour pressure of the most volatile constituent in the melt. The requirements of the liquid encapsulant are

1. That it be less dense than the melt.
2. That it be optically transparent.
3. That it be chemically stable in the environment.
4. That there should be no diffusion or convection of the volatile constituent through the layer. Hence it is desirable that the volatile constituents should be insoluble in the encapsulant.

For CdTe growth Boric oxide (B_2O_3) is a very suitable material for use as encapsulant. B_2O_3 is used to cover the CdTe charge, in a quartz crucible, to a depth of ~1cm. Growth of the CdTe crystal on a seed ensues at the interface of the two liquids. As the crystal is withdrawn from the melt it is covered with a thin film of B_2O_3, see fig. 2.2. This is an important aspect of the technique since the B_2O_3 film reduces loss of the volatile component from the grown crystal, while at the same time removing trace oxides and impurities from the CdTe. (A more detailed account of the LEC technique will be found in 2.5).

LEC has been applied to the growth of CdTe crystals by several groups of workers. Meiling and Leombruno, 1968 reported great difficulty in growing crystals larger than 5mm in diameter. This was attributed in part to the poor thermal conductivity of CdTe ($0.058 W.cm^{-1} deg^{-1}$ at $32.7^{o}C$). Vanderkerkof, 1971 also reported on this problem. He also noted difficulty with Cd loss from the periphery of the crystal and with discolouration of the B_2O_3 layer.

Mullin and Straughan, 1977 however did not have this problem. They used an over-pressure of 27 atmospheres of Nitrogen and achieved crystal sizes up to 10mm × 5mm × 50mm. They concluded that like other melt growth techniques this method does not produce the purest crystals due to Boron contamination from the liquid encapsulant.

Stockbarger Method

The Stockbarger method has been applied successfully to the growth of CdTe by several workers. (Yamada, 1960; Inoue et al, 1962)

In this method the molten material is contained in a carbonised silica quartz tube which has been sealed off under vacuum. The tube is mounted vertically (or horizontally) in a two zone furnace with a baffle to separate the regions which have a temperature difference of 50°-80°C. The silica tube had a constricted end to facilitate seeding for the growth processes, see fig. 2.3. After heating to about 1150°C for three hours the tube is lowered at a rate of ~2cm.hr^{-1}.

In 1960 Yamada obtained crystals of about 10mm in diameter × 50mm in length, they were p type material with resistivities of the order 10^2 - $10^3\Omega$.cm. If growth was effected under a "saturated" vapour pressure of cadmium then high resistivity p type crystals (10^6 - $10^8\Omega$.cm) were obtained.

Yamada, 1962 also grew n type CdTe crystals by introducing Indium or Gallium as dopant. He found however that the type of crystal (n or p) and the quality of crystals grown were very sensitive to dopant concentration. For example, an Indium dopant concentration of 10^{18}atoms.cm^{-3} produced polycrystalline n type CdTe, whereas an Indium concentration of 10^{16}atoms.cm^{-3} produced single crystal p type material.

Bridgman Method

If a tube containing CdTe is allowed to drop through a natural temperature gradient of a single furnace then recrystallisation of the material will occur. This is the basis of the Bridgman method of crystal growth, see fig. 2.4. Its advantages are in producing uniform ingot size and a more uniform distribution of impurities in the direction transverse to the

direction of growth. The main disadvantage of the original Bridgman technique is that if the melt is non stoichiometric the composition of the melt will change continuously as solidification takes place, thus changing the composition of the solid as it grows. The change in melt composition affects the electrical properties of the crystals by causing changes in the segregation coefficients of dopants (Lorenz and Blum, 1966). A modified Bridgman method developed by Kyle, 1971 permits control of melt stoichiometry and hence of the electrical properties of crystals produced.

In this modification the tube containing CdTe is elongated at one end so that a Cd or Te reservoir may be placed in the tube. Control of vapour pressure is achieved using a second furnace placed so as to heat this reservoir, see fig. 2.5. This second furnace operates at temperatures significantly below the temperature of the crystal growing furnace. The pressure of one of the components above the melt minimises vaporisation of the CdTe charge. As this pressure is kept constant, the melt composition and hence crystal composition is held constant. As the distribution coefficient of dopants is a function of component pressure (Lorenz and Blum, 1966) this is also kept fixed.

Kyle also noted the effect on the electrical properties of CdTe crystals that quenching has. He experimented using Indium doped CdTe. He reported that for CdTe doped with Indium and slowly cooled after solidification, the electrical properties of the crystal are predominantly determined by the amount of Indium in the crystal and the pressure of one of the components of the compound. CdTe doped with the same concentration of Indium and rapidly cooled (quenched) from high temperatures had electrical properties independant of the Indium content.

Zone Refining

Zone melting has been used to prepare single crystals of CdTe by several workers. De Nobel, 1959 prepared single crystal CdTe using a set up like that shown in fig. 2.6. In this set up a vapour pressure of Cd is maintained from a reservoir of Cd. In this procedure only part of the charge is molten at any one time. Melting and freezing are carried out progressively. If this process is repeated several times the procedure is called Zone Refining. De Nobel used a three zone

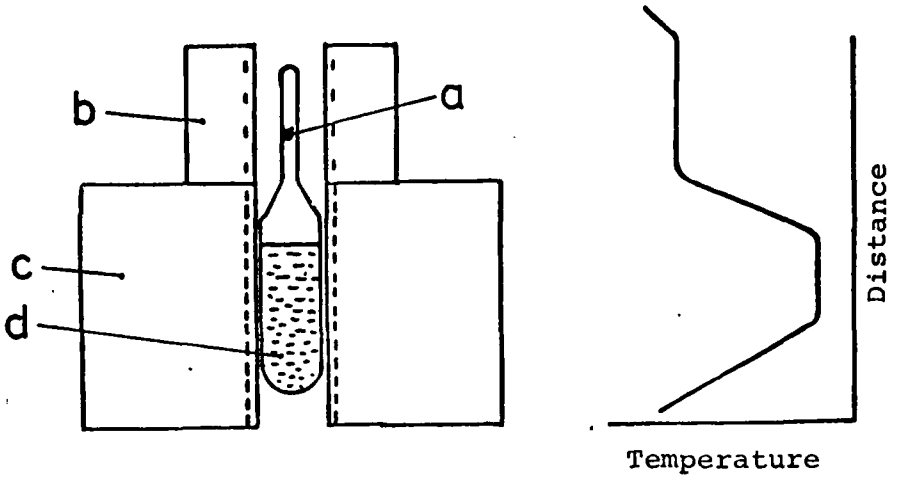

Fig. 2.5. Modified Bridgman Method and Temperature Profile as Used by Kyle (1971).

a. Cadmium reservoir: b. low temperature Furnace: c. high temperature Furnace: d. CdTe Charge.

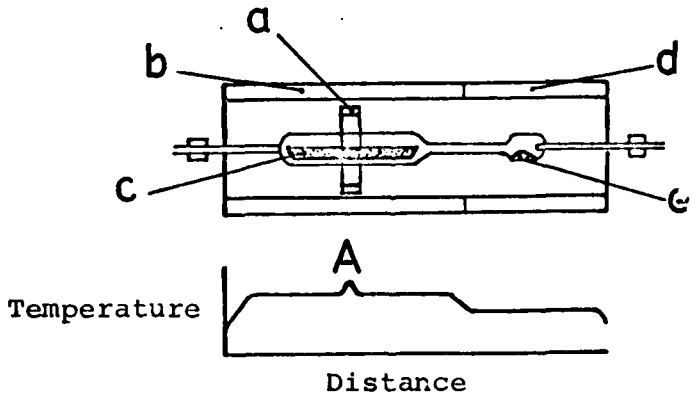

Fig. 2.6. Furnace Arrangement for Zone Melting Used by de Nobel (1959).

a. Molten Zone Furnace: b. High Temperature Furnace: c. CdTe: d. Low Temperature Furnace: e. Cadmium Reservoir.

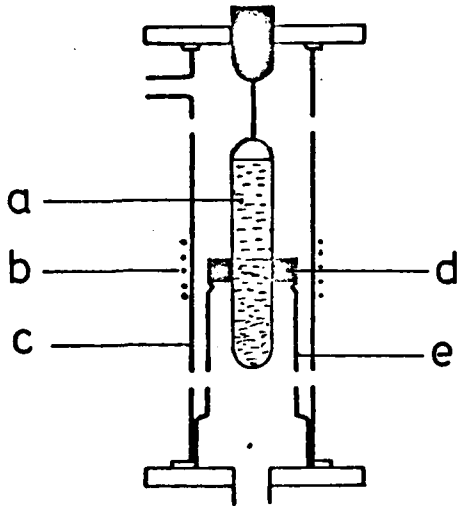

Fig. 2.7. Vertical Zone Refining Assembly as Used by Lorenz and Halstead (1963).

a. Quartz Enveloped CdTe Ingot: b. R.F. Coil: c. Quartz Tube: d. Graphite Susceptor: e. Quartz Susceptor Holder.

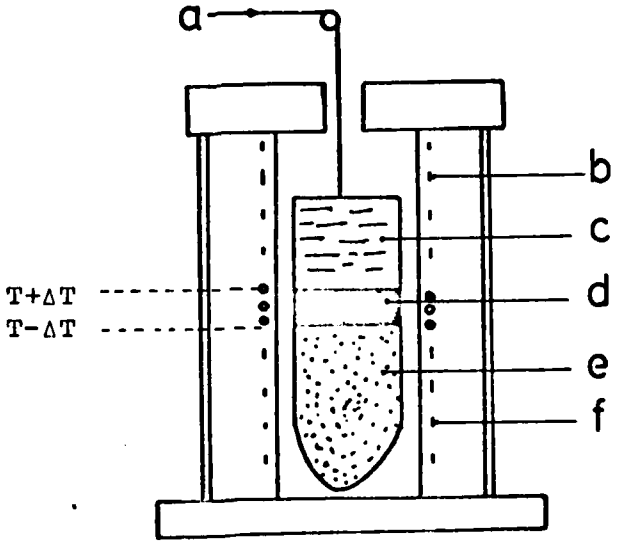

Fig. 2.8. Schematic Diagram of the Travelling Heater Method.

a. Lowering Mechanism: b. Pre-Heater: c. CdTe Charge: d. Tellurium Solvent: e. CdTe grown: f. After Heater.

furnace, permitting control of Cd Vapour pressure, ingot temperature and molten zone temperature. The quartz boat containing CdTe is moved through the temperature "kink" 'A' at $1cm.hr^{-1}$ and crystal growth proceeds with departures from stoichiometry that depend on the temperature of the Cd reservoir. De Nobel observed that when liquid CdTe has a composition which differs from the solid phase crystallising, the component present in excess is segregated as the solid-liquid interface. As at the melting point of CdTe both Cd and Te have appreciable vapour pressures, an excess in any one leads to the formation of gas bubbles at the interface which can produce a highly porous ingot if frozen out. This is overcome by an external Cd over pressure. He used various foreign atoms to dope his CdTe, eg. Cu, Ag, In, Au and Sb, and obtained crystals with dimensions 40mm × 10mm × 10mm.

Lorenz and Halsted, 1963 developed a vertical zone refining technique to produce high purity CdTe crystals with electron mobilities up to $1050cm^2.v^{-1}.s^{-1}$. at room temperature, see fig. 2.7. Single crystal size was up to several centimetres in length. Their technique had two main advantages over the horizontal three zone furnace technique as used by De Nobel. Firstly, it minimises the back diffusion of impurities via the solid phase, since the main part of the CdTe charge is at a temperature of less than 200°C. Secondly, CdTe is more dense in liquid form than in solid form so that any vapour generated in the molten zone should be confined to a volume travelling with the molten zone thus minimising transport of impurities by back diffusion via the vapour phase.

Triboulet and Marfaing, 1973 used vertical zone melting to produce high purity single crystals of CdTe. They produced single crystals of up to $3cm^3$ in volume. These crystals had electrical properties that were very dependant on the thermodynamic state of the material after synthesis, and as such is controlled by the vapour pressure of Cd used during preliminary growth by Bridgman method, eg. for P_{Cd} = 2-2.8 atm n type CdTe with a resistivity of 10-500 Ω.cm and an electron concentration of 10^{13} - $10^{14}.cm^{-3}$ is produced, if P_{Cd} = 1 atm then high resistivity p type material is produced. They also noted that the care taken in preparation of quartz tubes, synthesis of CdTe, temperature of the molten zone all had a marked effect on the quality

of crystal growth.

2.2.3 Solution Growth

Travelling Heater Method

The Travelling Heater method (THM) of crystal growth is a technique in which a molten solvent is made to migrate through a solid source material by the slow movement of the heater relative to the charge. (In reality this is impractical, so the charge is moved relative to the heater.) In this process dissolution of the charge material (CdTe) takes place at the hotter advancing liquid-solid interface and crystallisation of the charge material occurs at the cooler receding liquid solid interface, see fig. 2.8. The Composition versus temperature phase equilibrium determines the optimum growth temperature. Growth rate is determined by the rate of the liquid diffusion of the charge species through the solvent material.

The main advantages of this technique are in the preparation of bulk crystals of materials which decompose at their melting points, or of materials that require relatively high over pressures to prevent dissociation. With this technique highly reactive materials can be grown at temperatures considerably lower than their melting points. Hence, relative to melt growth techniques, less contamination from the crucible material occurs. Solution growth by the Travelling Heater method readily lends itself to initiating growth from a seed crystal. One of the side effects of this technique which may be an advantage or disadvantage, depending on the type of crystals required, is the fact that inherent to this type of processing, substantial purification of the charge material results from passing the liquid Te zone through the charge. This effect is enhanced, for CdTe, over zone refining since segregation of many impurities, metallic and non metallic, into liquid Tellurium is more pronounced than into liquid CdTe.

Bell et al, 1970 used this method to grow large single crystals of high purity CdTe. They used growth rates of 0.3 to 2.0cm.day^{-1}. Carrier concentrations of the order $5 \times 10^{9}.cm^{-3}$ to $10^{13}.cm^{-3}$ indicated that the crystals produced were semi-insulating. Taguchi et al, 1977 obtained fairly pure p type CdTe crystals using this method. They concluded that the p type conductivity was controlled

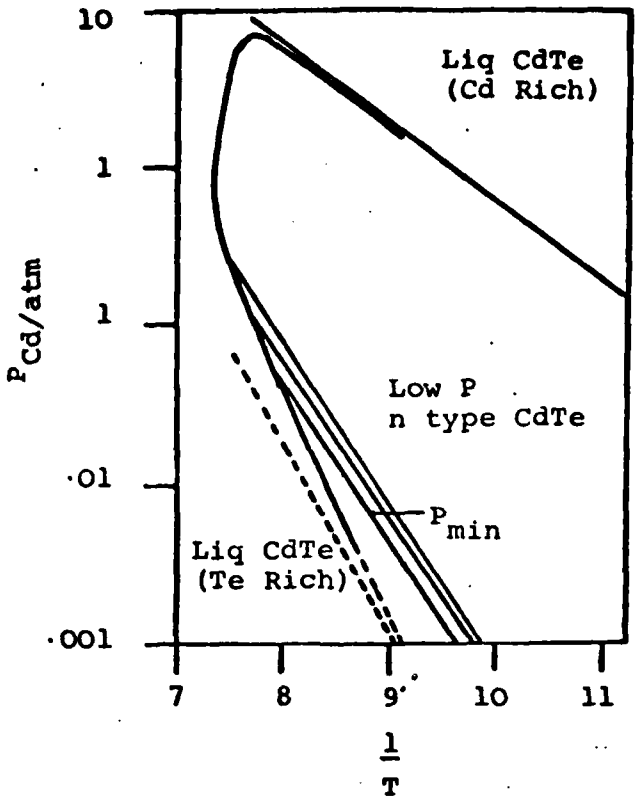

Fig. 2.9. Dependence of the CdTe Melting Point on the Cadmium Overpressure (Ray 1969).

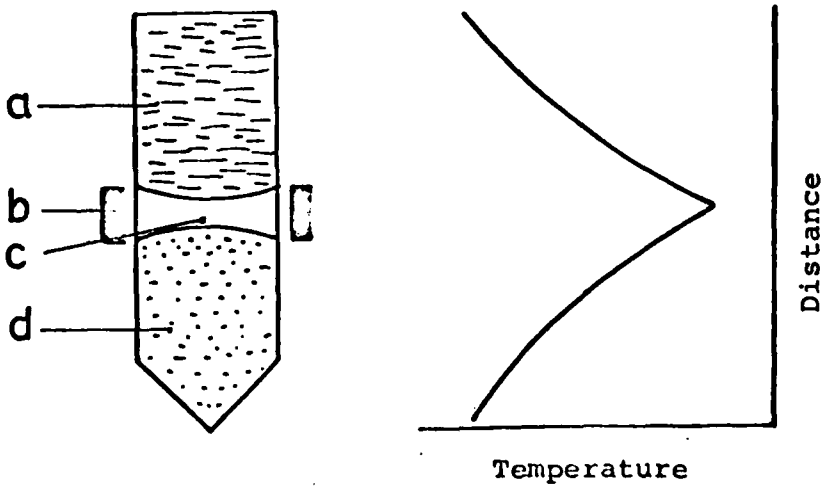

Fig. 2.10. Schematic Diagram of the Sublimation Travelling Heater Method.

a. feed CdTe: b. Stationary heater:
c. empty space: d. Regrown CdTe.

by acceptor complexes containing Cadmium vacancies, located at E_V + 0.15eV. They modified their system to obtain a controlled over pressure of Cadmium. They showed that a Cd over pressure of 3×10^{-3} atm. maximises the room temperature resistivity of undoped p type crystals.

The Travelling heater method using a Te solvent unfortunately presents two important intrinsic drawbacks, due to the composition of the grown crystal lying on the Te boundary of the homogeneity range of CdTe, see fig. 2.9. First the inevitable presence of Te precipitates, due to growth in Te rich conditions. Secondly, the necessity to compensate for the large concentration of intrinsic defects (Cd vacancies) possible at room temperature which leads to a great number of traps.

To reduce these drawbacks using classical THM, Triboulet, 1977 developed a growth technique using a similar arrangement. He called this SUBLIMATION THM. In this technique the tellurium molten zone is replaced by an empty space of approximately the same dimensions, see fig. 2.10.

By slow movement of the charge relative to the heater the empty space is made to migrate through the solid material. The displacement leads to a temperature difference between the sublimation interface and the growth interface, which induces a material flux from one to the other. An equilibrium condition exists between the sublimation rate, which depends on the sublimation interface temperature, and the growth rate, which depends on the thermal gradient between the two interfaces; and on the imposed lowering speed of the silica ampoule. Disagreement between these parameters leads to bad crystallisation.

The total pressure P ($P = P_{Cd} + P_{Te_2}$) over solid CdTe tends to reach a minimum. This provides the condition $P_{Cd} = 2P_{Te_2}$ (De Nobel, 1959) and as a consequence the vapour tends towards stoichiometry. They found that composition of the grown crystals lay, in the 3 phase line diagram (fig. 2.9), near the P_{min} line, at which $P_{Cd} = 2P_{Te_2}$. This was inside the homogeneity range and near the line of intrinsic pure CdTe. Hence the crystals should have no large excesses of Cd or Te and only a small concentration of foreign impurities. His results confirmed this.

2.3 Materials etc.

2.3.1 Synthesis of CdTe

Cadmium Telluride was synthesised directly by reaction of the elements Cadmium and Tellurium.

Cadmium and Tellurium used were both obtained from M.C.P. Electronics Ltd., Alperton, Wembley, Middlesex, England. They were both double zone refined and of 99.9999% purity. The cadmium when received showed evidence of surface oxidation and was therefore etched, prior to use, in a mixture of nitric acid and absolute alcohol. Tellurium was not treated chemically because of the risk of introducing undesirable impurities.

Reaction of Cadmium (Cd) and Tellurium (Te) starts at 550°C and continues above 800°C at which temperature the reaction is completed. At such temperatures though, CdTe tends to decompose markedly and no homogeneous phase will be obtained if this decomposition is not prevented. This can be done in two ways.

1. Prepare CdTe from Cd and Te under a vapour pressure of one of its components then the equilibrium in the equation

   $$CdTe(s) = Cd(g) + \tfrac{1}{2}Te_2(g)$$

   is shifted to the left and decomposition does not occur.

2. Carry out the reaction under a pressure of an inert gas. It is this second method that was employed to produce CdTe here.

The synthesis was carried out in a Malvern Czochralski High pressure crystal growth chamber - the C3000 work chamber, described later in section 2.5.

To produce undoped CdTe, stoichiometric amounts of Cd and Te were loaded into a quartz crucible and covered with a layer of Boric oxide (B_2O_3) liquid encapsulant. Boric oxide used was OPTRAN BORIC OXIDE for LIQUID ENCAPSULATION manufactured by BDH Chemicals Ltd., Poole, England. The crucible and contents were then loaded into a specially machined carbon susceptor and mounted in the centre of an RF induction coil in the centre of the chamber. The chamber was then evacuated, flushed several times with nitrogen and finally charged with Nitrogen to a chamber pressure of 500 p.s.i. By means of induction heating the

temperature of the susceptor and its contents were slowly raised. Temperature was monitored using a Platinum/Platinum - 10%Rhodium thermocouple buried in the carbon susceptor. The temperature was held stationary at 850°C for two hours to ensure that complete reaction had taken place. Periodically the melt was stirred using a motor driven tungsten stirrer. The temperature of the melt was then raised to 1150°C and held there for one hour.

After cooling the CdTe produced was extracted from the B_2O_3 by heating in distilled and deionised water. This dissolved the B_2O_3 leaving the charge of CdTe.

Doped material was produced using a similar technique. Doping material of the desired stoichoimetric ratio was added to the charge of Cd and Te prior to chemical reaction. Several different dopants were used:-

a) Indium

99.999% pure Indium was used. The material was scraped with a scalpel blade and washed several times in acetone and methanol to remove surface oxides prior to weighing. Various amounts of In were used (from 10 to 5000 ppm) to produce n type material of varying resistivity. The Indium was added to the Cd and Te charge, then reaction to form CdTe was promoted in the manner described above. Stirring of the melt was effected using a tungsten stirrer at ~1100°C.

b) Aluminium

Aluminium (99.99%) was prepared for inclusion in the melt by the same method as was used for indium i.e. scraping and washing in acetone/methanol. Various Aluminium concentrations were used, from 250 ppm to 5000 ppm, producing mainly p type material.

c) Chlorine

Chlorine used to dope CdTe was added to the melt in the form of $CdCl_2$. Again varying quantities were added and it was found that the type of material produced was very sensitive to the stoichiometry. Samples

doped with 400 ppm $CdCl_2$ were found to be p-type, whereas highly doped samples ($[CdCl_2]$ = 5000 ppm) came out n-type. In all cases however the material produced was highly resistive - of the order $10^7 \Omega$cm. for 400 ppm material to $10^9 \Omega$cm. for 5000 ppm material.

2.3.2 Ampoule Preparation

For several of the growth techniques used the cadmium telluride charge was placed in and sealed in quartz silica tubes under vacuum. This was done in our glassblowing workshop. Quartz is a very good material to use for these purposes because it is a high melting point material, it is optically transparent, it is relatively easy to work with and it is relatively cheap. It's main drawback is that metals generally react with the silica to form silicates. At high temperatures cadmium forms cadmium meta silicate ($CdSiO_3$). This reaction is more intense when traces of Cadmium oxide (CdO) is present. If this reaction is allowed to take place the CdTe sticks to the silica tube walls and results in breakage of the tubes as well as contamination of the CdTe charge by impurities within the silica. Hence it is desirable to prevent, where possible, contact between the CdTe and the silica tubes when at high temperatures, and to reduce any CdO presence. Reduction in the amount of CdO present is done, as described previously, by etching the Cadmium prior to reaction with Te. Preventing the CdTe coming into contact with the silicaballs is another problem.

For the LEC technique (see later) Boric oxide forms a protective layer between the CdTe charge and the quartz crucible. For other techniques however protection was effected by pyrolytically coating the inside of the ampoules with graphite. Two different techniques were used to this end.

The first technique used was that described by Triboulet and Marfaing, 1973. After production of the ampoule, by our glassblower, it was washed in an aqueous solution of Hydrofluoric acid (25%). It was then rinsed in doubly distilled deionised water and evacuated on a glass vacuum line to 10^{-6} torr for several hours, while being maintained at a temperature of over 1000°C. This was done using a specially wound furnace. The ampoule was then connected to a supply of pure benzene (Analar) and

vapour was drawn in. By "cracking" of the benzene carbon was deposited on the inner walls of the ampoule. This process was then repeated several times to produce a carbon coat of the desired thickness. The coat was then baked on at a vacuum of 10^{-6} torr and temp of over 1000°C for several hours.

The second method, devised by our glassblowers, is a derivative of the first method. It is quicker and easier to carry out. After production of the ampoule it is again washed out with HF (25%) and doubly deionised, distilled water. The ampoule was then put into a glassblowing lathe where it was continuously revolved and flamed by four oxygen-propane burners. The temperature of the tube was kept at ~1200°C. When the tube had been in this condition for 10 minutes, a drop of Analar benzene was admitted via a glass syringe system. The benzene immediately 'cracked' and a fine silvery coating of carbon was produced on the inner wall of the ampoule. This process was repeated several times to produce a carbon coat of the thickness required.

After many experiments with ampoules prepared by both methods it was found that there was no appreciable difference in the performance of the ampoules. It was therefore decided to prepare carbon coated ampoules by the second method for reasons of time, ease of production etc.

CdTe, produced previously, was crushed and loaded into an ampoule, coated with carbon. If a Cd or Te over pressure was to be used then a piece of Cd or Te was placed in the ampoule at the same stage. The ampoule was then connected to a vac line and evacuated to 10^{-6} torr. The Ampoule was flamed, using a hand held torch, to outgas the material. When outgasing had ceased and the vacuum reached 10^{-6} torr the ampoule was sealed off and a quartz hook attached.

2.4 Techniques for Determination of Crystal Quality

2.4.1 Seebeck Effect

An important method for studying semiconductors is the measurement of the Seebeck effect or Thermoelectric power. A temperature difference (ΔT) between the ends of a specimen gives rise to an emf $Q\Delta T$ mV. Q is defined as the Thermoelectric Power.

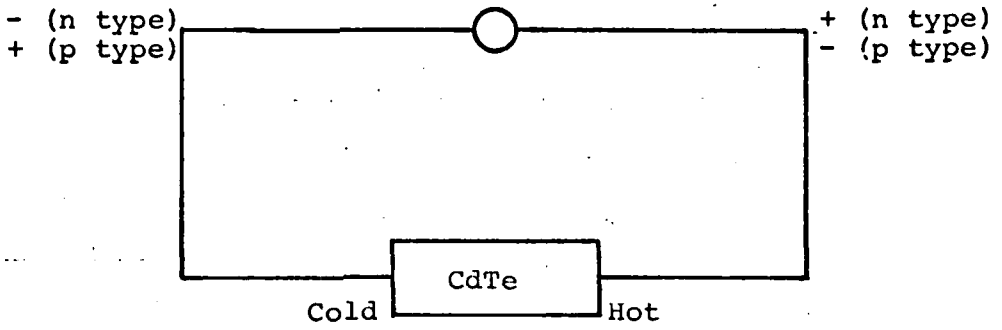

Fig. 2.11

To see the significance of the seebeck effect it is of interest to consider the peltier effect which is the inverse of the seebeck effect. When a current passes through a semiconductor, heat is absorbed at one semiconductor-metal junction and it is liberated at the other. The peltier coefficient (π) is expressed as the number of joules of heat liberated or absorbed reversibly per coulomb of charge passing through the junction. The Seebeck and Peltier effects are related by the Kelvin relationship

$$QT = \pi$$

If we consider an n type semiconductor in an applied field with metal contacts. The energy bands slope to the right due to the applied potential difference, which causes current flow from right to left (fig. 2.12). Electrons flow from left to right.

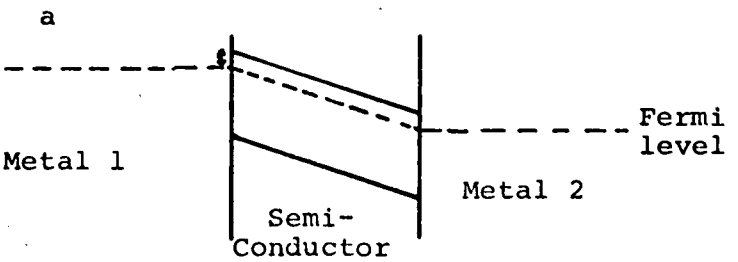

Fig. 2.12

$$a = E_C - E_F$$

Electrons trying to flow into the semiconductor from the Metal 1 on the left face an energy barrier equal to $E_C - E_F$. Only electrons with energy greater than this barrier can cross. Hence the metal contact on the left is depleted of most of its energetic electrons. At the right hand side there is no such barrier and electrons of excessive thermal energy are added to Metal 2. Hence there is a transferrance of heat from Metal 1 to Metal 2. For p type material the sign of the effect is reversed. This reasoning applies to the seebeck effect. The mobile charge carriers diffuse from the hot junction to the cold junction so that the cold junction acquires a potential of the same sign as the carriers. In fig. 2.11 heat is supplied to the right hand side and removed at the left, thus a potential difference is produced. Measurement of this voltage, its size and sign can give us information as to the type and quality of semiconductor present.

Experimental

The Thermoelectric effect was used simply to give a quick measurement of the type (n or p) of semiconductor material produced. As such only the sign of the voltage produced was of interest. The experimental set up is represented in fig. 2.13.

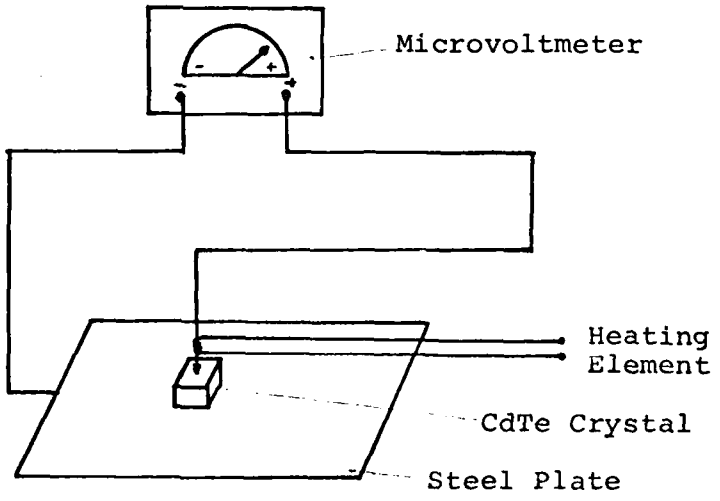

Fig. 2.13

Indium contacts were evaporated onto opposite sides of a crystal of CdTe. The Crystal was then fixed, using silver conducting paint, to a stainless steel plate which was connected to the negative junction of a Keithley null detector microvoltmeter, model no.155. The positive side of the microvoltmeter was a stainless steel probe heated by having a resistance heater (Nichrome Wire) attached to it. By placing the probe on the opposite surface of the crystal to the steel plate and heating the probe, build up of the potential difference between the two sides of the crystal could be monitored. By considering the sign of this voltage, and the side of the χ tal that was heated, the type of charge carriers and hence the type of semiconductor could be determined.

2.4.2 Hall Effect

Use of the Hall effect is an important method for obtaining information of carrier concentrations, and mobility in semiconductors. The experimental considerations are as shown in fig. 2.14.

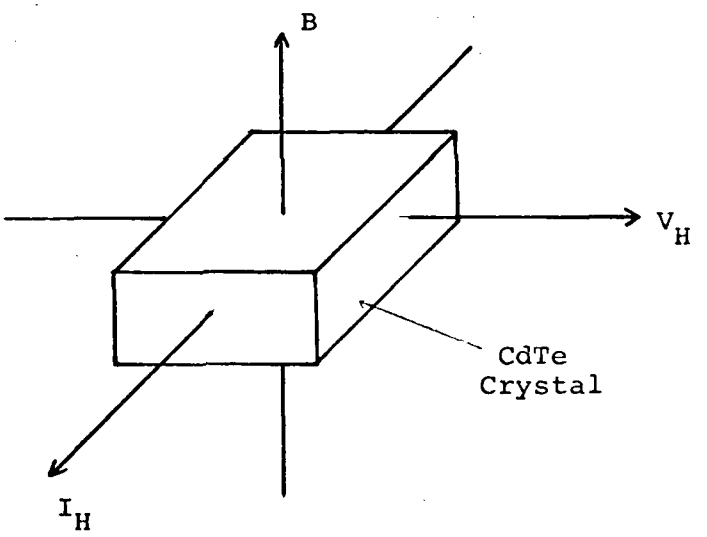

Fig. 2.14

A Direct current (I_H) is passed through the material and a magnetic field (B) is applied at right angles to to the direction of current flow. A transverse

voltage develops (V_H), the sign of which depends on the type (n or p) of material being investigated. This voltage is proportional to the current and field, and inversely proportional to the crystal thickness in the direction of the magnetic field. A constant or proportionality R, the Hall coefficient is given by the relationship:

$$V_H = \frac{R\ I\ B}{T} \quad \text{or} \quad R = \frac{V_H\ T}{I\ B}$$

T = Crystal thickness

This relationship is derived from consideration of the force produced on a charge carrier under the above conditions. Consider an n type semiconductor where n is the number of charge carriers an μ is the mobility of the charge carriers. ε_H is the field generated across the sample normal to Current I and field B and is given by

$$\varepsilon_H = \frac{V_H}{W}$$

V_H = Hall voltage

W = Width of Crystal

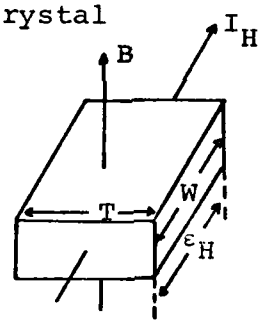

Fig. 2.14 a

The current density J is defined as

$$J = \frac{I}{W\ T} \ .$$

In n type semiconductors, the charge carriers are electrons

$\therefore$ Force = B e $\bar{v}$

e = charge on electron

$\bar{v}$ = average velocity of charge carriers

in equilibrium then

$$B\ e\ \bar{v} = e\ \varepsilon_H$$

since current density $J = n\ e\ \bar{v}$

$$\text{then } \varepsilon_H = \frac{1}{ne} J\ B$$

so that the Hall Field ε_H is given by

$$\varepsilon_H = R\ J\ B$$

$R = \frac{1}{ne}$ is the Hall Constant

Knowing the current density, J, and the magnetic field B, we measure V_H and hence ε_H, hence we have a measure of R the Hall coefficient and thus n the number of charge carriers.

$$R = \frac{1}{ne} = \frac{\varepsilon_H}{J\ B} = \frac{V_H\ T}{I\ B}$$

The sign of V_H also tells us the nature of the charge carriers, either electrons or holes, and hence the type of material (n or p type).

If the conductivity (σ) is measured (see 2.4.3) then with use of the Hall coefficient R_H we can get a direct value of the mobility μ. i.e.

$$\sigma = ne\ \mu \quad \text{and} \quad R = \frac{1}{ne}$$

$$\therefore \quad \mu = R\sigma$$

Mobility of charge carriers gives an indication of the purity of a crystal. Mobility drops as the number of impurities in a crystal increases. Consider the drift velocity of electrons in an electric field ε, then the electrons will be accelerated. In a perfect crystal the acceleration (A) is given by

$$A = \frac{-e\varepsilon}{m^*}$$

m^* is the effective mass of the electron

this implies that the velocity of an electron under these conditions increases with time. Ohm's law however implies that this velocity is constant and the electron is not accelerated

$$\sigma = \frac{J}{\varepsilon} = \frac{ne\bar{v}}{\varepsilon}$$

hence $\mu = \frac{\bar{v}}{\varepsilon}$

However electrons can be scattered by thermal atomic vibrations (phonons) and impurities, hence the mobility will be affected.

a) Scattering by Phonons

The mobility is given by

$$\mu_L = 3.2 \times 10^{-9} \frac{Cu}{\varepsilon_1} \frac{m}{m^*}^{5/2} T^{-3/2}$$

Cu is an averaged elastic constant.

ε_1 is change in position of band edge due to change in volume of unit cell.

m = mass of e

m^* = eff. mass of e .

hence μ_L varies $T^{-3/2}$

b) Scattering by Impurities

Calculations of the mobility associated with scattering at charged defects are fairly crude. However the Conwell-Weisskopf, 1950 mobility relationship based on simple Rutherford scattering appears to be a reasonable representation for most situations.

$$\mu_I = \frac{2^{7/2} \chi^2 (KT)^{3/2}}{\pi^{3/2} (m^{*\frac{1}{2}} q^3 Z^2 N_i) \ln[1+(3\chi KTrq^2 N_I{}^{3/2})^2]}$$

μ_I is mobility associated with the charged defect scattering.

χ is the dielectric constant.

qZ is the charge associated with the defects.

N_i is concentration of the defects.

m^* is the density of states effective mass.

This equation has been modified by Debye and Conwell, 1954 and by Brooks, 1955 to treat the scattering more realistically.

$$\mu_I = \frac{3.2 \times 10^{17}\ x^2}{N_I \ln (1 + x^2)}\ T^{3/2}$$

where $x = \dfrac{1.8 \times 10^5 T}{N_I^{\frac{1}{2}}}$

hence μ_I varies as $T^{3/2}$

To a good approximation the mobility associated with the various scattering processes can be determined by adding reciprocally the mobilities that would exist if each process were the only one active.

i.e.

$$\frac{1}{\mu_T} = \frac{1}{\mu_I} + \frac{1}{\mu_L}$$

$$= aT^{-3/2} + bT^{3/2}$$

hence at low temperatures the contributions from impurities ($aT^{-3/2}$) dominates, whereas at high temperatures scattering due to lattice phonons is predominant. Thus if a graph is drawn of total mobility against temperature the affect on mobility can be seen (fig. 2.15).

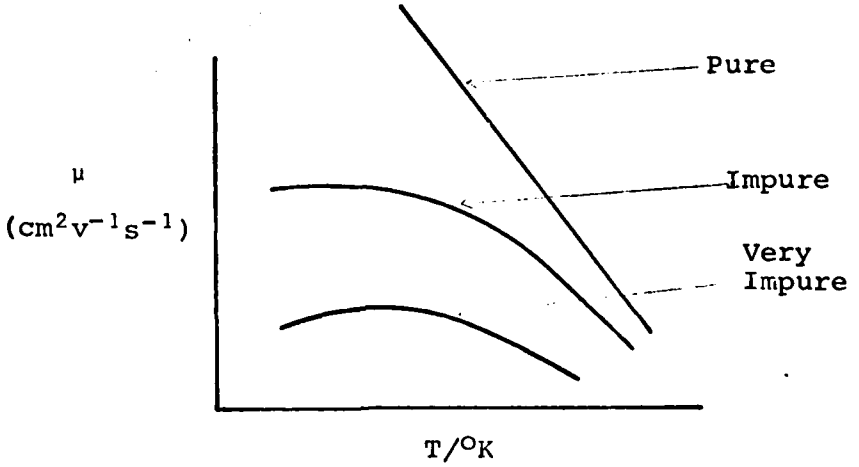

Fig. 2.15

Experimental

For measurement of Hall effect a crystal of CdTe was mounted in a probe and inserted in the Hall effect circuit shown in fig. 2.16.

A crystal of CdTe was cut into the form of a cube using a low speed diamond crystal sawing machine designed at R.S.R.E., Malvern, Worcester, England. The dimensions of the crystal were measured using the Scanning Electron Microscope. Four ohmic contacts were evaporated onto two pairs of opposite faces of the crystal. The metal used as ohmic contact was Indium, which, after evaporation, was alloyed by heating to 150°C in a vacuum of 10^{-4} torr for 10 minutes. The crystal was then attached to a small glass slide with impact adhesive. Fine stainless steel wires were attached to the four Indium ohmic contacts using silver conductive paint. Care was taken to ensure that contacts were made directly opposite each other on opposite faces. Conductivity measurements were made using contacts 1 and 3 or 2 and 4 (see later, 2.4.3). For Hall effect measurements the voltage generated between probes 1 and 3 was measured, on the application of a direct current between probes 2 and 4, while a magnetic field, B $wb.m^{-2}$, was applied perpendicular to the plane of the diagram.

The Current was measured in mA using a Keithley Electrometer, model no. 602, voltage was measured in mV using a Keithley null detector microvoltmeter, model no. 155, and magnetic field was measured in webers.m^{-2} (1 $wb.m^{-2} = 10^4$ gauss) using an AEI gaussmeter Type FB22.Form B3.

From these measurements values of mobility and carrier concentrations could be calculated.

2.4.3 Conductivity Measurements

The electrical conductivity is defined as the proportionality factor between the current density and the electric field. In an n type semiconductor material conductivity is due to electrons. The amount of conduction is determined by the number of electrons and their ease of movement in an applied electric field. This is called their mobility. The drift velocity of carriers, and is measured in units of $cm^2.v^{-1}s^{-1}$. i.e.

$$\sigma_n = \mu_n q n$$

σ_n = conductivity due to electrons - measured in $ohm^{-1}\ cm^{-1}$.

μ_n = mobility of electrons - in $cm^2\ v^{-1}\ s^{-1}$.

q = charge on electron = 1.6×10^{-19} coulombs.

n = no. of charge carriers (electrons).

In general for a semiconductor then

$$\sigma = q(n\ \mu_n + p\ \mu_p$$

where μ_n, n, q are as previously defined.

μ_p = mobility of holes.

p = no. of holes.

if the material is n type, $p = 0$

if the material is p type, $n = 0$.

the resistivity of the material is given by

$$P = \frac{1}{\sigma} \text{ - ohm. cm.}$$

hence measurement of resistivity gives conductivity, and hence the value of μ n.

Experimental

The resistance, r, of a crystal was determined by measuring the voltage drop between two probes when a direct current was passed through the crystal. By reversing the direction of current the homogeneity of the crystal was checked. From these measurements the specific resistance, (resistivity) ρ was obtained by means of the relation

$$\rho = \frac{r\ w\ T}{l}$$

l = distance between probes

w = width of sample

T = thickness of sample.

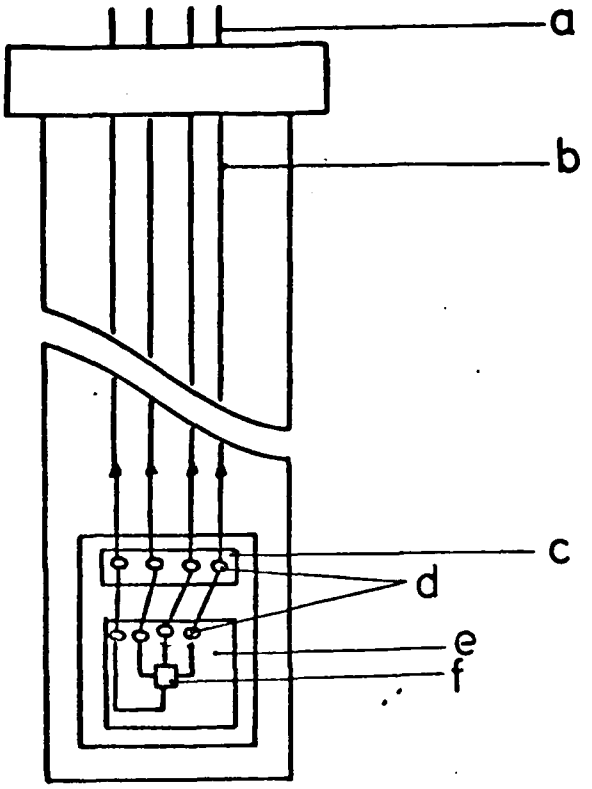

A.

Fig. 2.16. A. Hall Effect Probe.

a. B.N.C. Sockets: b. Insulated Wires:
c. P.T.F.E. Block: d. Silver Paste:
d. Glass Slide: f. CdTe Crystal.

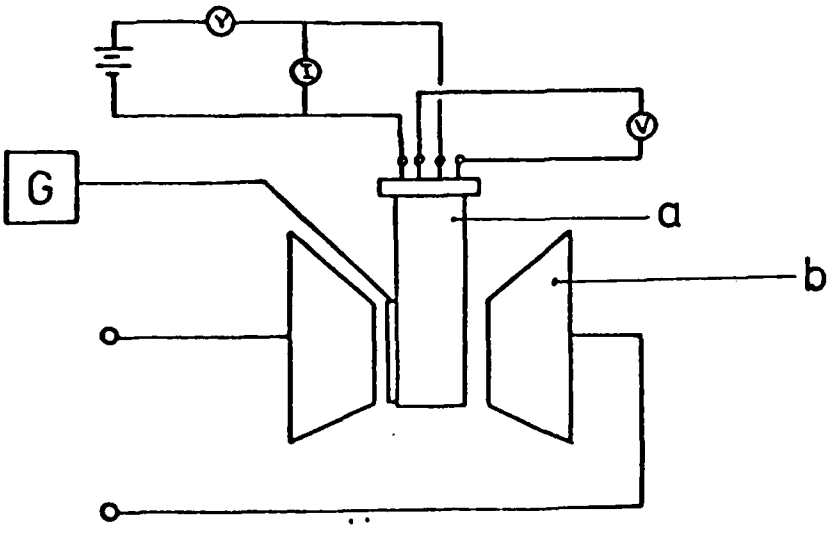

B.

Fig. 2.16. B. Hall Effect Circuit.

a. Hall Effect Probe: b. Electromagnet:
c. Gaussmeter.

The crystal resistance was measured at the same time, in the same apparatus as Hall effect measurements were taken. Only two of the contacts on the crystal were used.

2.5 Crystal Growth Methods used here and Results

A. Melt Growth

1. Liquid Encapsulant Growth

a) The Crystal Puller

Liquid encapsulant growth (LEC) of CdTe was carried out using a Malvern Czochralski crystal puller fitted with a C3000 high pressure work chamber. This is a commercial crystal growth system produced by Metals Research Ltd., Melbourn, Royston, Herts, England.

The C3000 high pressure chamber is designed for operation at internal pressures up to 200 atmospheres and has in fact been tested up to 300 atmospheres. The three main sections were machined from solid billets of austentic stainless steel, and were bolted together rather than welded. The chamber is water cooled. The main body of the chamber is machined to embody a reinforcing flange which gives added strength and also provides a convenient mounting point for viewing and diagnostic equipment. Two viewing ports are fitted at a convenient angle to allow observation of the crystal growth process. To one of these windows a Pye Television camera was fitted to enable monitoring to be continuous during high pressure operation. Double windows were fitted in each port. The outer window contains the pressure (tested to 300 atmospheres) and the inner window limits the amount of volatile material reaching the outer window. The Inner window is close to the crucible and is thus at a high enough temperature to prevent condensation of volatile material onto it.

The top plate contains the pull rod seal, which is a composite neoprene/PTFE high pressure unit capable of holding pressures

during pulling and rotational motions. It is rated at 400 atmospheres. The top plate also serves as a housing for the pull rod which is precision ground from stainless steel and is tapped to allow a variety of seed holders to be used. The bottom plate is mounted on the lower side of the main puller chamber, and is fitted with vacuum/ high pressure ceramic insulated RF feed throughs. The bottom plate also provides a support for the crucible and susceptor. An adjustable screw fitting allows easy adjustment of crucible position within the RF coil. There is also an insulated lead through to enable a thermocouple to be mounted inside the chamber to measure such things as susceptor temperature etc. Access to the chamber is obtained by lowering the bottom plate which is sealed to the main body of the chamber by eight stainless steel bolts (1" diam.) and a neoprene 'O' ring backed by a PTFE spacer ring. The entire chamber was designed to comply with the ASME Boiler and Pressure Vessels Code section 8 and the British Pressure Vessels Code BS1500.

Heating of the crucible and contents is achieved by RF induction heating of a carbon susceptor. The RF generator and saturate reactor provide a controllable and stable source of RF power at a nominal frequency of 450 KH_z. It has impedance matching facilities to enable a variety of susceptors to be used. The Saturable reactor provides a continuously variable stable source of three phase AC power to the main generator, which is mounted separately from the reactor. The generator contains an oscillator of rugged design. It is protected by a comprehensive system comprising

a) a water flow relay and pressure switch to ensure minimum water requirements,

b) lead (Pb) targets, in the water connection to the anode of the valve, to present electrolysis,

c) A D.C. Current overload relay,

d) a grid proportional under current relay system,

e) a filament and grid cooling fan.

The Generator high tension power supply is a full wave three phase system. To avoid power supply surges, resistance starting is incorporated through a time delayed twin contactor circuit. The output circuit is of med/high impedance and incorporates an impedance matching coil. A three position isolation switch is fitted giving off/test/run facilities. This is interlocked with a figure lock, an essential safety feature which ensures that the H.T. or RF power cannot be applied with an open crucible.

The pull rod lift and rotation mechanism gives accurate and precisely controlled lift and rotational motion to the pull rod. It has a built in pressure compensation which reduces wear of the drive mechanism and ensures that maximum precision and flexibility of control can be maintained at operating pressures up to 200 atmospheres. The lift and rotation mechanism incorporates separate and continuously variable controls for lift and rotation. The servomotors for lift and rotation both incorporate DC generators. The DC generator voltage output is proportional to the rotational speed. This is compared to an adjustable reference voltage and any difference between the two is amplified and applied to the motor field so minimising the differences caused by changes in motor field. In this way rates of lift and rotation could be held constant.

The puller was fitted with a sophisticated gas pressure control system. This enabled us to charge the chamber to a required over pressure of an inert gas or to evacuate the chamber. Evacuation was effected using an Edwards ES50 rotary vacuum pump. For the growth of CdTe oxygen free nitrogen supplied by B.O.C. was used as the inert gas. This

was supplied in bottles pressurised to 3000 p.s.i. In theory we could therefore pressurise the chamber to 3000 p.s.i. but in reality we rarely worked with pressures greater than 500 p.s.i.

b) Experimental Technique

The CdTe charge was contained in a quartz silica crucible, which was housed in a specially machined carbon susceptor, see fig. 2.17. Several susceptor shapes were tried but the final design arrived at provided the best temperature gradients especially at the bottom of the crucible. CdTe (doped or undoped) was loaded into the crucible and covered with a layer of B_2O_3 to a depth of seven millimetres. The crucible was then placed in the carbon susceptor and the whole lot placed in the centre of the RF coil. The Crucible was placed such that the level of the top of the B_2O_3 layer was just above the top of the susceptor. This enabled an adequate temperature gradient to be set up (fig. 2.17).

The temperature profile of the melt was measured initially by using thermocouple (Pt-Pt/10%Rh) encased in a quartz silica tube and lowered into the melt via the pull rod. This was compared with the temperature of the carbon susceptor, measured by another thermocouple (Pt-Pt/10%Rh) buried in the susceptor. If future experiments temperature measured was that of the carbon susceptor.

In the first experiemnts a clean tungsten rod was attached to the pull rod and used to pull crystals, but this was later replaced by a piece of CdTe, grown previously by the stockbarger method, fashioned into a seed and held in a chuck type seed holder, made in our workshop (fig. 2.18).

The technique used to grow crystals by the L.E.C. method was as follows. After setting up the crucible etc. described above the high pressure chamber was closed and bolted

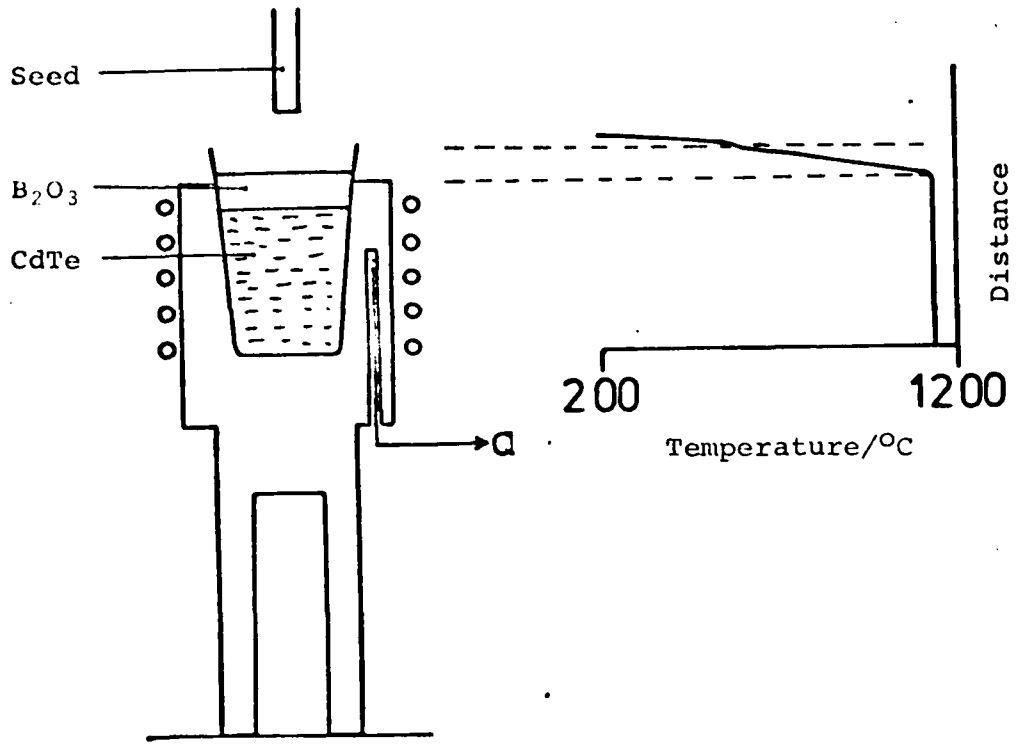

Fig. 2.17. Apparatus and Temperature Profile Used by US in the Growth of CdTe Crystals by the LEC Method.

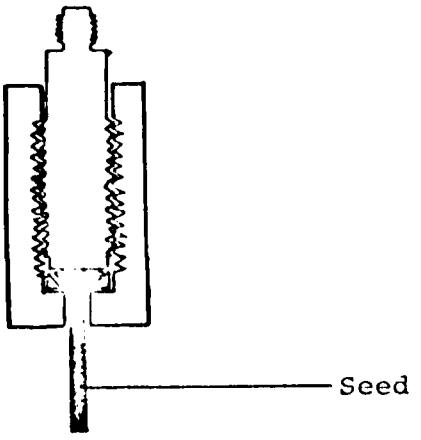

Fig. 2.18. Chuck Type Seed Holder Used in the LEC Method.

CRYSTAL No.	RESISTIVITY(ρ) /Ω.cm.	MOBILITY(μ) /$cm^2v^{-1}s^{-1}$	Carrier Concentration /cm^{-3}
LEC 1.1	2×10^{-2}	490	3×10^{17}
LEC 2	5×10^{-2}	350	2×10^{17}
LEC 3	3×10^{-1}	700	5×10^{16}
LEC 6	5	200	8×10^{15}
LEC 8	8×10^{-2}	120	1×10^{17}

TABLE 2.1

Typical electrical Characteristics of undoped n type CdTe crystals grown by LEC

(all measurements carried out at room temperature ~ 293 K)

together. It was then evacuated to 10^{-3} torr. Nitrogen was then admitted to the chamber to a pressure of 250 p.s.i. The chamber was then re-evacuated and recharged with N_2. This process was repeated four times to ensure that the atmosphere in the chamber consisted just of oxygen free nitrogen, since traces of oxygen and other gases caused erosion of the carbon susceptor etc. at high temperatures. The chamber was finally charged to a working pressure of 500 p.s.i. An overpressure of 500 p.s.i. was used as experiments using pressures below 500 p.s.i. showed that absorption of Te from the melt by B_2O_3 occurred and that Cd vapour losses were seen.

The whole apparatus was enclosed in a "Safe" area surrounded by heavy chain mail. When all the water, gas, etc. had been on for about ten minutes the RF power was switched on and gradually increased until the temperature of the susceptor was ~1150°C. The system was left at this temperature for about one hour before any further steps were taken. This was to ensure that all of the charge was molten and that the whole system inside the chamber had reached a state of equilibrium. When the charge was molten the seed crystal (or tungsten rod) was lowered through the molten B_2O_3 and into contact with the molten CdTe. This process was monitored continuously by television. The seed was rotated continuously throughout the growing process to neutralise any asymmetries in the heating. Typical rates of rotation were 5-10 r.p.m. The seed was then slowly pulled from the melt at rates typically of the order 0.5 $cm.hr^{-1}$. Reasonably shaped ingots could be grown by this method, but it was found that the depth of the B_2O_3 layer had a marked effect on the type of growth seen. Too shallow a depth of B_2O_3 resulted in an inadequate layer of B_2O_3 being drawn up with the crystal, resulting in cadmium vapour loss from the surface of the crystal. Too great a depth produced bulbous shaped crystals whose diameter gradually increased and decreased in a

periodic manner. Nygren, 1973, noted the same phenomena when he grew GaP crystals by the LEC method. He noted that the repeat period correlated with the depth of the B_2O_3 and that the way to grow crystals of uniform diameter was to employ a programme of power reduction during crystal growth.

c) Crystal Growth Results

Using a manual programme of RF power reduction i.e. reducing RF power to keep temperature of the CdTe melt just about $5^{o}C$ above the melting point of CdTe, ingots of up to 70mm × 20mm diameter were grown. B_2O_3 was removed by dissolving the B_2O_3 in hot water. Crystals of size up to 10mm × 5mm × 3mm were grown using this method.

Electrical characterisation of the crystals was carried out using the methods of Thermoelectric effect, Hall effect and Conductivity measurements described previously. Some typical results are presented in table 2.1.

Undoped material generally came out as n type material with low resistivities, i.e. $\rho \sim < 10\ \Omega$ cm. when measured at room temperature. Carrier concentrations were generally in the range 10^{16}-10^{17} cm^{-3} with mobilities ranging from 50 to 800 $cm^2\ v^{-1}\ s^{-1}$. The high concentration of carriers, considering the material to be undoped, was probably due to impurities picked up during the growth process. Mullin and Straugham, 1977 found this to be the case for their LEC grown CdTe crystals. They noticed consistently that Boron and Bromine impurities were present in fairly high concentrations in all their crystals. The Boron originated from the B_2O_3 layer and the Bromine from the Bromine/Methanol etch used to clean up the CdTe charge prior to LEC growth. As Boron is a potential donor in CdTe the inability to control the Boron concentration in LEC grown CdTe crystals is a large

drawback to growth of tailored crystals by this technique.

2.5 A.2. Fast Vertical Bridgman

a) Apparatus

Fast vertical Bridgman growth of CdTe was carried out inside the C3000 high pressure chamber of the Malvern Czochralski crystal puller. The D.C. servomotor controlling lift was suitably modified to enable the pull rod to be lowered at a controllable rate instead of raised as was the mode for LEC growth. A Carbon susceptor suitably machined and supported by three tungsten legs was placed in the centre of the RF coil (fig. 2.19). This provided a temperature profile as shown also on fig. 2.19. The temperature profile was measured using a Pt-Pt/10%Rh thermocouple attached to the pull rod of the susceptor. Several different shapes and dimensions of carbon susceptors were experimented with, each giving different temperature profiles. The final shape used gave a narrow temperature zone 'A' of about 1cm at 1120°C. Zone B above the 'hot' zone A was at a temperature of ~830°C. This region controlled the vapour pressure of Cd and allowed use of the solid-liquid vapour equilibrium to adjust deviations from stoichiometry of the compound. A temperature of 830°C for zone B gave a Cd overpressure of 2.1 atm (see appendix 2.7). For experiments where different Cd over-pressures were required, different susceptors of basically the same design as that in fig. 2.19, but different dimensions were used. The temperature below the molten zone - zone C provides for slow cooling and an annealing region. For samples to be quenched a susceptor was used which gave a temperature profile shown if fig. 2.20. After passing the hot zone the whole ampoule could be kept at a temperature of 1000°C. The chamber was then rapidly opened and the ampoule immersed in a bath of cold water.

b) Experimental Procedure

CdTe (doped or undoped) was loaded into a quartz silica ampoule, 17mm in diameter, rounded at one end and coated on the inside with pyrolytic carbon. The ampoule was then evacuated to 10^{-6} torr and sealed off. A quartz silica hook was attached to the top of the ampoule through which the ampoule could be attached to the crystal puller pull rod.

The crystal puller was sealed and the chamber evacuated to 10^{-3} torr using the rotary pump. The reason for evacuation is two-fold. First, a lack of air in the system prevents corrosion of the carbon susceptor when at high temperatures, which would affect the temperature gradients. Secondly a lack of air in the system means that there are no convection currents set up to vibrate the ampoule and thus affect crystal growth quality. It was noticed in the first experiments that fairly large movements of the ampoule were occuring. These were attributed to convection currents between the very hot carbon susceptor (1180°C) and the chamber walls a distance of 1½" away and water cooled (temp. 40°C). Removal of the atmosphere, via evacuation, from the chamber reduced these convection current effects to virtually zero.

After the carbon susceptor had been heated to the desired temperature which gave the desired temperature profile the system was allowed to equilibrate for 30 minutes. The ampoule was then lowered through the centre of the susceptor. Various growth rates and temperature profiles were experimented with, but it was found that for the particular experimental arrangement used here a growing, or Ampoule lowering rate, of $2cm.hr^{-1}$ and a temperature profile as shown in fig. 2.19 which correlated to a carbon susceptor temperature of 1180°C produced the best crystal growth. The Ampoule lowering procedure was monitored using the Television system as used for LEC crystal growth monitoring.

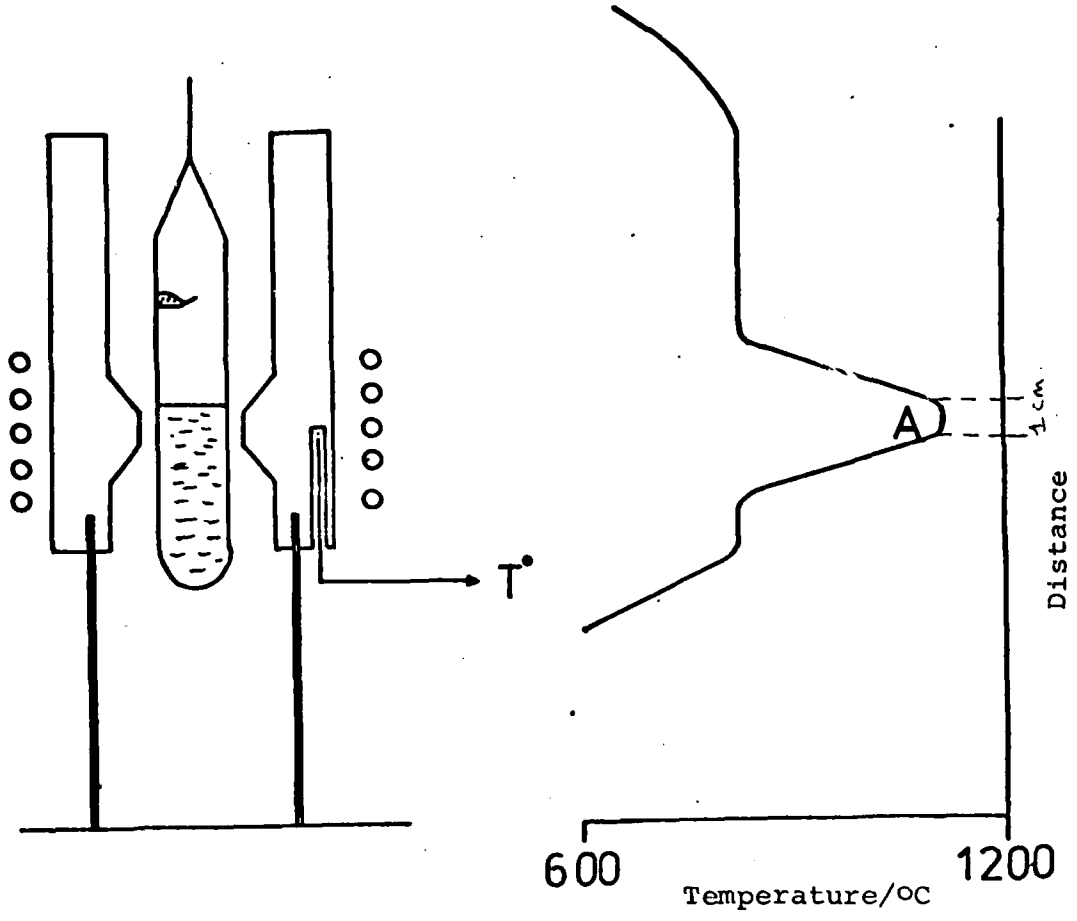

Fig. 2.19. Apparatus and Temperature Profile Used for 'Slow Cooled' Fast Vertical Bridgman Growth of CdTe.

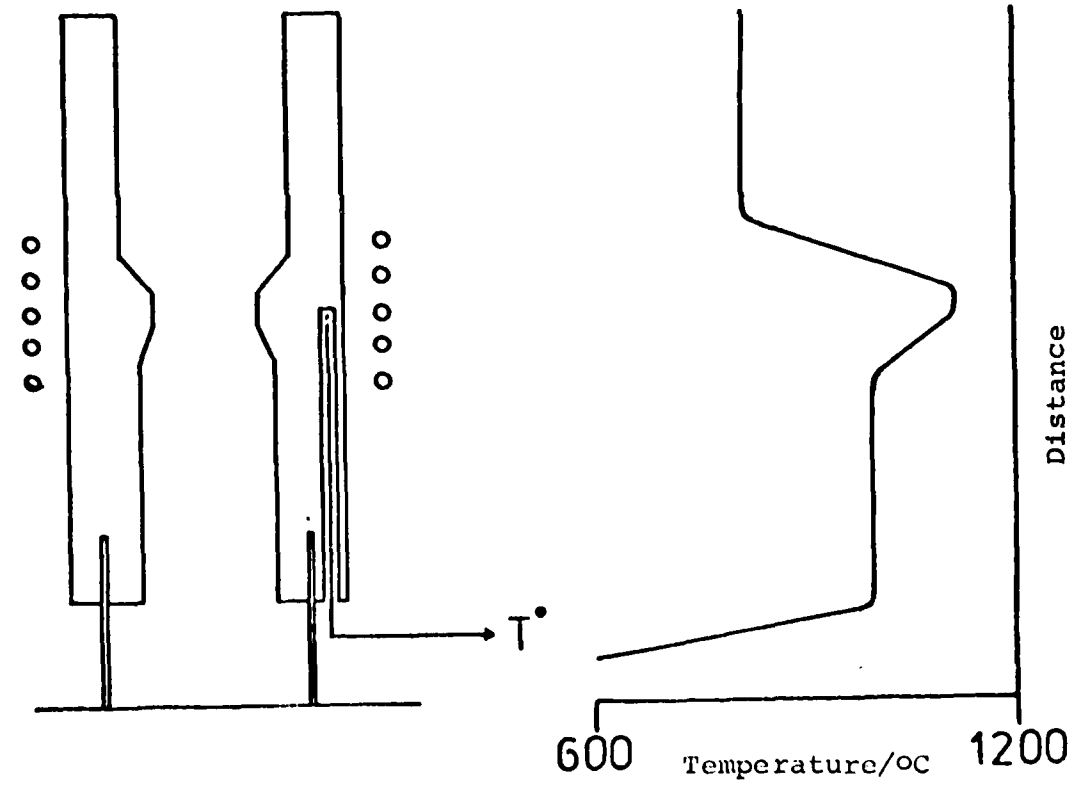

Fig. 2.20. Apparatus and Temperature Profile Used for 'Quenched' Fast Vertical Bridgman Growth of CdTe.

CRYSTAL No.	TYPE (n or p)	P_{Cd}	QUENCHED(Q) or SLOW COOLED(S)	DOPANT	DOPANT LEVEL /atoms.cm^{-3}	RESISTIVITY(ρ) /Ω.cm.	MOBILITY(μ) /cm^{2}v^{-1} s^{-1}	Carrier Concentration /cm^{-3}
FVB 9	n	2.1	S	-	-	250	750	10^{14}
FVB 11	p	1	S	-	-	10^6	-	-
FVB 36	n	2.1	S	In	2×10^{18}	1	500	10^{17}
FVB 40	n	2.1	Q	In	2×10^{18}	10^5	-	-
FVB 48	p	2.1	S	Al	10^{18}	10^2	80	10^{15}
FVB 49	n	2.1	S	Al	1.5×10^{18}	10	5.2×10^2	1.5×10^{16}
FVB 19	p	2.1	S	Cl_2	10^{18}	10^5	-	-

TABLE 2.2

Typical electrical properties of CdTe Crystals grown by FVB

(All measurements carried out at room temperature)

c) Results

This method of crystal growth produced ingots of material 50mm long × 17mm diameter. Inside the ingots single crystals up to 20mm × 10mm × 10mm were found.

Electrical properties of crystals, both doped and undoped were investigated using the methods of Thermoelectric power, Hall effect and conductivity previously described. Some typical results are presented for undoped CdTe and crystals doped with Indium, Aluminium and Chlorine in table 2.2.

If we consider first of all the crystals of CdTe grown with undoped CdTe and Indium doped CdTe it will be seen that the electrical properties vary greatly. It appears that these properties are dependent on the vapour pressure of Cd employed during the growth process and on the rate of cooling of crystal material after growth has taken place. For instance, Undoped CdTe grown at a Cd overpressure of 2.1 atmospheres and slow cooled produced n type CdTe with a resistivity of 250Ωcm mobility of 750cm $v^{-1}s^{-1}$ and an electron carrier concentration of $10^{14}cm^{-3}$ when measured at room temperature. If undoped CdTe was grown under the same conditions as before except that the Cd overpressure was kept at1 atmosphere then high resistivity p type material was produced.

The effect of rate of cooling on the crystals can be seen in the results of crystals taken from ingots FVB 36 and FVB 40. In both cases CdTe doped with the same amount of Indium (2×10^{18} atoms.cm^3) was used. The same Cd overpressure (2.1 atm) was used. The only different parameter was in the rate of cooling. FVB 36 was slow cooled and FVB 40 was rapidly cooled or 'quenched'. There was quite a dramatic change in the electrical properties of the crystals produced. FVB 36, slow cooled, produced n type crystals of low resistivity - 1Ωcm, mobility of 500$cm^2v^{-1}s^{-1}$ and electron carrier concentration of $10^{17}.cm^{-3}$. Quenched crystals (FVB 40) however produced n type

material of high resistivity ~$10^5 \Omega$cm. In a paper published in 1971 Kyle reported similar results for crystals grown by his modified Bridgman method. He found that CdTe doped with Indium and slow cooled produced crystals whose electrical properties were determined predominantly by the amount of Indium put into the crystals, and the pressure of one of the components of the compound. CdTe doped with Indium and quenched from over 1000°C produced crystals with electrical properties independant of the Indium concentration. Hence as far as CdTe undoped and doped with Indium are concerned good quality crystals can be grown to required electrical properties providing that adequate control over the rate of cooling of crystals after growth and over the vapour pressure of Cd during growth is maintained.

CdTe crystals doped with Aluminium proved to be not as reliable as those grown with Indium. As the results in table 2.2 indicate there is a very fine dividing line between the amount of alumium needed to produce p type material and the amount required to produce n type material, i.e. $10^{18} \rightarrow 1.5\ 10^{18}$ giving carrier concentrations of $10^{15}.cm^{-3}$ for p type material and $1.5 \times 10^{16}.cm^{-3}$ for n type material.

Chlorine doped crystals of CdTe produced mostly p type material unless the concentration of Chlorine used was very high when n type material could be produced. Typically using Chlorine starting concentrations of 10^{18}atoms.cm^{-3} it was found that p type material was formed even with a Cd overpressure of 2.1 atmospheres and slow cooling of the grown crystals. With a starting concentration of 10^{19}atoms.cm^{-3} slightly n type material of high resistivity could be produced. This occurrence was noted by other workers. Agrinskaya and Matreev, 1977 noted that crystals doped with 10^{17} atoms.cm^{-3} of Chlorine or less resulted in p type crystals with carrier concentrations in the range 10^{11}-10^{15}. Crystals doped with 2×10^{18} atoms.cm^{-3} appeared n type with a carrier concent-

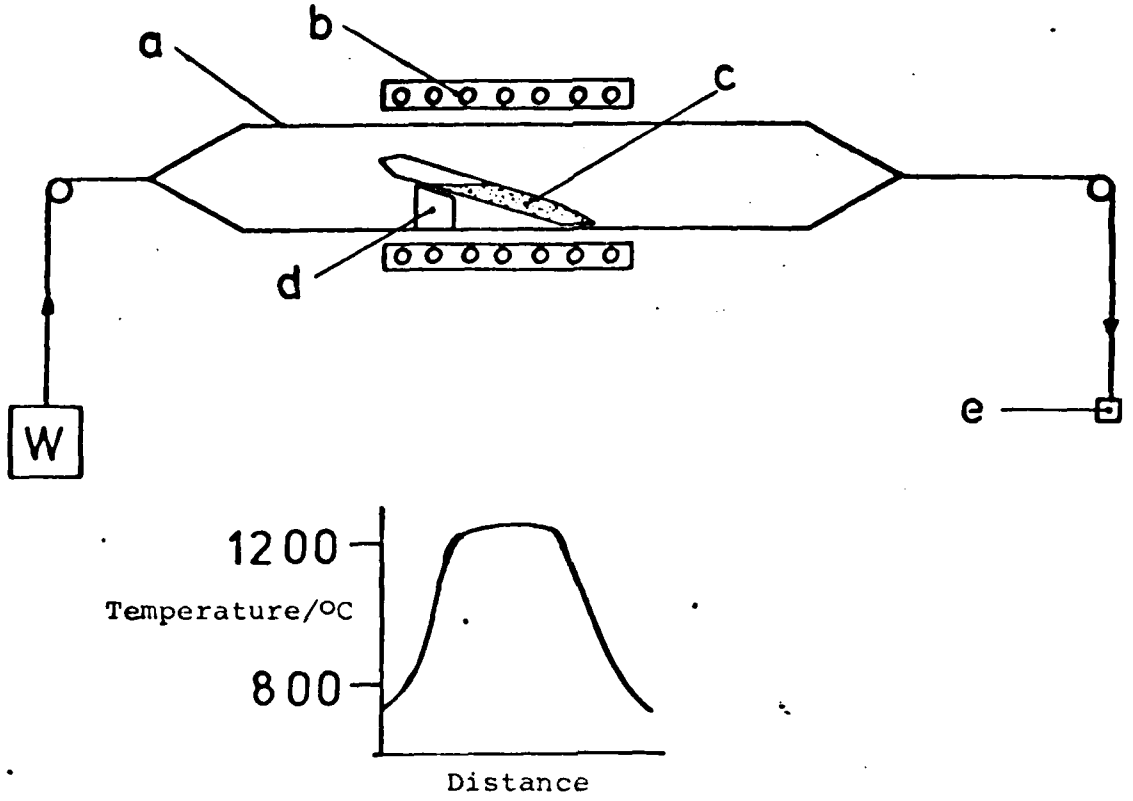

Fig. 2.21. Schematic Diagram and Temperature Profile of the Furnace and Ampoule Used in the Horizontal Stockbarger Method of CdTe Crystal Growth.

a. Mullite Tube: b. High Temperature Furnace: c. Quartz Ampoule and CdTe Charge: d. Quartz Support Block: e. D.C. Servomotor: W. Tension Weight.

CRYSTAL No.	RESISTIVITY(ρ) /Ω.cm.	MOBILITY(μ) /$cm^2 v^{-1} s^{-1}$	Carrier Concentration /cm^{-3}
$S_{1.1}$	10	450	10^{16}
$S_{1.2}$	50	150	10^{15}
$S_{1.3}$	1500	70	3×10^{14}
$S_{1.4}$	1200	80	2.5×10^{4}

TABLE 2.3

Typical electrical characteristics of n type CdTe crystals (undoped) taken from the same ingot after growth by the stockbarger method

(All measurements carried out at room temperature)

ration of the order $10^{17}.cm^{-3}$.

Again as in the case of Aluminium doped CdTe it would appear that it is the concentration of dopant that determines the type of electrical behaviour shown by the crystal. There is also a very fine dividing line between the concentrations that produce n type and p type material.

Hence it could be concluded that of the dopants used Indium is the most predictable and as such Fast vertical Bridgman growth appears best suited to growing tailored crystals of Indium doped CdTe.

2.5 A.3. Stockbarger Growth

a) Apparatus

The apparatus used is shown in fig. 2.21. The furnace is a platinum wound commercial furnace made by JMM*, Through the centre of the furnace is run a Mullite tube supported by two free running PTFE wheels, one at either end of the furnace. One end of the mullite tube is attached via a pulley system to a D.C. Servomotor and the other end to a tension providing counter balance. Using this method it is possible to move the tube through the furnace at a determined rate e.g. $2cm.day^{-1}$. The temperature of the furnace is regulated by Pt-Pt/10%Rh thermocouples buried in the furnace and linked to a temperature controller which keeps the furnace at any pre set temperature required. At the best operating temperature, found by experiment, the furnace had a temperature profile as shown in fig. 2.21.

b) Experimental Method

Ampoules were prepared, as described previously, by carbon coating silica quartz. CdTe (doped or undoped) was introduced and the ampoule sealed under vacuum of 10^{-6} torr. The Ampoule was introduced to the mullite tube with the furnace on, and supported inside the tube at an angle of ~30°C by a suitably shaped piece of quartz. The

furnace was then switched on to the desired temperature and the mullite tube pulled through the resulting temperature gradient. As the CdTe comes into the decreasing temperature gradient in region A, solidification and hence crystal growth of the CdTe takes place in the pointed end of the ampoule. Typical pulling rates are $2cm.day^{-1}$.

c) Results

Ingots containing large single crystals, 10mm × 10mm × 10mm were successfully grown. It was found that for the particular experimental arrangement used here a growth rate of $2cm.day^{-1}$ gave best results. Transport measurements however demonstrated the non-uniformity of the doping in these crystals. It was found that crystals taken from various parts of the growth ingot differed quite markedly in their electrical characteristics. This is typified by the results of conductivity and Hall measurements shown in table 2.3. Here the results are taken from ingot designated S_1 crystal 1 i.e. $S_{1.1}$ was taken from near the pointed end of the ingot and ingots ^{2,3,4} from progressively further back in the growth ingot. As can be seen the n type crystals (undoped) vary from low resistivity (10Ωcm) to fairly high resistivity (1200Ωcm).

2.5 B. Solution Growth - Travelling Heater Method

a) Apparatus

The Travelling heater method apparatus used is shown in fig. 2.22. This consists of a stationary heater with a motorised pulley system which provides for movement of the CdTe charge relative to the heater. The furnace, built at our laboratory, consisted of three resistance heaters, a relatively short pre heater (A) provides a temperature zone for the solvent, the main heater (B) and an after heater (C) which subjects grown crystals to subsequent annealing. The pre heater and after heater are linked together and made of the same material Nichrome Tape with a resistivity of ($23\Omega.m^{-1}$). They were controlled by the same

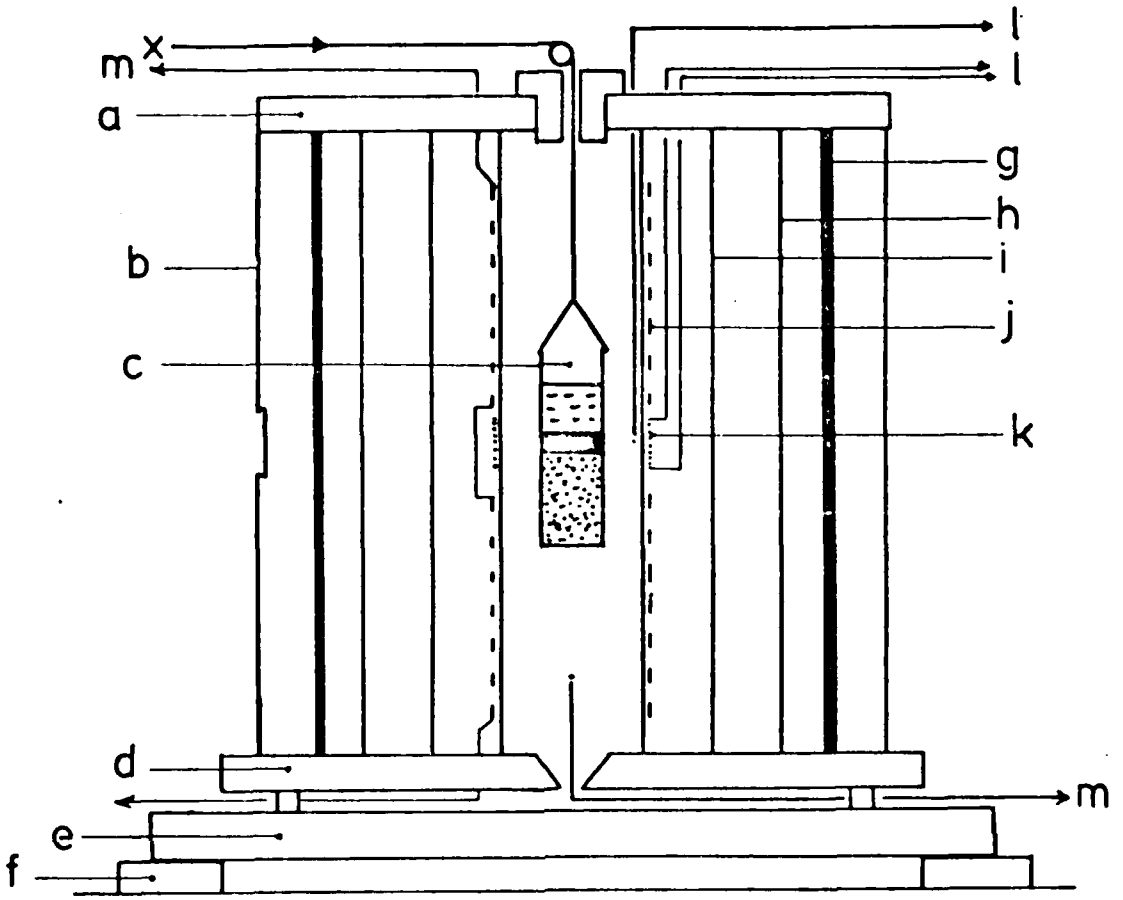

Fig. 2.22. Travelling Heater Method Furnace Construction.

a. Asbestos Top Plate: b. Aluminium Shield with Mica Windows: c. THM Ampoule: d. Asbestos Bottom Plate: e. Cast Iron Base: f. Rubber Supports: g. Steel Support Rods: h. Quartz Tube: i. Quartz Tube: j. Pre-Heater: k. Main Heater: l. Temperature Control and Thermocouple of Main Heater: m. Temperature Control and Thermocouple of the Pre- and After Heaters: x. Ampoule Lowering Mechanism.

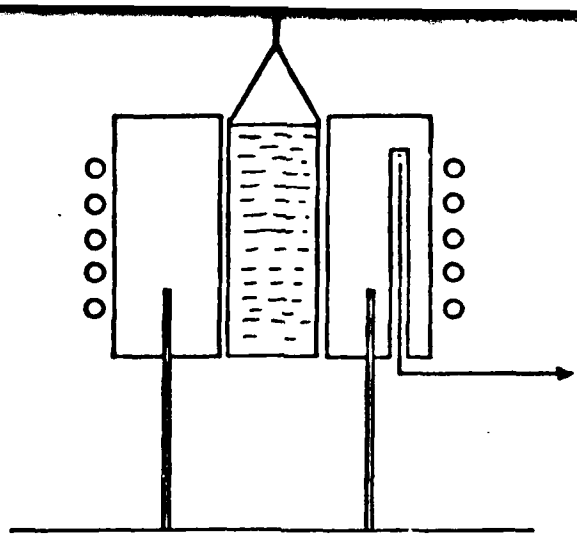

Fig. 2.23. Apparatus Used to Produce the CdTe Charge for Use in the THM Ampoule.

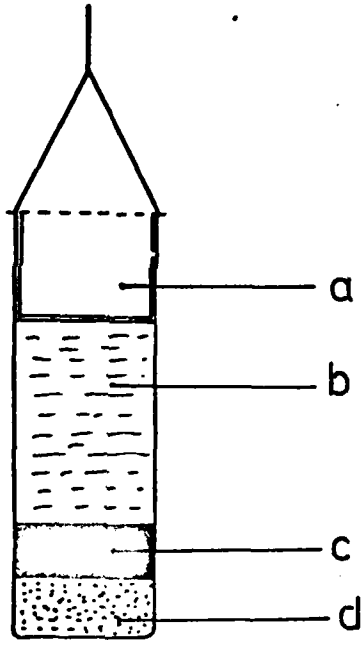

Fig. 2.24. THM Ampoule Construction.

a. Quartz Plug: b. CdTe Charge: c. Tellurium Solvent: d. CdTe Grown.

temperature controller and monitored by the same thermocouple.

The main heater was a lightly wound Nichrome Wire heater (23Ω.m^{-1}). This was made by winding nichrome wire round the quartz inner tube and cementing it in place using high temperature alumina cement. (The nichrome wire was later replaced with platinum wire - see later).

The heating elements were protected from convection currents etc. by two clear tubes, the inner one quartz and the outer one pyrex, placed concentrically around the heater tube. Around these were then placed an aluminium shield with plexiglass (later mica) windows to allow monitoring of the crystal growth. The whole rig was bolted to a solid iron base and placed on rubber feet to prevent vibrations.

A D.C. servomotor was housed on a separate shelf above the furnace by a system of gears and pulleys the ampoule could be lowered at a predetermined rate for several weeks non stop.

b) Material Preparation and Experimental Method

For crystal growth by the travelling heater method feed material with a density as close to 100% as possible is desirable. This prevents the absorption of liquid solvent by the feed material through the capillary action of structural voids, and will also prevent the occasional detachment of the liquid solvent during crystal growth. This latter effect results from the decrease in volume of CdTe which results when theoretically dense crystals are formed from less dense feed material. Feed material was made in the Malvern Czochralski crystal puller high pressure chamber using a carbon susceptor and ampoule of special design (see fig. 2.23). The Ampoule diameter 'd' was the same as the diameter of the ampoule to be used for the crystal growth. CdTe produced earlier was introduced to the ampoule which was

evacuated and sealed. The CdTe was heated up to 1150°C then cooled with the result being a solid ingot of CdTe. This was to be the CdTe charge.

The ampoule for the travelling heater method is shown in fig. 2.24. This was a carbonized quartz ampoule of diameter 'd'. It contained a CdTe seed crystal, a layer of solid Te and the CdTe charge produced above. A quartz plug was inserted and the ampoule evacuated to 10^{-6} torr and sealed. A stainless steel wire was attached and the ampoule inserted into the upper heater (A) of the furnace. The furnace was switched on to operating temperatures and the ampoule slowly lowered through the temperature gradients. Typical lowering rates were 0.3 to 1.0cm.day^{-1}. Various main heater operating temperatures were used from 650°C to 900°C (at 650°C the solubility of CdTe in liquid Te is about 15% which is quite sufficient for equilibrium crystal growth from solution). Typical pre heater and after heater temperatures were of the order 300-450°C.

One major design problem was that of the long term reliability of the main heater element. To obtain an air temperature in the quartz tube of 900°C the nichrome wire element had to be operated at temperatures in excess of this. In the original design a broad main heater was used but this produced only small CdTe crystals. This was due to the Tellurium solvent layer becoming too broad and thus to diffuse resulting in an uneven diffusion of Solute through the solvent. Using a narrower main element to achieve the same temperature region meant operating the Nichrome wire at higher temperatures. This resulted in the element burning out, usually before a crystal growth run could be completed.

To overcome this problem different winding materials were used. The first of these was Tungsten. Unfortunately due to the rigidity of the tungsten wire it was found to be very hard to produce element

CRYSTAL No.	TYPE n or p	DOPANT	RESISTIVITY(ρ) /Ω.cm.	MOBILITY(μ) /$cm^2v^{-1}s^{-1}$	Carrier Concentration /cm^{-3}
THM 1	p	-	10^4	~80	~10^{13}
THM 2	n	Cl (1000ppm)	1100	600	9×10^{12}
THM 4	p	-	10^3	80	10^{13}
THM 6	p	Cl (1000ppm)	10^2	150	10^{12}
THM 8	p	Cl (5000ppm)	10^8	35	10^9

TABLE 2.4

Typical electrical properties of CdTe crystals grown by THM

(all measurements carried out at room temperature)

windings without "kinks" being formed in the wire. On heating these kinks caused hot spots which resulted in a very short lifetime for the element. Latterly platinum wire was used instead of nichrome. Platinum 0.25mm in diameter resistance $5\Omega.m^{-1}$ produced by Engelhard Industries Ltd., was used. This was a more malleable material than tungsten and as such element windings, kink free, were easier to produce. The main heater produced had a hot zone 1cm broad and was run continuously for periods of up to 18 days.

Growth was carried out on undoped CdTe using two types of molten zones. First was just Tellurium to produce undoped CdTe crystals. The second was Tellurium with Cadmium Chloride ($CdCl_2$) added to produce chlorine doped CdTe.

c) Results

The results of the travelling heater method were encouraging. Large single crystals (15mm × 10mm × 5mm) were grown by this method. Electrical characterisation of these crystals was carried out by the methods of Thermoelectric power, Hall effect and conductivity measurements. Some typical results as shown in table 2.4.

Undoped material generally came out as p type material of fairly high resistivity i.e. 10^3-$10^6\Omega$cm with mobilities in the range 50-150cm^2v^{-1} s^{-1} and carrier concentrations of the order of $10^{13}cm^{-3}$ e.g. Crystals THM 1 and THM 4. The high resistivity of the undoped material is linked to one of the side effects of the THM method, that is in the purification of the CdTe caused by the movement of the Tellurium zone through the CdTe (see before).

Material doped with Chlorine however was not as predictable as the undoped material. In table 2.4 the concentration of Cl quoted are the concentrations of $CdCl_2$ added to

the Te solvent zone prior to crystal growth. As can be seen there is a large variation in electrical properties which seem to be caused by the change in Cl concentration i.e. from highly resistive p type material to n type material of medium resistivity.

Conclusion

The Travelling heater method as set up works satisfactorily and produces reasonably large single crystals of CdTe. However doping of the material by this method seems to be uncertain and does not seem to lend itself to producing tailored crystals of desired electrical characteristics. If the desire is for high purity undoped p type crystals of high resistivity (as in the case for nuclear detection) then this method would seem to be ideal for this.

2.6 General Conclusions

As has been shown there are numerous ways of producing good quality crystals of cadmium telluride. Each method has its own advantages and disadvantages. Some are more controllable and predictable than others. By careful definition of the electrical characteristics, physical dimensions etc. of the required crystals beforehand it is possible to chose a growth method which will best provide crystals needed. For example, for nuclear detectors high purity high resistivity CdTe is needed, whereas for production of Schottky barriers low resistivity material with carrier concentrations in the range 10^{16}-10^{17}.cm^{-3} are required.

For nuclear detector work then it would seem appropriate to grow crystals by the travelling heater method since this method consistently produces high purity, high resistivity and high mobility material with low carrier concentrations. For Schottky barrier work, however, CdTe grown by the method of fast vertical Bridgman growth would seem most appropriate since control of the electrical characteristics by use of Cd overpressures, dopant concentration, rate of cooling etc. is relatively straightforward and crystals of low resistivity, low mobility with carrier concentrations in the range 10^{16}-10^{17}.cm^{-3} can readily be grown. Liquid encapsulation also provides crystals of the correct

type for Schottky barrier formation but lack of control over contamination by Boron from the Boric oxide makes the process less predictable than the fast vertical Bridgman method.

2.7 Appendix

The Vapour Pressure of Cd and Te

The particles of a solid can escape into the vapour phase to establish a vapour pressure. The particles of a solid do not all have the same energy, there is a distribution in which most of the particles have energy near the average, but some have less while others have more. Those particles which at any one time are of higher than average energy and are near the surface of the material can overcome the attractive forces of their neighbour and escape into the vapour phase. If the solid is enclosed in a container eventually there will be enough particles in the vapour phase so that the rate of return of the particles to the material will be equal to the rate of escape. At this point a dynamic equilibrium is set up, in it there is an equilibrium vapour pressure characteristic of the solid. Since the escaping tendency of the particles depends on the magnitude of the intermolecular forces in the particular material considered the equilibrium vapour pressure will differ from one substance to another. For instance if the attractice forces in the solid are small as with a molecular crystal such as solid hydrogen the escaping tendency is great and the vapour pressure is high. Whereas in an ionic crystal with large binding forces then vapour pressure is low.

The vapour pressure of a material is also dependent on temperature, the higher the temperature the more energetic the particles and the more easily they can escape. The more that escape the higher the vapour pressure. Fig. 2.24 shows how the vapour pressure of a typical substance changes with temperature. At absolute zero the particles have no escaping tendency so vapour pressure is zero. As temperature is raised so the vapour pressure rises. It rarely gets to be very high before the solid melts. Above the melting point the vapour pressure curve is that of a liquid. Fig. 2.25 shows the vapour pressure curves of Cd and Te. Data is from "The Handbook

of Physics and Chemistry (58th Edition)".

As is indicated on the diagram at a temperature of 1095°K(822°C) Cd has a vapour pressure of 2.1 atmospheres whereas at 800°C the vapour pressure is 1.7 atmospheres. Hence in methods like the Fast vertical Bridgman crystal growth method keeping a piece of Cd at a temperature of 822°C in an enclosed ampoule will provide a vapour pressure or over-pressure of 2.1 atmospheres, keeping the Cd at 765°C gives an overpressure of 1 atmosphere.

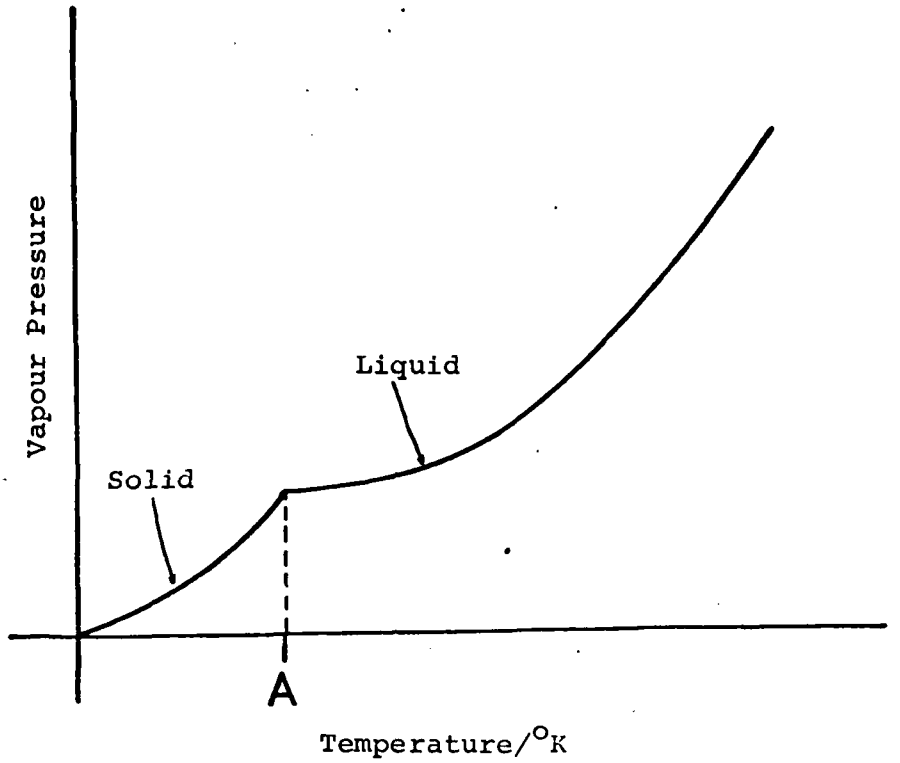

Fig. 2.25. Temperature Variation of Vapour Pressure of a Typical Substance: A is the Melting Point.

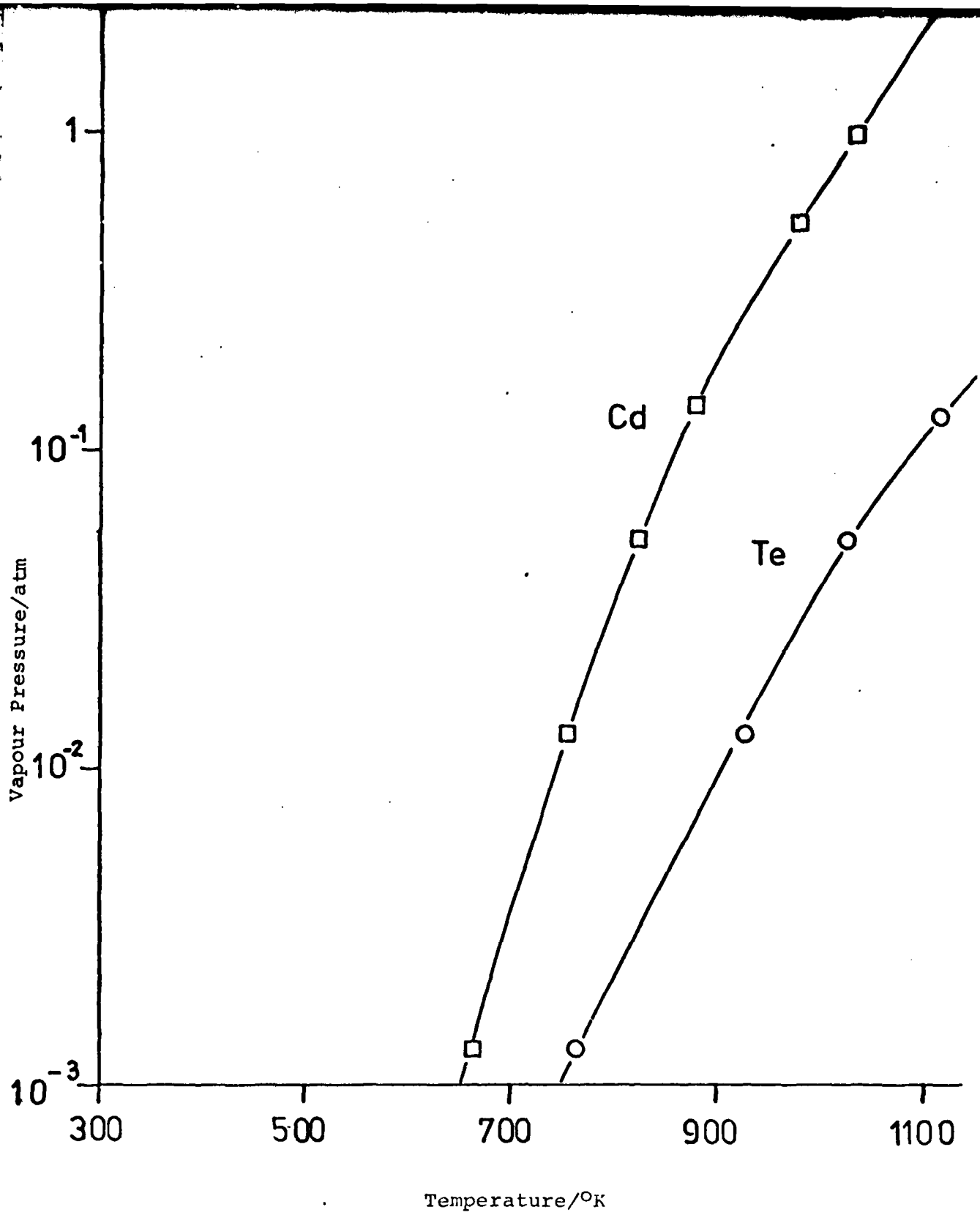

Fig. 2.26. Vapour Pressure Against Temperature Curves for Cadmium and Tellurium (C.R.C. Handbook of Chemistry and Physics, 58th Edition.).

THE CADMIUM TELLURIDE SURFACE

INTRODUCTION

Cadmium Telluride (CdTe), as mentioned earlier, has potentially a large number of applications. The fabrication of devices on CdTe however is fraught with many difficulties, many of which are due to the fact that the physical properties of the solid are poorly understood. A major obstacle is the lack of understanding of the nature of the surface of the material. The properties at the surface of a solid are always different from the bulk properties for the rear in that the surface forms the boundary of the solid and is subjected to physicochemical interaction with the surrounding medium. Single crystals are generally subjected to chemical etching during device fabrication and it is known that many etchants give rise to surface layers which may significantly influence device performance (STRAUSS 1977). As such it is perhaps somewhat surprising that very little effort has been made to characterise these surface layers.

The intention of the series of experiments described in this section has been to try and characterise the surface of CdTe and to look at the affect on the surface that various surface preparations, commonly used, have. A review of the little work already published on this subject is presented. Sample preparations and experimental techniques used are described. The results show what large variations occur in the CdTe surface when different surface preparations are used. The best methods for obtaining clean stoichrometric surfaces are outlined.

3. REVIEW OF PUBLISHED WORK

It appears that the first serious investigation into the nature of the CdTe surface, and its affect on device performance, was that carried out by BODAKOV et al in 1960. They noticed that by clamping a metal onto the surface of n-type CdTe a rectifier could be produced. It was thought that this was due to the creation of a p-type layer at the surface with a p-n transition layer between the outer layer and the bulk n-type material. By leaving p-type crystals exposed to air at room temperatures for a long time they noticed that conducting layers formed at the crystal surface which didn't form a p-n transition region with the bulk material. The formation of surface layers with hole conductivity, due to Cadmium vacancies, was believed to be stimulated, principally, by the oxygen in the air. In 1962 INOUE et al looked at the surface chemistry involved and the resultant surface species evolved when CdTe was subjected to various etchant procedures. They noticed that different etchants produced different surface

layers, and that by choice of etchant one could preferentially remove one species of atom from the surface e.g. HNO_3 or HF would preferentially react with Cd, leaving the surface Tellurium rich. In 1971 ZITTER used surface Raman Spectroscopy to look at tellurium layers so formed on CdTe. He concluded that the Te rich layer on the surface was polycrystalline Tellurium and was generally of the order of 100 atomic layers (~500Å) thick, after 40-50 minutes immersion in a 15% HNO_3:H_2O solution. In 1975 ZITTER and CHAVDA looked at some electrical and photovoltaic properties associated with these layers. They compared the I-V Characteristics of a metal point contact to unetched CdTe and CdTe etched in HNO_3 solution with a resultant thick Tellurium layer. Both were found to be rectifying with a typical diode type curve being seen. The only difference between etched and unetched samples was that the etched samples had a "softer" reverse breakdown. In these samples the contact between the metal point and the surface layer of Te was found to be ohmic so they concluded that the rectification occurred between the Tellurium layer and the CdTe substrate. Photovoltaic effects were also observed which were dependant on the presence of the Te layer e.g. resolved peak at 1.4 eV (0.88μ) is seen in unetched CdTe. As the Te layer grows on the surface this peak reduces and finally disappears. In 1973 TOUSKOVA and KUZEL looked at the rectifying contacts of n-type CdTe. They noted that the fundamental electrical properties of the diodes formed were strongly dependant on the surface treatment of the crystals prior to metal precipitation. Although they didn't carry out an investigation into the reasons for this dependance. 1975 saw the publication of a paper by AKOBIROVA et al on the mechanism of rectification at a metal-CdTe contact. They looked at contacts to n- and p-type material and concluded that the nature of the rectification is independant of the method of metal deposition and the nature of the surface, etched or cleaved in air. They proposed that on oxidation, the CdTe surface reacts to form a Cadmium oxide semiconductor surface of n-type material. This Cd loss from the CdTe should result in formation of a layer rich in Cd vacancies which could act like doubly charged acceptors to increase p-type conductivity i.e. producing a p^+-type layer. Rectification at the metal n-type contact occurs, then, at barriers which appear between the base and the p^+-type layer. In 1977 SIFFERT et al, in an attempt to represss polarisation in CdTe detectors (characterised by a progressive decrease of both pulse amplitude and counting rate with time after the bias voltage is switched on) tried several experiments. One of these involved boiling the etched (presumably in Br_2/CH_3OH) samples for a few minutes in H_2O_2. Using Secondary Ion Mass Spectrometry (SIMS) they showed that an oxidised surface rich in cadmium is produced presumably, the concluded, by forming a semiconductor layer similar to CdO. Also in 1977 PONPON and SIFFERT carried out a SIMS analysis of the surface

region of a CdTe sample etched in a Bromine/Methanol etchant. They noted an increase in the Cadmium concentration at the surface compared to Tellurium. A bromine presence was also noted. In 1978 TAKEBE et al looked at the Schottky Barriers formed by evaporating metals onto vacuum cleaved, air cleaved and etched CdTe surfaces. They reported that barriers produced on vacuum cleaved surfaces were, for certain metals, different to those produced by evaporation of metals onto air cleaved or etched surfaces. They suggested that this change in electrical behaviour was a function of the thickness of the surface layer formed on the crystal, either by exposure to air or etching, and/or the surface state density.

In 1979 HAGE-ALI et al from Strasbourg published work which investigated the surface properties of CdTe and their effect on the detection properties of CdTe detectors. They used the methods of SIMS, Rutherford Back Scattering (RBS) and ellipsometry to look at polished, etched and oxidised surfaces of CdTe. They found that different surface treatments leave the CdTe surface in very different chemical states. For samples etched in Bromine/Methanol RBS measurements showed that the surface of the CdTe was left in a cadmium enriched state with 46% more Cd on the surface than in the case of an air cleaved sample. SIMS measurements on the etched surface revealed the presence of traces of Bromine and CH_n radicals on the surface even after thorough cleaning in methanol. They also noted slight oxidation of the Tellurium, probably as a film of TeO. Oxidised samples produced by boiling etched samples in a H_2O_2:NH_4OH solution showed a different surface to that of the etched crystals. SIMS showed large peaks due to TeO, TeO_2 and TeO_3. The presence of TeO_3 on the surface as an individual species is improbable since below 300°C it decomposes to TeO_2. It is possible though that the TeO_3 radical was sputtered from a heavier molecule e.g. $CdTeO_3$ present on the surface. Looking then at the characteristics of surface barrier detectors produced on these different CdTe surfaces they noticed differences in performance which were hard to explain.

In 1979 EBINA et al published results of an electron loss (low energy) spectroscopic investigation of clean and oxidised surfaces of CdTe. Their findings suggested that adsorbed oxygen preferentially combines with surface Tellurium atoms rather than surface cadmium atoms with the most probable resultant surface species being TeO_2.

3.1 SAMPLE PREPARATION

Samples used were of n-type CdTe, doped with Indium and grown by the method of Fast Vertical Bridgman. Resistivities were typically of the order 10-50 Ω cm. In device fabrication previously reported (see CORNET et al 1970,

TOUSKOVA et al 1972, GABAS et al 1977) several etchants have been used to "prepare" the CdTe surface prior to metal evaporation. It has been reported that these preparations lead to a wide variation in the electrical properties of these devices, so it was therefore decided to investigate the effect that these preparations had on the CdTe surface stoichrometry.

Samples of CdTe were mounted on sample holders made, usually, of Aluminium or stainless steel. The crystals were attached using silver epoxy adhesive. This is an electrically conducting epoxy resin which was 'cured' by heating to 120° for twenty minutes in an evacuated quartz furnace. As this method of attaching crystals to the sample holder involved some surface contamination the process was carried out prior to any of the surface preparations described below. After attachment to the sample holder was effected the crystals were cleaved using a new scalpel blade, to reveal an uncontaminated (110) surface of CdTe on which the surface preparations were carried out.

1. Air Cleave

Preparation of air cleaved surfaces was achieved by cleaving along the (110) plane a CdTe crystal in air with a new scalpel blade. Samples were then left in air for a period of 48 hours prior to insertion into a UHV chamber.

2. Vacuum Cleave

CdTe cleaves readily only along the (110) plane. This fact was utilised in the design of a cleaver for use in UHV systems at pressures in the region of 10^{-10} torr. Crystals were mounted such that the (110) faces were parallel to the plane of the crystal holder. After a vacuum of 10^{-10} torr was attained, crystals were manoevered inside the UHV system until a position was reached where the crystal was under the scalpel blade (spot welded to the cleaver) and the plane of the sample holder, and hence the (110) plane of the CdTe sample, was parallel with the scalpel blade. The crystal was then cleaved by giving a sharp knock to the cleaver. Good vacuum cleaves were obtained by this method.

3. Bromine-Methanol (Br_2-MeOH)

Samples were cleaved in air and immediately immersed in a 1:1 solution of Bromine:Methanol for 30 seconds. Samples were then removed and washed several times in methanol, including an ultra sonic bath rinse, before insertion into the vacuum chamber.

4. Potassium Bichromate ($K_2Cr_2O_7$)

Samples were cleaved in air and immediately immersed in solution 1 for 30 seconds, taken out and immersed for

30 seconds in Solution 2. Solution 1 was made up of 10 cm^3 HNO_3, 20 cms H_2O and 4 gms $K_2Cr_2O_7$. Solution 2 was made up of 10 cms^3 of Solution 1 + 5 mg $AgNO_3$. Samples were rinsed thoroughly in deionised, distilled water.

5. Nitric Acid (HNO_3)

Samples were cleaved in air and immediately immersed in concentrated nitric acid for 30 seconds. Samples were then removed and vigorously rinsed (in ultra sonic bath) in deionised distilled water.

6. Ethylene Diaminetetra Acetic Acid (EDTA)

Samples were cleaved in air and immediately immersed in a molar solution of EDTA for 30 seconds, then removed and washed in deionised, distilled water.

7. Hot Sodium Cyanide (NaCN)

Samples were cleaved in air and immediately immersed in a boiling solution of molar NaCN for twenty minutes, then washed in deionised, distilled water several times.

8. PBr_2

After cleaving in air samples were immersed in P solution for 30 seconds, followed by 60 seconds in PBr_2 solution, then washed several times in deionised distilled water. P solution was 10 cm^3 conc. HNO_3, 10 cm^3 conc. HCl, 5 cm^3 H_2O. PBr_2 solution was 10 cm^3 of solution P and 10 mg Br_2.

3.2 EXPERIMENTAL TECHNIQUES

It was mentioned before, briefly, that the outer atomic layers of a solid can be looked upon as a phase with properties different from those of both the bulk material and the gas phase around it. Traditionally non-destructive testing of this surface region has been very difficult but in recent years techniques have been developed which investigate these layers. In most of the techniques electrons are involved either through being bombarded against a surface or through being generated and emitted from within the atoms of the surface layers on the addition of some stress, in the guise of electrons, radiation etc., to the surface. The techniques of this type which were used here were Auger electron spectroscopy (AES), Photoelectron Spectroscopy (PES), Low Energy Electron Spectroscopy (LEED) and are described below, along with the different UHV systems in which they were housed.

Auger Electron Spectroscopy (AES)

One of the most popular and convenient methods of identifying the chemical nature of surface atoms is AES. Basically the technique consists of bombardment of the surface with a beam of electrons, with energy up to 5 KeV and analysis

of the electrons ejected from the surface. The process is illustrated in fig.3.1. The incident electron excites an electron from a core level (k). An electron from a higher lying level such as the valence band is then able to fill the core hole thus releasing energy. This energy is captured by yet another electron which, if the energy gained is sufficient may be emitted from the solid as an auger electron. The energies associated with the emitted Auger electrons are characteristic of the emitting atoms and for a given atom always occur at nearly the same kinetic energy regardless of the incident beam energy. In AES the exact energy of the emitted electron is complicated by many processes such as the fact that the Auger electron is emitted from an ion rather than a neutral atom. As the process is not a direct one Auger lines are therefore quite broad. Subtle changes in binding energies due to chemical effects may sometimes be observed. The Auger features in the energy distribution N(E) are usually very small in amplitude consequently, the spectra are differentiated electronically and dN(E)/d(E) is displayed. Electron beam excitation makes possible the use of a finely focussed high current spot, allowing rapid chemical identification and high spatial resolution. The vast range of applications of AES means that the technique has been reviewed extensively elsewhere and the reader is directed to these sources for a comprehensive treatise on the theory of AES. i.e. RIVIERE 1972, CHANG 1974, GALLON and MATHEW 1972.

Photoelectron Spectroscopy (PES)

Photoelectron spectroscopy is essentially a simple process in which a photon of energy $h\nu$ absorbed by the solid excites an electron to an energy sufficiently high to enable it to escape over the work function barrier, W, at the surface. The kinetic energy, E_k, of an emitted electron is then measured and from this the energy level E_i from which an electron originated may be calculated. Approximately

$$E_k = h\nu - (E_i + W)$$

where E_i is referred to the Fermi level. This equation is only approximate since it assumes that if an electron is removed from a system containing N electrons then the energies associated with the remaining (N-1) electrons remains unaltered. Obviously these electrons may relax lowering the energy of the system and this relaxation energy will be carried away by the excited photoelectron. In addition if one considers the case where one has a localised level, such as in an adsorbed atom on the surface of a solid, then, if a hole is created in this level, by emission of an electron, the hole will have the appearance of a positive charge and will consequently attract electrons from the solid towards it. This charge will screen the hole. Thus Binding energies of the levels associated with the adsorbate are lowered with

respect to their values in isolated atoms.

The experimenter may measure the total number of photoelectrons emitted i.e. the yield, and can use the photon energy as a variable. Alternatively one can measure the way the emitted electrons are distributed in energy i.e. N(E) is measured as a function of emitted kinetic energy. Traditionally PES has been divided into two regimes depending on the energy of the exciting photon. Ultra violet photoelectron spectroscopy (UPS) covers the range up to $h\nu \approx 50eV$, the photon sources usually being inert gas discharge lamps. The second regime involves X-ray sources, the photoelectrons in this case being excited by Aluminium Kα radiation (1486eV) or Magnesium Kα radiation (1236eV) typically. This method is normally referred to as X-ray photoelectron Spectroscopy (XPS) and unless an X-ray monochromator is used the large linewidth of the X-rays leads to rather poor energy resolution. However many core levels are accessible and the technique has found widespread application for surface chemical analysis, since the core levels act as a fingerprint for emitting atoms. Information on the bonding of atoms to neighbouring atoms may be obtained. The exact binding energies of the core levels are sensitive to the way the outermost electrons are distributed and small "chemical shifts" of the binding energies of a given level may often be observed for the same atom in different solids or molecules. These shifts yield information about chemical bonding and are one of the main reasons for the success in surface chemistry of ESCA (Electron Spectroscopy for Chemical Analysis). Auger electrons are also observed in XPS spectra.

In general then XPS is used to investigate the chemistry of the surface and UPS to study the electronic structure associated with the outer layers of solids. For a detailed account of the theory of UPS the reader is directed to a review of UPS given by FEUERBACHER and WILLIS (1976). A review of ESCA was presented by BRUNDLE in 1974 and 1972. The texts listed below are also recommended.

'Electron Spectroscopy, Theory Techniques and Application', edited by Brundle and Baker, 1977. 'Photoemission in Solids', edited by Cardona and Ley, 1978. 'Handbook of X-ray and Ultra-violet photoelectron Spectroscopy', edited by D. Briggs, 1977.

Low Ener Electron Diffraction (LEED)

If an electron beam of well defined energy Ep is incident on a solid then an energy distribution of scattered electrons will be of the form shown in fig.3.1a

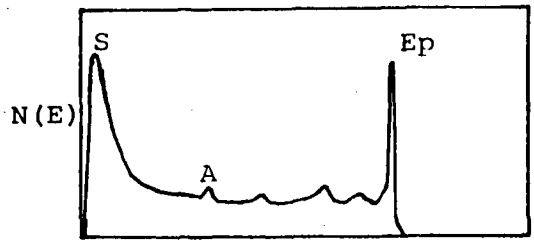

Fig.3.1a

(S : Secondary electrons; A : Auger electrons; Ep : Elastically scattered electrons)

A group of electrons are scattered elastically with energy Ep. From the distribution of these elastically scattered electrons in space it is possible to derive information about the crystallography of the solid surface, providing it is ordered. This is the method of LEED. This method is comparable in many ways to X-ray diffraction of a bulk material. In a crystal the regular arrangement of atoms represents a grating to the electron, and diffracted beams appear at angles which depend on the interatomic spacings. Unlike X-rays, though, electrons, with a wavelength of ~1Å, can penetrate only a few atomic layers without undergoing inelastic collisions. LEED is therefore specific to the surface of a solid. The observed diffraction pattern is thus determined by the two dimensional periodicity of the surface plane. This method is therefore an important source of data on the structure of surface layers. LEED has been reviewed extensively before and the reader is directed to the following references for a fuller discussion of LEED. i.e. PENDRY 1974; MITCHELL 1973.

Electron Beam Effects

For some time it has been thought possible that subjecting the surface of CdTe to an electron beam for any length of time had the effect of disordering the surface. Very few reports on CdTe have appeared where electron beams have been used to probe the surface. EBINA in 1979 noted that during oxidation of the CdTe surface, oxygen uptake was increased drastically when the surface was irradiated with an electron beam. It was decided, therefore, to carry out our own investigations on any such phenomena so as to gain a yardstick as to how much emphasis one should place on the results of electron induced effects on CdTe.

We used two techniques to monitor the electron beam effect:- AES and UPS. The experiments were carried out in UHV system 1 and UHV system 2.

In the Auger experiments the primary electron beam was left on the sample for a period of time. During this time Auger spectra were recorded and examined for changes. This

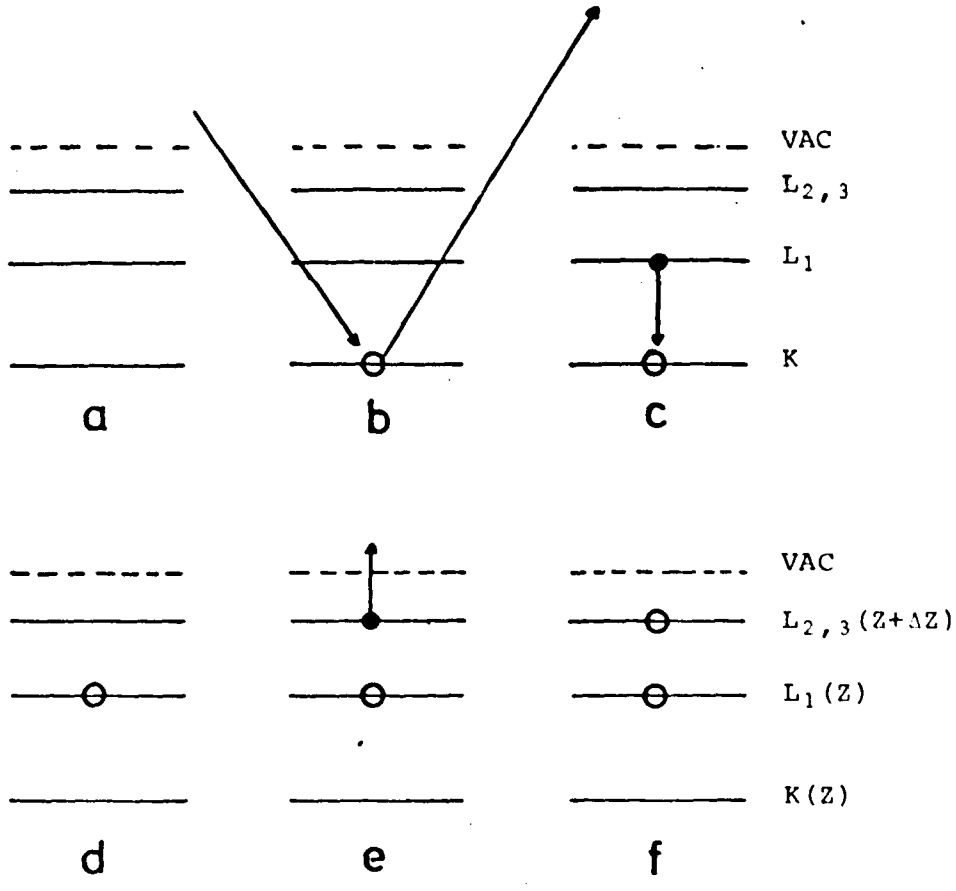

FIG.3.1 Auger Process for an isolated atom. The Transition is labelled $KL_1\ L_{2,3}$.

a. Neutral atom, atomic number Z.
b. Ionisation of an inner shell by the primary electron.
c. Transition of electron from level L_1 to fill hole in level K.
d. The approximate situation after redistribution of the Coulombic Field.
e. Ejection of an auger electron with energy $\approx[K(Z)-L_1(Z)-L_{2,3}(Z+\Delta Z)]$.
f. Doubly ionised final state.

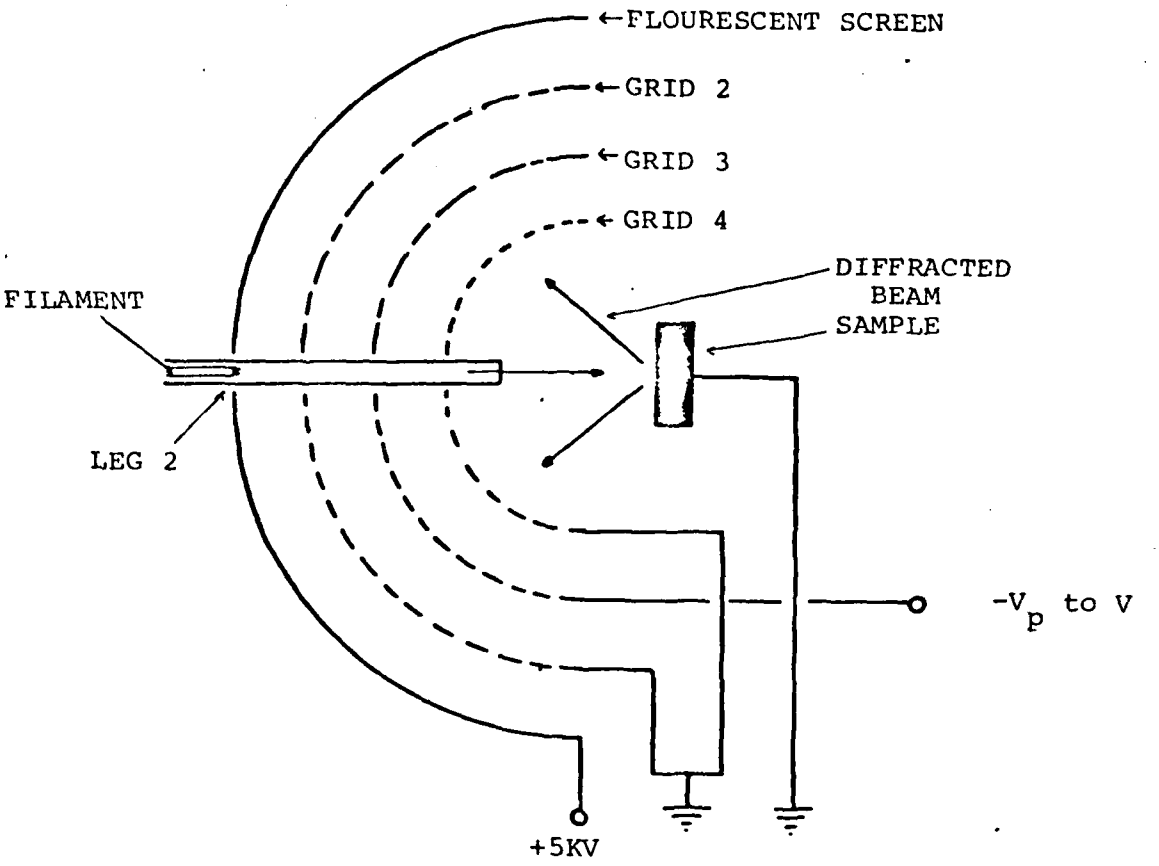

FIG.3.2 LEED optics.

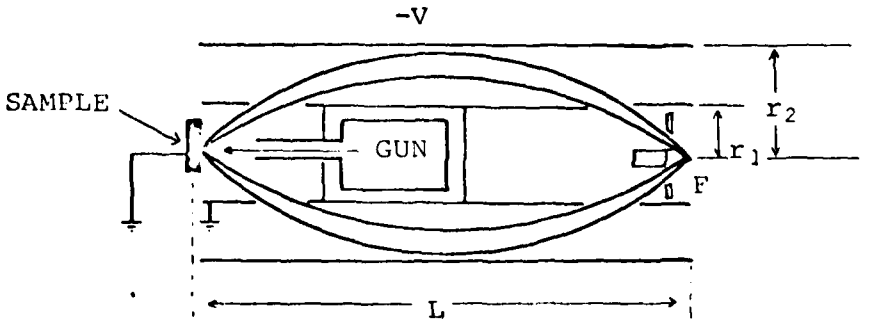

FIG.3.3 Mode of Operation of a Cylindrical Mirror Analyser as used in Auger Electron Spectroscopy with integral electron gun.

experiment was carried out on both vacuum cleaved and air cleaved samples.

For UPS measurements a sample was cleaved in vacuum, of ~10^{-9} torr, and immediately an Electron Density Curve (EDC) was recorded very accurately. An electron beam was then made to impinge on the vacuum cleaved surface and EDC's recorded at various time intervals. The spectra were examined and various new peaks, peak shifts etc. noted. This experiment was not carried out on air cleaved CdTe as the EDC for air cleaved CdTe does not reveal much structure.

Vacuum Systems

System 1

This Ultra High Vacuum (UHV) system contained the techniques of AES, LEED and an ion gun to facilitate depth profiling. Also included were facilities for metal evaporations. The main chamber was a ten inch diameter stainless steel vessel pumped by a 140 l. s^{-1} getter ion pump with bakeable magnets and magnetic shielding. Evacuation from atmosphere was achieved using two zeolite based sorption pumps. The system was surrounded by bakeout ovens which, after bakeout at 250°C, allowed vacuums of up to 10^{-10} torr, as measured by an ion gauge, to be obtained. The Chamber was connected through a right angle bend to the ion pump, which was positioned well away from the LEED and AES facilities. These were both mounted on 8" diameter side ports. A viewing window was positioned on an 8" port opposite the LEED optics. A UHV cleaver was mounted on one of the 2¾" side ports. On the top 6" diameter port was mounted a sample manipulator, the VG Ltd. universal manipulator - *UMD1*, which allowed for movement in the three cartesian axes as well as rotation about the vertical and tilt. Samples were mounted and connected to a carousel on the UMD1 so that they could easily be moved to different ports in the same horizontal plane. An ion gun was attached to a 2¾" side port and arrangement was made so that the focus of the ion gun beam was at the Auger sample position, so that etching and AES could be carried out without moving the sample. Metal evaporators were made and mounted in suitable side ports. Controlled gas inlet facilities were obtained by use of a bakeable leak valve attached to the relevant gas bottle (O_2, Cl_2 etc...) situated below the bakeout ovens.

Leed Optics

A standard '3' grid retarding field analyser with an integral electron gun was used. The filament of the electron gun was made of Rhenium with lanthium hexaboride and was capable of producing a fine beam of monoenergetic electrons with focus and energy variable within the range 1-5 KeV. Three concentric stainless steel mesh grids with an Aluminium

screen coated with fine grain phosphorescent material, together with the electron gun, were mounted on an eight inch flange and attached to one of the eight inch side ports of the chamber. The system operated with grid G_4 and the sample at earth potential to provide a field free space for incident and back scattered electrons (see Fig.3.2). Grid G_3 was placed at a retarding potential in order to separate elastically scattered electrons from those that had suffered energy losses due to interactions with the sample. Grids G_2 and G_4 were strapped together to shield G_3 from field penetration from the screen. The screen was at a potential of 5 Kv so that elastically scattered electrons that passed the grid system were accelerated onto the phosphors, which then fluoresced to produce an optical display. The LEED pattern was observed through a 6" viewing window and could be recorded on film. Two small magnets placed outside the system near the LEED optics directed the electron beam normal to the sample surface. The sample earthing also prevented any sample charging.

Auger Electron Spectrometer

The Auger electron spectrometer used in this system was a Cylindrical Mirror Analyser (C.M.A.). This is a dispersive analyser where only electrons within a narrow energy range reach the detector. It has a good signal to norse ratio with a very rapid scan time (>1000 eV s^{-1}) and a resolving power of ~200. The resolving power is very dependant on sample position and on minimising the spot size of the exciting source. The CMA consists of two concentric electrodes and an electron multiplier surrounded by magnetic shielding to neutralise the earths magnetic field or other magnetic influences. The CMA had an integral electron gun which produced primary electrons with which to bombard the sample. Beam currents up to 100 μA with beam energies of 200-3000 eV and a beam size of 20 μM diameter were available. X and Y deflection plates provided control for fine beam adjustment to maximise resolution and to enable scans to be taken over small areas. Complete electrostatic shielding was provided so that potentials applied to the gun did not affect the trajectories of electrons being analysed. The inner cylindrical electrode had 'gridded' apertures at the ends of the cylinder. Secondary electrons from the sample pass through the inner cylinder entrance aperture towards the outer cylinder. A negative potential is applied to the outer cylinder and electrons of selected energy range are deflected through the exit aperture at the other end of the inner cylinder. Electrons are then focussed near the analyser axis and pass through a thin annular exit aperture to give precise definition of their energy. A 15 stage Be-Cu electron multiplier detected and amplified the secondary electrons that passed through the exit aperture. This amplified signal was sent to the control unit. Fig.3.3 shows diagramatically

the operation of the CMA, r_1 and r_2 are the radii of the inner and outer cylinders. Electrons were emitted with kinetic energy E from sample S on the axis of the analyser, positioned so that emission angle = $42^{\circ}18^{1}$. Focussing of the electrons occurred at point F, so that

$$\frac{E}{eV} = 1.31 \ln \frac{r_1}{r_2}$$

where r is voltage between cylinders. Sweeping the retarding voltage on the outer cylinder and measuring the resultant current, proportional to energy distribution N(E) x Energy E, the energy distribution curve of electrons originating from the sample surface if generated. As the Auger signal in the N(E) distribution is very weak compared to background noise, the CMA is operated in such a mode as to record an output proportional to dN(E)/dE. This is done using a modulation technique i.e. a small modulation of between 0.5v and 20v peak to peak at a frequency of 17 K H_Z is superimposed on the deflection voltage V. The A.C. component of the output current was passed to a lock-in amplifier where it was compared to a reference signal of 17 K H_Z. All components of frequency other than that of 17 K H_Z were rejected. A phase shifter was required so that the phases of the analyser and reference signals were kept in phase. The output from the lock-in amplifier, a d.c. voltage, was applied to the Y axis of an X-Y recorder. A voltage proportional to the retarding voltage on the deflection electrode was applied to the X axis.

If the modulation superimposed on the retarding voltage V is of the form $A\sin\omega t$ then current, as a function of V, can be expanded as a Taylor Series.

$$I(V+A\sin\omega T) = I(V)+I'(V)A\sin\omega T+\frac{I^{11}(V)}{2!}A^2\sin^2\omega T$$

$$+\frac{I^{111}(V)}{3!}A^3\sin^3\omega T+\cdots\cdots\cdots$$

subscripts ^{1}, ^{11}, ^{111} ... represent the first, second, third ... differentials. Upon rearrangement algebraically and trigonometrically then

$$I(V+A\sin\omega T) = I(V)+[\frac{A^2}{4}I^{11}(V)+\frac{A^4}{64}I^{1V}(V)+\cdots\cdot]$$

$$+[AI^{1}(V)+\frac{A^3}{8}I^{111}(V)+\cdots\cdot\cdot]\sin\omega T$$

$$+[\frac{A^2}{4}I^{11}(V)+\frac{A^4}{48}I^{1V}(V)+\cdots\cdot]\cos 2\omega T$$

$$+\cdots\cdot\cdot$$

collection of the first harmonic gives

$$[AI^{1}(V)+\frac{A^3}{8}I^{111}(V)+\cdot\cdot]\delta m\omega T$$

where amplitude is proportional to $I^1(V)$, neglecting A^3 and higher powers. The current from the CMA is given by

$$I_{CMA} = C_{CMA}\ E\ N(E)$$

where C_{CMA} is a constant of the analyser. dE is proportional to dV, hence the first harmonic is proportional to dI_{CMA}/dE

$$\frac{dI_{CMA}}{dE} = C\left(E\frac{dN(E)}{dE}+N(E)\right) = \frac{dN(E)^*}{dE}$$

This distribution qualitatively exhibits the same structure as dN(E)/dE itself. It is enhanced at higher energies with respect to dN(E)/dE because of the factor E and shows a higher background at lower energies because of the additive N(E). The Spectrum $dN(E)^*/dE$ was directly plotted by the CMA.

Fig.3.4 is a block diagram of the CMA control units which enable dN(E)/dE to be recorded. The CMA analyser control unit was the 981-2601 model supplied by VARIAN which allowed auger electron analysis in the range 0-3 KeV with sweep widths of 0, 50, 100, 200, 500, 1000, 2000 eV, with a vernier control and a centre of sweep energy from 0-2 KeV. Sweeprates were variable and rates of 0.05-5.0 sec. $sweep^{-1}$ and 0.5-50.0 min. $sweep^{-1}$ were available. Modulations of 0.5, 1.0, 2.0, 5.0, 10.0 and 20.0 volts peak to peak were possible at an oscillator frequency of 17 KH_z. The reference and modulation signal were supplied by a HEWLETT PACKARD 200 CDR wide range oscillator, and a BROOKDEAL 9501 lock-in amplifier provided amplification and phase sensitive detection. Auger curves were plotted on a HEWLETT PACKARD 7035B X-Y recorder, and for display of the elastic peak an oscilloscope with X-Y deflection plates and high gain was used.

Sample alignment was obtained by first of all observing the light spot from the gun filament, through a side port, and positioning the sample so that the light spot was on its surface. To observe the electron beam position relative to the light spot and also to focus the electron beam to a minimum spot size a fluorescent screen was used. By displaying the elastic peak on an oscilloscope the sample could be adjusted to obtain the optimum elastic peak indicating the best position for auger spectroscopy. To obtain maximum sensitivity the amplitude of the modulating signal was usually kept below 5 volts peak to peak.

Depth Profiling Facility

This facility consisted of an Ion gun mounted on a 2¾" side port and arranged so that the axis of the ion gun was coincident with the axis of the CMA at the sample position, and at an angle of 80° to the CMA axis. The Ion gun was a cold cathode source with ion extraction, acceleration and focussing.

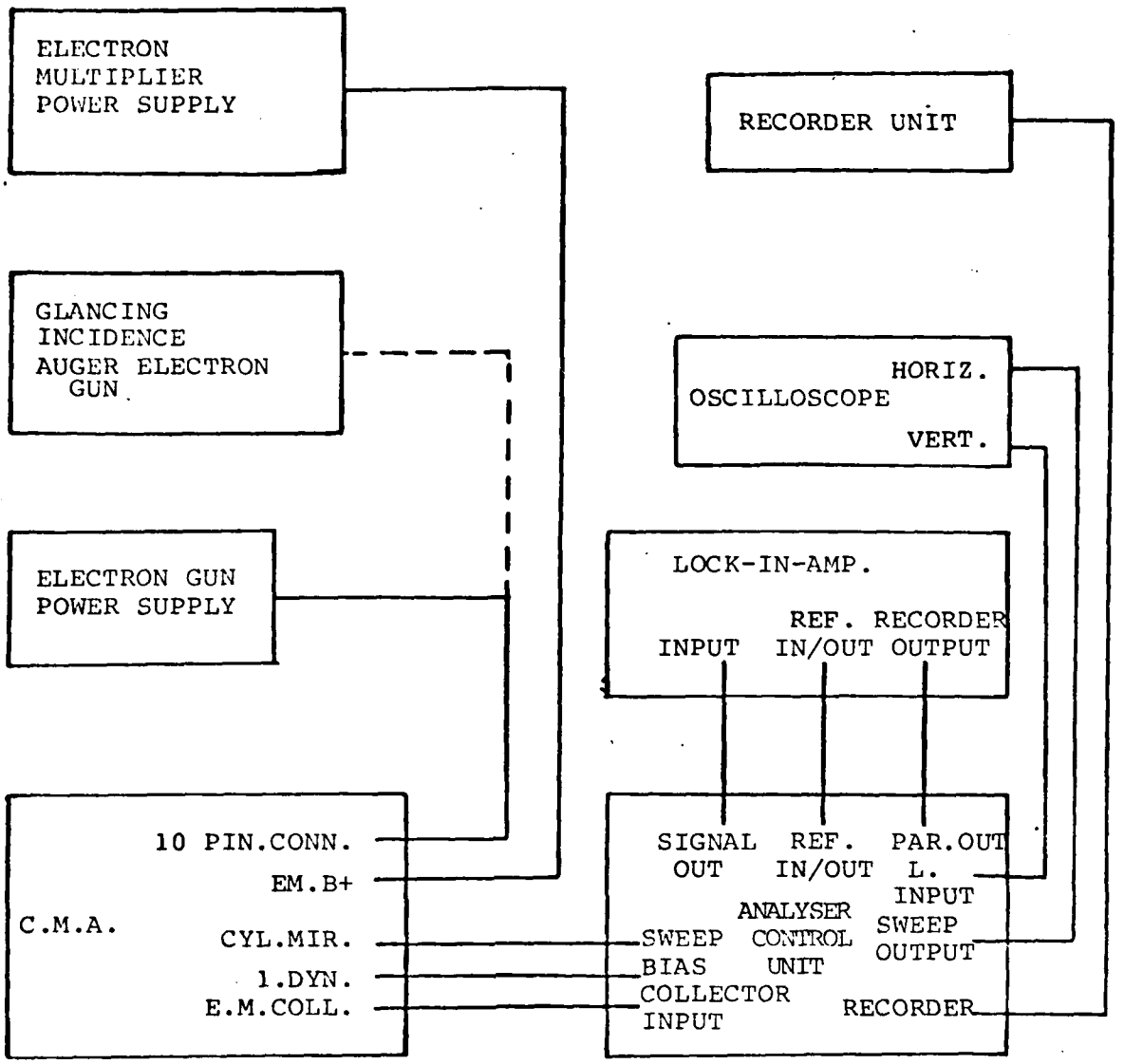

FIG.3.4 CONTROL SET UP as used in our Auger Electron Spectrometers.

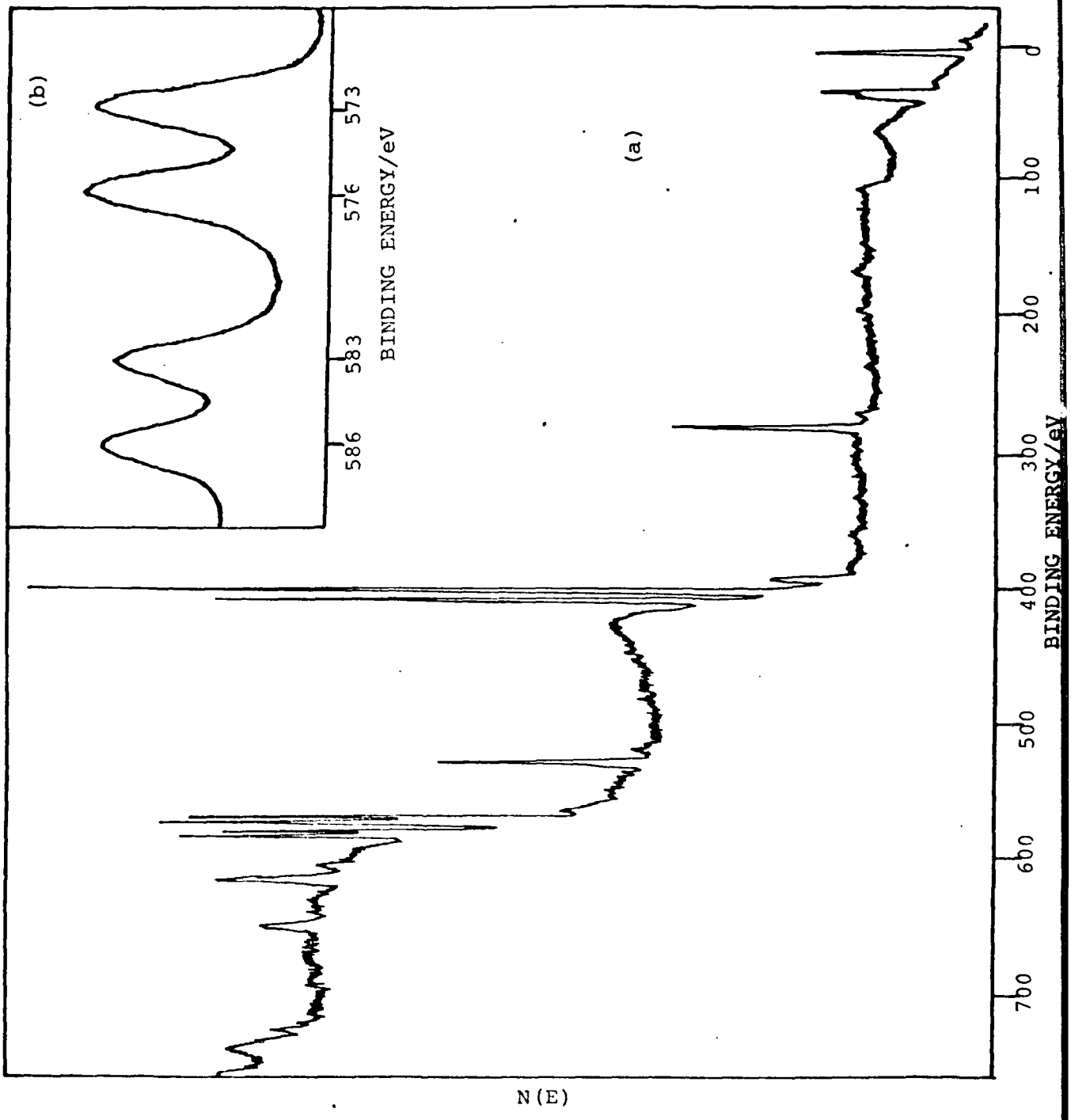

FIG.3.5 a. XPS spectrum of Air Cleaved CdTe.
b. XPS spectrum of the Te_{3d} region showing splitting of the $3d_{5/2}$ and $3d_{3/2}$ emissions due to the presence of TeO_2.

The ion beam energy was variable from 0-10 KeV with a beam diameter variable from 2-20 mm controlled by the potential applied to the focus electrode. Pure Argon was admitted to the ion gun at a pressure of 5×10^{-6} torr, controlled by a UHV leak valve. At an operating pressure of 5×10^{-6} torr target currents of 9×10^{-5} amps at 2 KeV to 3×10^{-4} amps at 10 KeV were obtained, measured by a microammeter on the gun control unit.

Samples were mounted so that the surface normal of the sample made an angle of 10° with the CMA axis. This meant that the Argon Ion beam bombarded the sample surface at a glancing angle of 20°. The sample was electrically insulated from the sample holder, but was electrically connected to a lead through at the top of the chamber via a loose insulated wire. This enabled ion current at the sample to be measured. The sample surface could be viewed while etching was in progress via a glass port beside the sample. To prevent the ion gun magnet interferring with the CMA resolution a μ-metal shield was positional round the outside of the CMA. As Argon ions were capable of producing Auger and other secondary electrons the ion gun was switched off while Auger spectra were recorded. One of the drawbacks of this UHV system was that the ion pump could not be isolated from the UHV system so Argon pressures of $>5 \times 10^{-6}$ torr could not be used. Therefore to obtain sufficient etch rates, high ion energies had to be used i.e. >5 KeV.

Sample Holders and Crystal Cleaver

Samples were mounted on special aluminium plates, which could be attached to the carousel of the UMDI manipulator. The plates were so designed that when attached to the manipulator they were insulated electrically from it. This was done using machined ceramic holders. Electrical contact was then made to the plate using an insulated wire attached to an insulated lead through in the flange which contained the manipulator. Samples were attached to the plates using a silver epoxy resin which was cured by heating to $120^{\circ}C$ for twenty minutes in an evacuated quartz furnace. The Cleaver consisted of lever system attached to a bellows attached to one of the 2¾" side ports. It was constructed such that whenever a sharp knock was given to the bellows, an upper 'jaw' was made to close against a stationary lower 'anvil'. To this upper jaw was attached, either by screws or by spotwelds, a scalpel blade. This blade was replaced frequently ensuring a good cutting surface all the time. Samples were mounted such that the 110 face was parallel to the sample plate. By manoeuvring the sample to the cleaver and ensuring that the scalpel blade and sample plate were parallel then samples could be cleaved fairly easily and successfully.

System 2

The second ultra high vacuum apparatus used consisted of a stainless steel cylindrical chamber constructed for the purpose of studying angle resolved photoemission. The Chamber was pumped by an EDWARDS E04 oil diffusion pump backed by an Edwards Ed100 rotary pump. A VG Ltd. liquid nitrogen cooled vapour trap was used. Evacuation from atmosphere was achieved using a CENCO HYVAC 14 rotary pump connected to a 2¾" diameter port on the bottom of the chamber. Bakeout ovens were constructed to allow the whole UHV chamber etc. to be baked to 250°C giving, when cold, a pressure of 10^{-10} torr when measured by a nude ion gauge. The diffusion pump was connected directly, via the liquid nitrogen trap, to the chamber via one of the eight inch side ports. On an opposite 8" port a viewing window was positioned and on another 8" port was placed an Ultra violet Helium discharge lamp (see later). An X-ray source (twin anode - Aluminium and Magnesium) was mounted on a 2¾" side port in the same horizontal plane as the UV lamp. The photon beams from both these sources were made to impinge on the sample at its experimental position on the chamber central axis. On the top 6" port was mounted a VG Ltd. High Precision specimen translator, the HPT1. This allowed for movement of the sample in the three cartesian axes, as well as rotation through ±180° about an axis normal to the surface of the sample. A UHV cleaver was mounted on another 2¾" port which enabled crystals to be successfully cleaved on UHV. A hemispherical analyser was mounted on a platform and positioned on top of a cylindrical support, rigidly attached to a 6" diameter flange, with the axis of the cylinder in alignment with a 2¾" port at the centre of the flange. This 6" flange, which contained two other 2¾" ports in addition to the one mentioned above, was attached to the bottom 6" port of the UHV chamber. A rotary drive mechanism, mounted on the 2¾" port at the centre of the flange and connected to the platform through the centre of the cylindrical support, allowed the platform, and hence the analyser, to be rotated through 180° about the axis of the chamber. This arrangement enabled the analyser to sample electrons emitted from a sample positioned at the centre axis of the chamber. Electrical connections were made through a multi-lead through attached to one of the other 2¾" ports on the bottom 6" flange, and attached to the analyser by insulated leads inside the cylindrical support.

Facilities for gas admission through a bakeable UHV needle valve, metal evaporation from metal filaments and ion depth profiling were all available from various sideports.

Electron Energy Analyser

A VG Ltd. 150" hemispherical analyser is used for collection and energy analysis of emitted photoelectrons. The

analyser acts as a narrow pass filter letting through only electrons within a narrow energy range $E + \Delta E_0$. It consists of two concentric hemispheres, with an entrance hole 1 mm in diameter in the Hertzog plate. Detection is thus confined to a small angle of emission with resulting angular resolution of $\sim 2^{\circ}$. The pass energy of the analyser, E_0, is determined by the potential difference between the hemispheres and the radii of the two hemispheres (R_1 and R_2) i.e.

$$\Delta V = 2V_0 \, R_0 \frac{(R_2 - R_1)}{R_1 R_2}$$

and

$$E_0 = eV_0$$

and

$$R_0 = (R_1 + R_2)/2$$

the energy resolution of the analyser is given by $E_0/\Delta E_0$ where ΔE_0 is the full width at half maximum of the energy distribution after analysis of a monochromatic electron beam. This ratio is constant for the analyser ΔE_0 will decrease linearly with E_0. Energy resolution is greatest then at low pass energies and the analyser in use in this system had an energy resolution of 0.1 eV at a pass energy of 20 eV.

Photoelectrons emitted from the sample are retarded, or accelerated, to pass energy, E_0, by applying a potential difference between the sample and the Hertzogplate. If the kinetic energy of the photoelectron with respect to the fermi level, E_F, is E and the retarding voltage is R then

$$E = R + E_0 + W$$

W is the work function of the analyser. The binding energy of the photoelectron is then given by the Source energy minus kinetic energy. In UPS the source energy, for HeI, is 21.2 eV and for XPS source energies of 1486.6 eV and 1253.6 eV are produced by Aluminium Kα and Magnesium Kα respectively. A pass energy of 20 eV was used for UPS, while for XPS passenergies of 2, 5, 10, 20 and 50 were available from a VG Ltd., Spectrometer control unit which applied the potential difference between the hemispheres.

In XPS electrons were accelerated or retarded by a voltage from a variable power supply of 0-1.5 KeV which allowed the kinetic energy starting position of the scan to be selected. This supply was in series with a ramp generator which could be switched to give kinetic energy scan ranges of 10, 30, 100, 300 or 1000 eV in times variable from 30-30,000 seconds. The photoelectrons which passed through the analyser were collected and amplified by a channel electron

multiplier. The output pulses were fed through a d.c. isolating capacitor to an amplifier and ratemeter. The scan was controlled by the ramp generator incorporated in the VG Spectrometer control unit, and the EDC's were plotted directly by a BRYANS X-Y chart recorder.

In UPS the scan giving rise to the energy distribution curve (EDC) is controlled by a NICOLET Computer, and signal averaging is obtained by collecting the EDC's for a given number of scans, displayed on a TEKTRONICS display unit, and then recording on paper using a BRYANS X-Y chart recorder.

UV and X-ray Photon Sources

The Ultra Violet source used was a VG Ltd. model 22-101 gas discharge lamp in which the discharge was confined by a small quartz capillary tube. Helium gas, which passed through a liquid nitrogen cooled sorption gas purifier containing 5Å molecular sieve, was admitted to the lamp via a bakeable UHV leak valve, and discharge at ~0.5 torr to give HeI radiation at 21.2 eV energy with high photon yield. Pressure in the UHV chamber was kept in the low 10^{-9} torr range by two stage differential pumping provided by an Edwards ED50 rotary pump and an Edwards EO_2 oil diffusion pump. A UV lamp power supply provided 5 KV for starting the discharge and a 1 KV current stabilised supply variable from 20-50 mA was used to run the lamp. A Bellows unit with three studs on the lamp allowed the lamp to be aligned for maximum signal. Spot size of the photon beam on the sample surface was ~3 mm diameter.

The X-ray photon source was a VG Ltd MK II X-ray tube which had a twin anode, magnesium on one side and Aluminium on the other. This gave the facility of two independent X-ray lines - Mg K_α at 1253.6 eV and Al K_α at 1486.6 eV. The X-ray assembly was mounted on a 2¾" flange and a bellows arrangement allowed the source to be moved in the direction of the sample to increase intensity of the photon beam at the sample surface. The photon spot size on the sample was ~5 mm in diameter.

UHV System 3

The third UHV system available to us was a commercially available ESCA III spectrometer produced by VG Ltd. This was coupled to a VG data system 3000 data acquisition system. This provides automatic control of the retard and analyser voltages on the ESCA III spectrometer control of the XY plotter and storage of spectra on magnetic tape. The 3000 series incorporated the following hardware:-

1. A DIGITAL EQUIPMENT CORP. (DEC) PDP8e computer with 12,288 words of core memory, with a double TD8E magnetic tape.
2. A VT8E integrated graphic/alpha numeric visual display.

AD-A086 991 NEW UNIV OF ULSTER COLERAINE (NORTHERN IRELAND) SCH--ETC F/G 20/2
GROWTH AND APPLICATION OF CADMIUM TELLURIDE.(U)
JAN 80 R H WILLIAMS, M H PATTERSON DA-ERO-77-G-026

UNCLASSIFIED NL

2 2

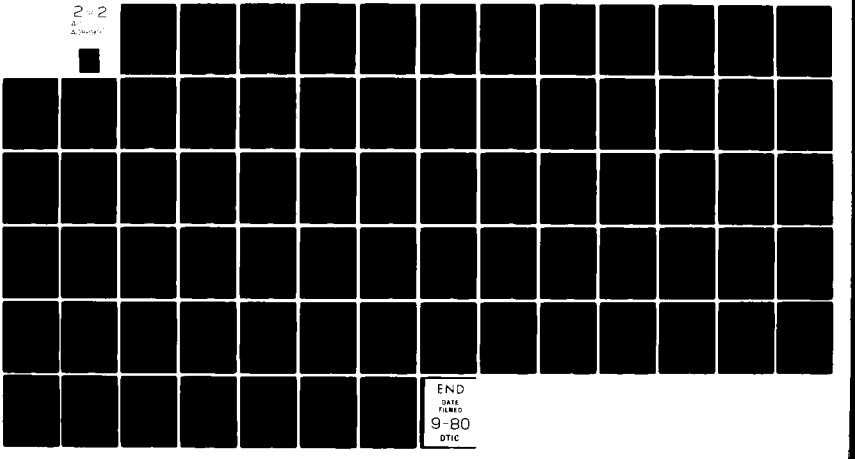

END
DATE FILMED
9-80
DTIC

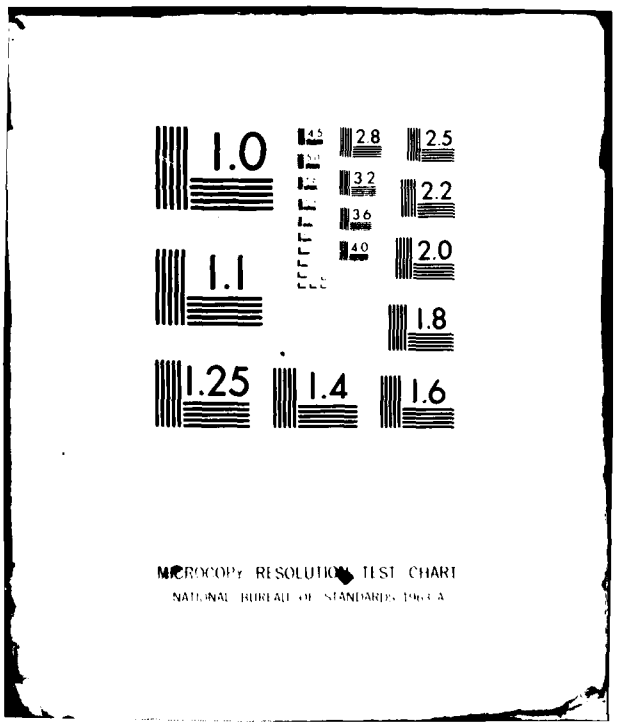
1.0
1.1
1.25
1.4
1.6
1.8
2.0
2.2
2.5
2.8
3.2
3.6
4.0
MICROCOPY RESOLUTION TEST CHART
NATIONAL BUREAU OF STANDARDS 1963-A

3. An ASR33 teletypewriter.

4. A VG data systems Ltd designed interface to provide connection between the analogue circuitry of the electron spectrometer and the digital electronics of the computer.

5. A VG Computer Spectrometer control unit.

Among the facilities afforded by this system were:- acquisition and averaging of data; data presentation on Binding energy or kinetic energy axes; quadratic smoothing of data; deconvolution of multiple peaks by Fourier transform; peak synthesis; background correction and spectral subtraction; spectra comparisons; peak position determinations; differentiation or integration of spectra.

The spectrometer itself was basically very similar in nature to UHV system 2, although there were several mechanical differences. The UHV chamber consisted of two parts - an analyser chamber which was continually evacuated to UHV and a preparation chamber. The preparation chamber was let up to atmosphere to admit new samples. It was possible to seal off the analyser chamber from the prep chamber during this operation. Evacuation of the prep chamber from atmospheric pressure was done by an Edwards ED100 rotary pump and evacuation to UHV achieved using an Edwards E04 oil diffusion pump backed by an Edwards ED100 rotary pump. The analyser chamber was also evacuated by an Edwards E04 oil diffusion pump backed by an Edwards ED100 rotary pump. In addition a VG Ion pump was used on the analyser chamber. After bakeout vacuums of $\sim 10^{-10}$ torr were available. The manual spectrometer control unit, Helium gas discharge lamps, X-ray sources etc. were all more or less as those described in UHV system 2. Facilities for metal evaporation, Argon Ion etching were also available. One extra facility available was that incorporated into the sample holder was aresistance heater and thermocouple. This allowed us to heat samples at temperatures of up to $600^{\circ}C$ in Vacuum. The sample probe also contained channels for passing liquid nitrogen through so that if needed the samples could be cooled in vacuum to sub-zero temperatures.

One of the unfortunate drawbacks of this system was that only non-angle resolved photoemission could be carried out in the system. Any angle resolved studies therefore had to be carried out in UHV system 2.

3.3 RESULTS

1. Air Cleaved CdTe

The surface of air cleaved CdTe was investigated using XPS, UPS, AES and LEED. Most information as to the nature of

this surface came from the results of XPS measurements. These were carried out in UHV system 3, the VG Ltd ESCA III spectrometer. These measurements showed the presence of O, C, Cd and Te on the surface, see Fig.3.5a. It is interesting to note that the 4d emission line and also the $3d_{5/2}$ and $3d_{3/2}$ emission lines of Tellurium are split. The splitting in the 3d levels was measured at 3.0 eV. This is shown in Fig.3.5b Comparison of Binding energies calculated for these peaks with the Binding energies of Tellurium 3d when the Tellurium is in different chemical states (BAHL et al 1977) leads to the conclusion that the chemically shifted Tellurium 3d and 4d emissions observed here are due to the presence on the surface of TeO_2 as well as Te in the form of CdTe. The difference in Binding energies of Te_{3d} lines in TeO_2 and elemental Te was measured by Bahl et al as 3.0 eV. This figure is in agreement with the figure we obtained here. The presence of TeO_3 on the surface instead of TeO_2, can be ruled out for two reasons. Firstly the splitting caused by Te being in TeO_3, not elemental Te, is measured by Bahl at 4.2 eV. Secondly TeO_3 is unstable and reverts to TeO_2 below 300°C. The most prominent feature of the spectrum, however, are the emissions at 405 and 412 eV due to Cd $3d_{5/2}$ and Cd $3d_{3/2}$ emissions. These emissions are unsplit and would indicate that Cd present is in the form of CdTe and not as CdO. According to GAARENSTROM et al 1977, Cd metal produces $3d_{5/2}$ emission at 404.9, CdTe produces Cd $3d_{5/2}$ at 405.0 and Cd O produces Cd $3d_{5/2}$ at 404.2 eV. Hence presence of CdO on the surface would have produced a noticeable splitting of the Cd 3d lines. Also evident in the spectrum are substantial emissions due to oxygen (O is at 532 eV Binding energy). This is understandable if TeO_2 is present in the surface, and due to Carbon (C is at 284 eV B.E.). The Cd:Te (unoxidised ratio) was ~2.5:1.

Heating this surface in a vacuum of 10^{-7} torr to 400°C leads to a gradual reduction in both the oxygen and TeO_2 emissions. Heating for 120 minutes reduces emissions due to oxygen and TeO_2 to zero and increases the emissions due to unoxidised Te to a peak height equivalent to that of the Cd emissions. Carbon emissions are also reduced substantially Fig.3.6. In fact the Cd:Te ratio was measured at ~0.95:1.

Auger electron spectroscopy was carried out in UHV system 1. This revealed the presence of C, Cd, Te and O. The O and Te peaks were of approximately the same intensity. The Cd:Te ratio was ~1.5:1 see Fig.3.7.

No identifiable LEED pattern was seen with air cleaved CdTe.

UPS spectra were recorded in UHV system 2, but no worthwhile results were forthcoming. There was a lack of identifiable structure in the spectra, Fig.3.8, caused by the 'enveloping' effect of the oxygen EDC.

FIG.3.6 XPS Spectrum of Air Cleaved CdTe after heating to 450°C for 40 minutes in a vacuum of 10^{-7} torr.

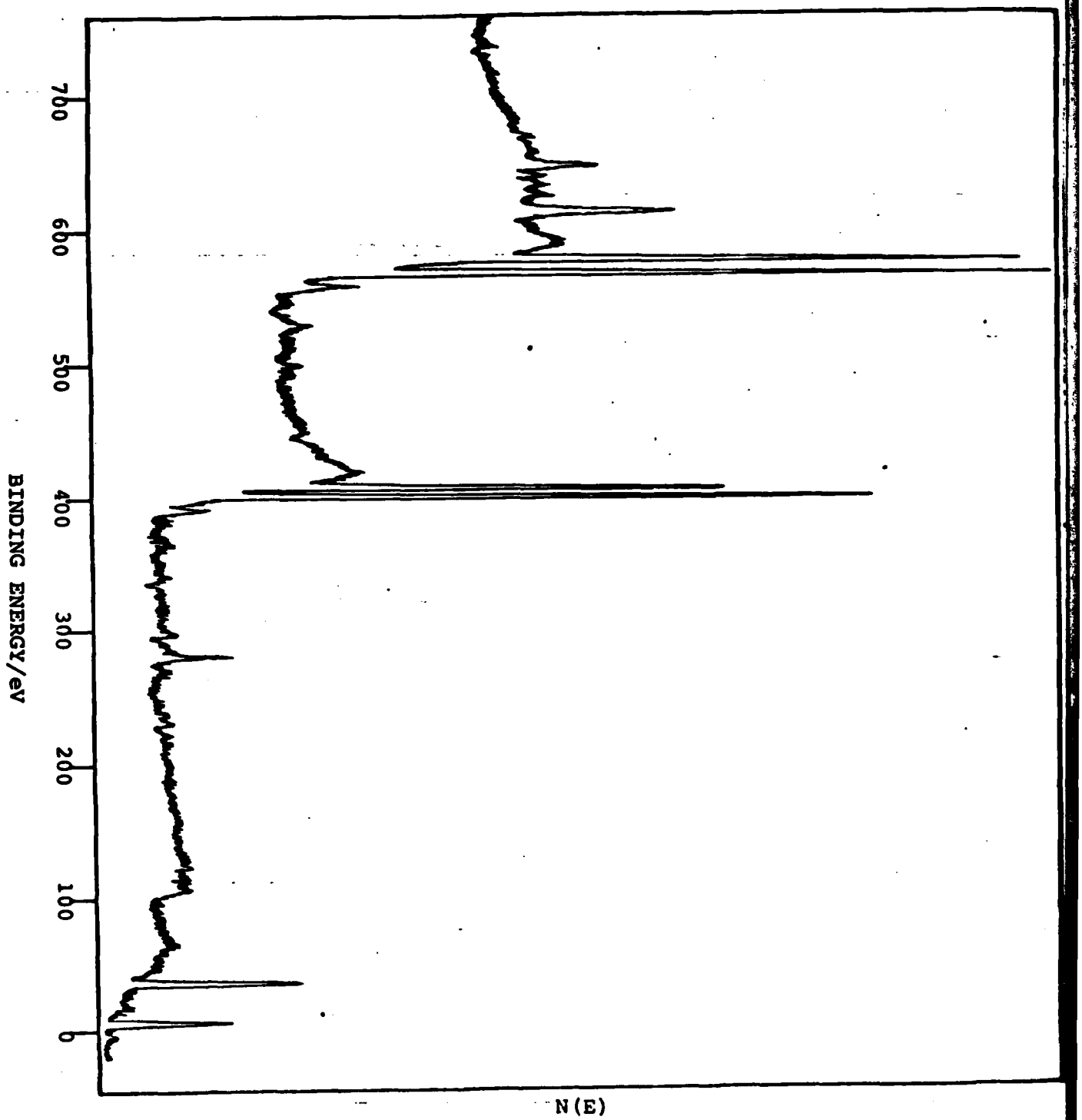

FIG.3.7 AES Spectrum of Air Cleaved CdTe.

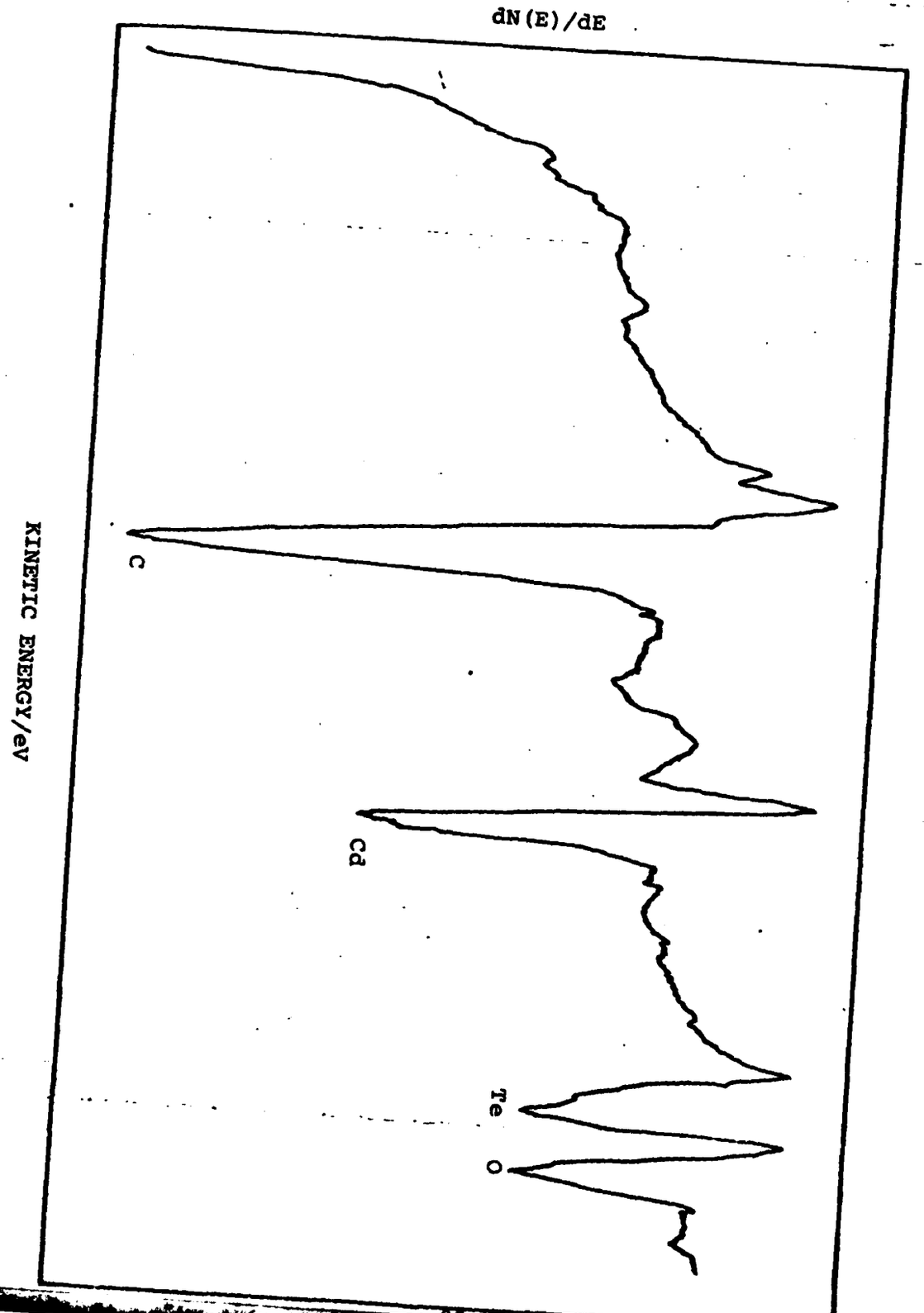

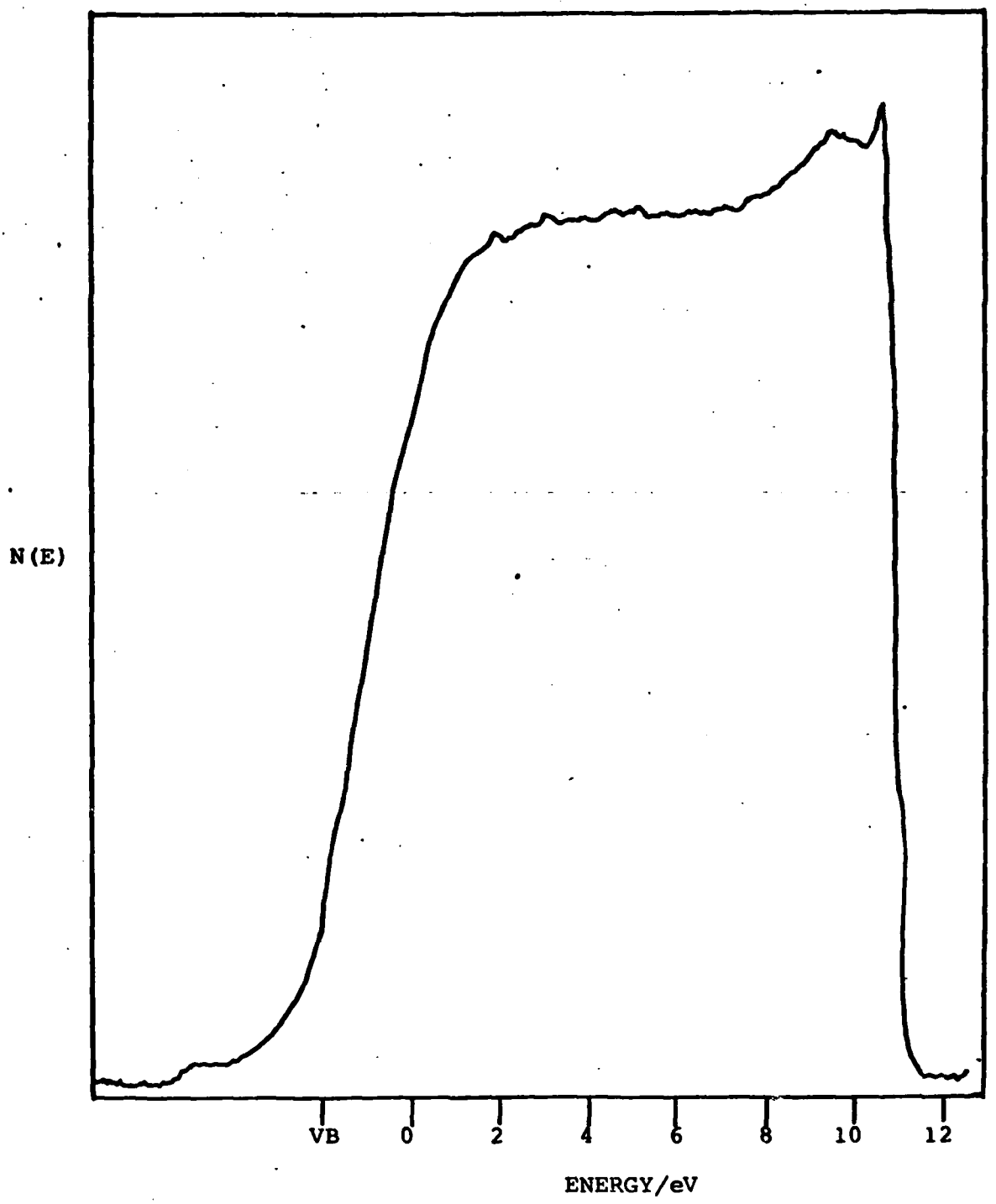

FIG.3.8 UPS Spectrum of Air Cleaved CdTe. HeI (21.2eV) radiation was used.

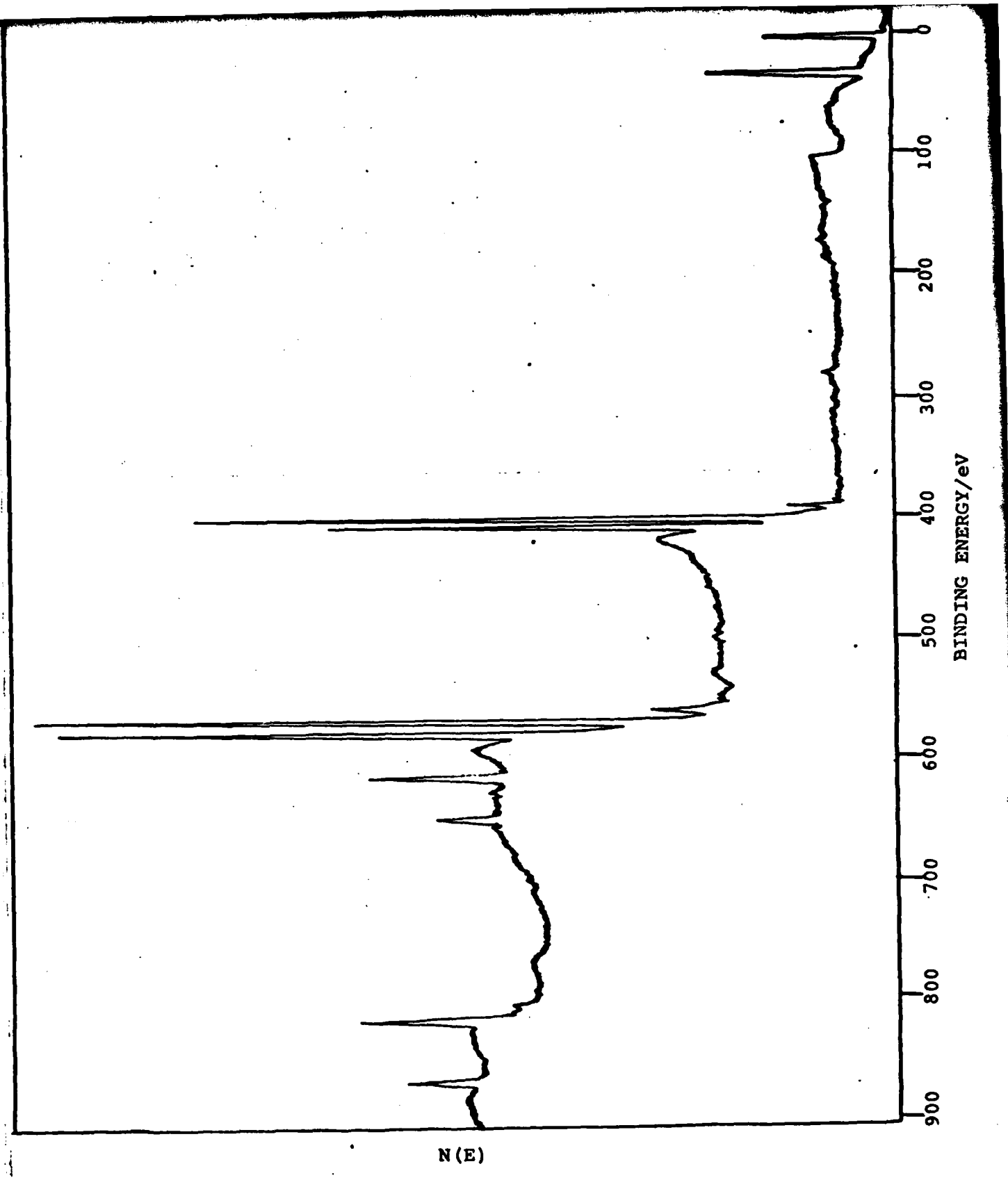

FIG.3.9 XPS Spectrum of Vacuum Cleaved (10^{-9} torr) CdTe.

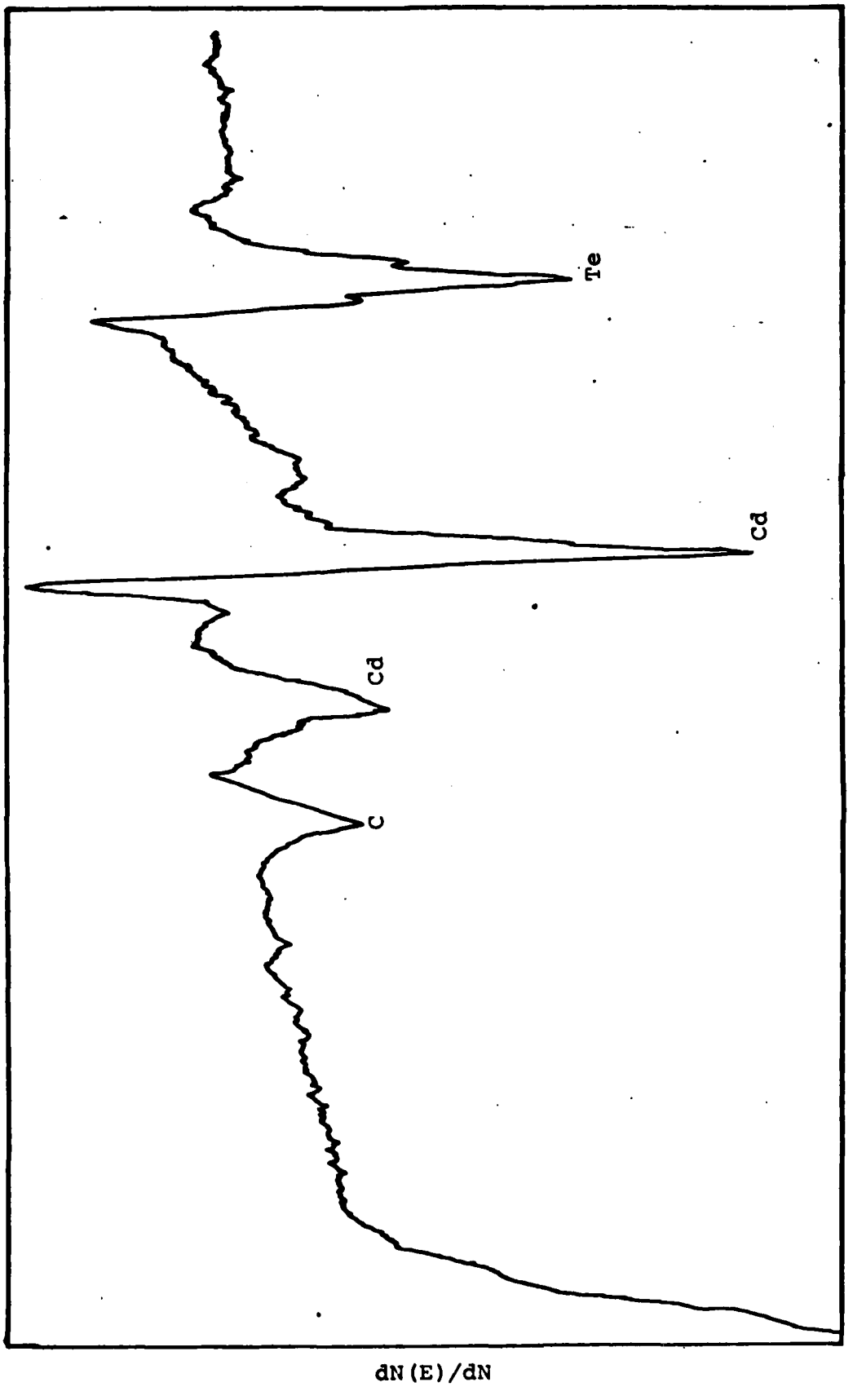

FIG.3.10 AES Spectrum of Vacuum Cleaved (10^{-9} torr) CdTe.

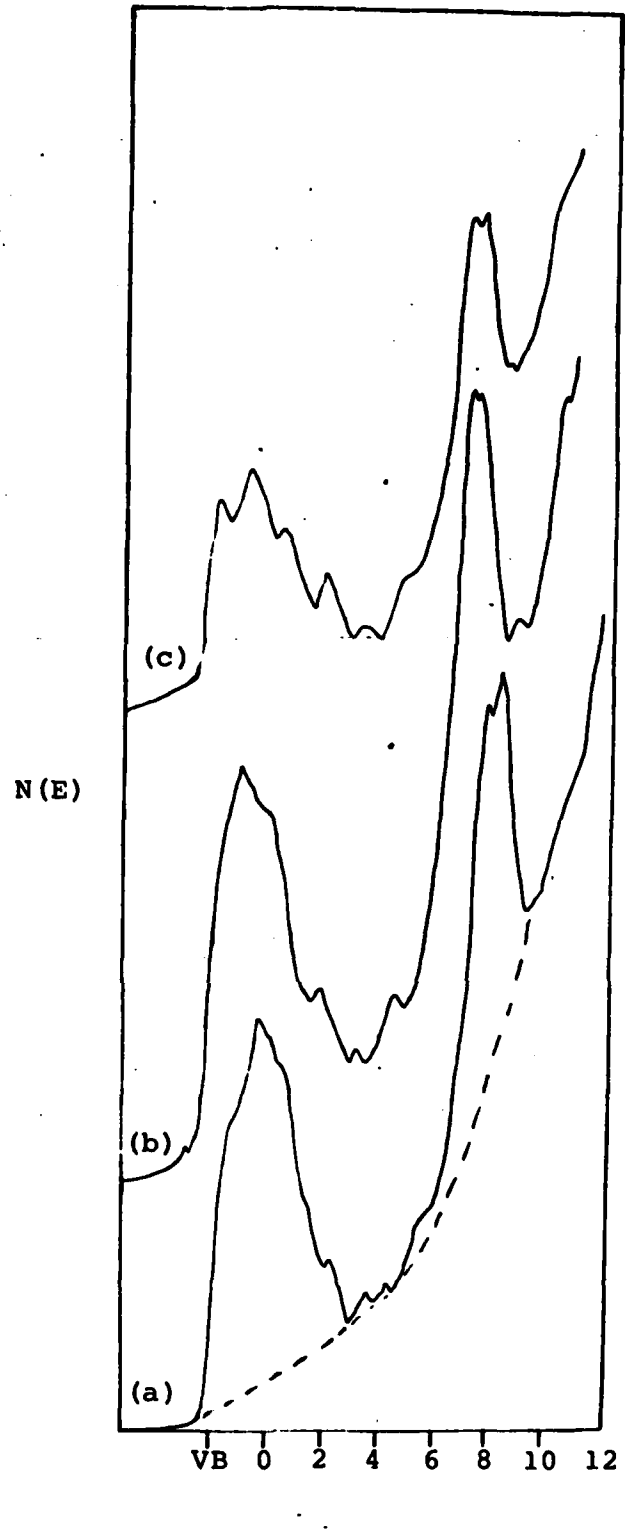

FIG.3.11 a. UPS Spectrum of Vacuum Cleaved (10^{-9} torr) CdTe.
b. UPS Spectrum of Vacuum Cleaved CdTe after exposure to a 3KV electron beam for 30 secs.
c. as b. with 5 minutes electron beam exposure.

2. Vacuum Cleaved CdTe

The vacuum cleaved surface of CdTe was investigated by XPS, UPS, AES, LEED.

The XPS spectra differed markedly from the XPS spectra recorded for air cleaved CdTe (Fig.3.9). The most noticeable difference was seen in the emissions due to Tellurium. The lines were no longer split, instead single lines larger in height than those of Cd were seen. The Cd:Te ratio was measured as 1.5:1. The Te 3d peaks were located at 573 eV and 583 eV which corresponds to those values reported for unshifted Tellurium metal positions. No oxygen was evident in the spectra and although there is a carbon presence it is very small. It could be said then that there is no TeO_2 or any other oxide of Te or Cd present on the surface of vacuum cleaved CdTe.

AES spectra were recorded in UHV system 1. The spectrum is shown in Fig.3.10. The Cadmium peaks at 277, 321, 376 and 382 eV kinetic energy are well defined as are the Tellurium peaks at 483 and 491 eV kinetic energy. There are no carbon or oxygen peaks.

An attempt was made to obtain a LEED pattern immediately after recording of the Auger spectra was complete but no pattern could be seen. If however LEED was attempted immediately after vacuum cleavage, and prior to AES, a LEED pattern was discernible for a short period of time. After this short period of time, sometimes as little as 10 seconds, the LEED pattern would become "streaky" and the end result would become very indistinct. These observations would indicate that the electron beam, used in AES and LEED, was having some disordering influence on the CdTe surface. This effect was investigated later using UPS.

A UPS spectrum of a good vacuum cleaved surface of CdTe is shown in Fig.3.11. The valence band information appears superimposed on a background due to secondary electrons, that increases smoothly with increasing binding energies. The area below the dotted line is taken to represent the contribution from the inelastic electrons so that the area above this line should represent the contributions from electrons emitted without suffering losses. Looking at the spectrum, the first peak, from the Valence Band Edge, arises from the top part of the valence band and is composed primarily of the Tellurium 5p orbitals. The second peak at Binding energies ~5 eV arises from an admixture of the Te 5p with Cd 5s orbitals. Below these p like bands are seen the sharp peaks at Binding energies ~10.5 eV due to the $J = {}^5/_2$ and $J = {}^3/_2$ components of the Cd 4d core levels. The doublet is just resolved here with a splitting of 0.7 eV. A small shoulder just to the left of the Cd 4d levels may be associated with

the Tellurium s levels.

This sample was then irradiated with an electron beam and careful measurement was made of the resulting spectra. Initially there is a movement of energy levels towards the valance band edge by ~0.6 eV, see Fig.3.11 as measured by the position of the top of the Cd 4d bands. As the length of time to which the surface was exposed to the electron beam was increased, so we see more structure appearing in the lower energy part of the spectra. Indicating that some rearrangement of atoms within the surface layers is occurring.

3. Bromine-Methanol Etch

XPS spectra were recorded for several samples of CdTe etched in Bromine-Methanol. These all showed emissions at the same Binding energies as the spectra for air cleaved CdTe. In some cases, though, there were extra emissions. This was due to presence of Bromine on the surface, evidence by the Bromine 3d emission at 70 eV. It was noted that the presence of the Bromine on the surface was dependant simply on the thoroughness of the rinsing procedure carried out after etching. It was found that rinsing the crysal once or twice in methanol after etching was not enough to remove the Bromine. Bromine only disappeared from the surface after a rinsing procedure which included rinsing in methanol in an ultra-sonic water bath for ~20 minutes had been employed. It is noted that when Bromine was seen on the surface of CdTe, the emissions at 405 and 412 eV due to Cadmium $3d_{5/2}$ and $3d_{3/2}$ were larger than for a sample with a Bromine free surface. A Bromine free spectrum is shown in Fig.3.12(a). It is seen that there are emissions due to Cd, Te, O and C. The tellurium 3d and 4d emissions are split by the same magnitude as was seen in air cleaved CdTe, i.e. 3d levels split by ~3.0 eV Fig.3.12(b). It was thus concluded that the splitting was due to the presence of Tellurium in the surface in two forms CdTe and TeO_2. The main difference between this spectrum and that for air cleaved CdTe is in the ratios of peak heights. If one looks at the peak height ratios of the Te_{3d} emissions in air cleaved CdTe one sees Te in CdTe:Te in TeO_2 ratio of ~1:1. In Bromine-Methanol etched surfaces this ratio has risen to 1:1.5 i.e. The surface layer produced by etching in Bromine-Methanol contains a greater proportion of surface Tellurium in the form of TeO_2 than is seen in the surface produced by cleaving in air. The Cd, O and C emissions are all unsplit. The ratio of Cd:Te (Te in unoxidised state) was measured as 1.5:1.

On heating to 450°C in a vacuum of 10^{-6} torr the spectrum began to change. After 120 minutes at this temperature the splitting in the Te 3d emissions disappeared, the Oxygen peak reduced, but the Carbon peak became prominent see Fig.3.13.

FIG.3.12 a. XPS Spectrum of the CdTe surface after etching in Bromine-Methanol, and then thoroughly rinsed.
b. XPS Spectrum of the Te_{3d} region.

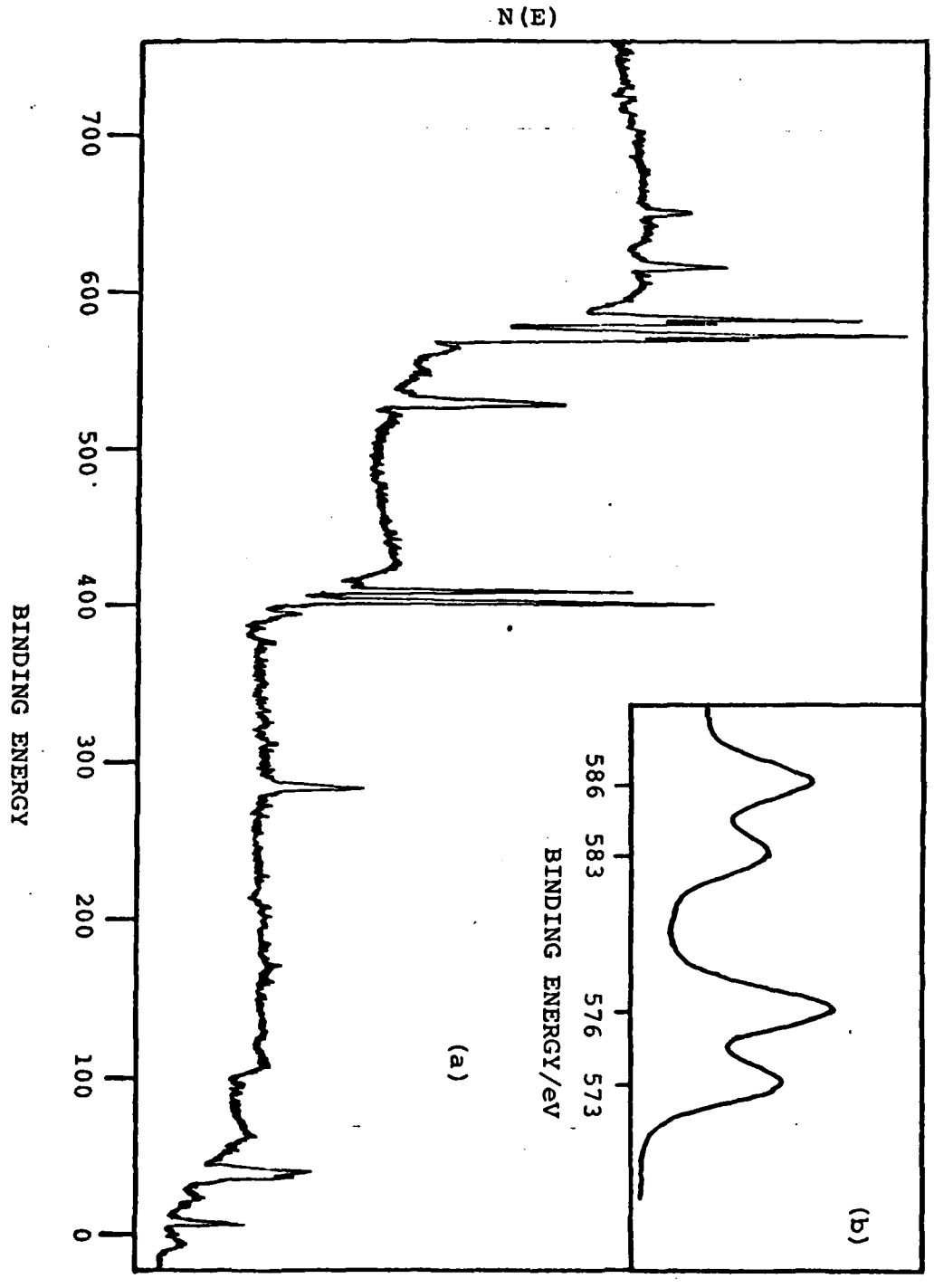

FIG.3.13 XPS Spectrum of CdTe surface, etched in Bromine-Methanol, then heated to 450°C for 60 minutes in a vacuum of 10^{-7} torr.

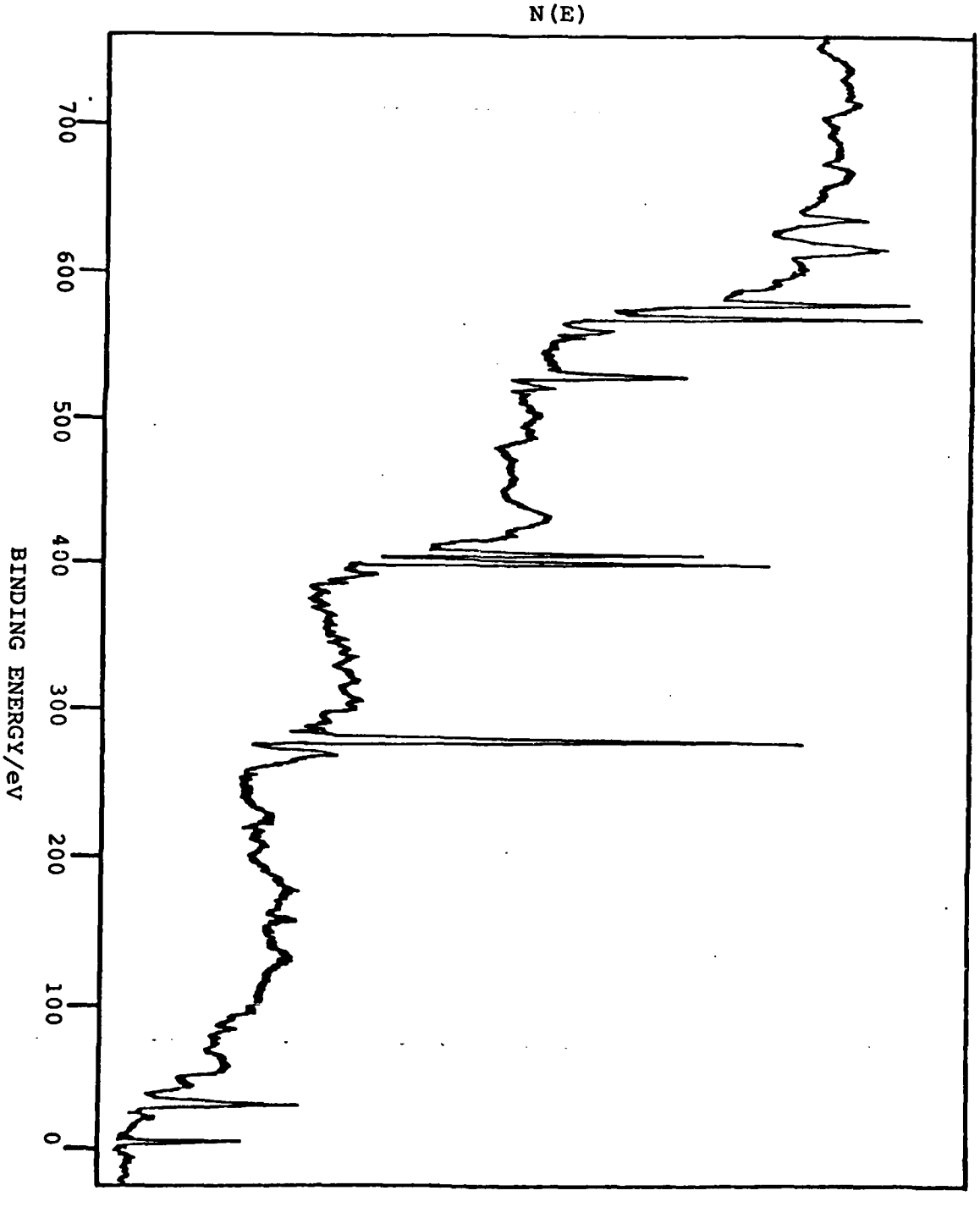

FIG.3.14 XPS Spectrum of the CdTe surface after etching in Potassium Bichromate Solution.

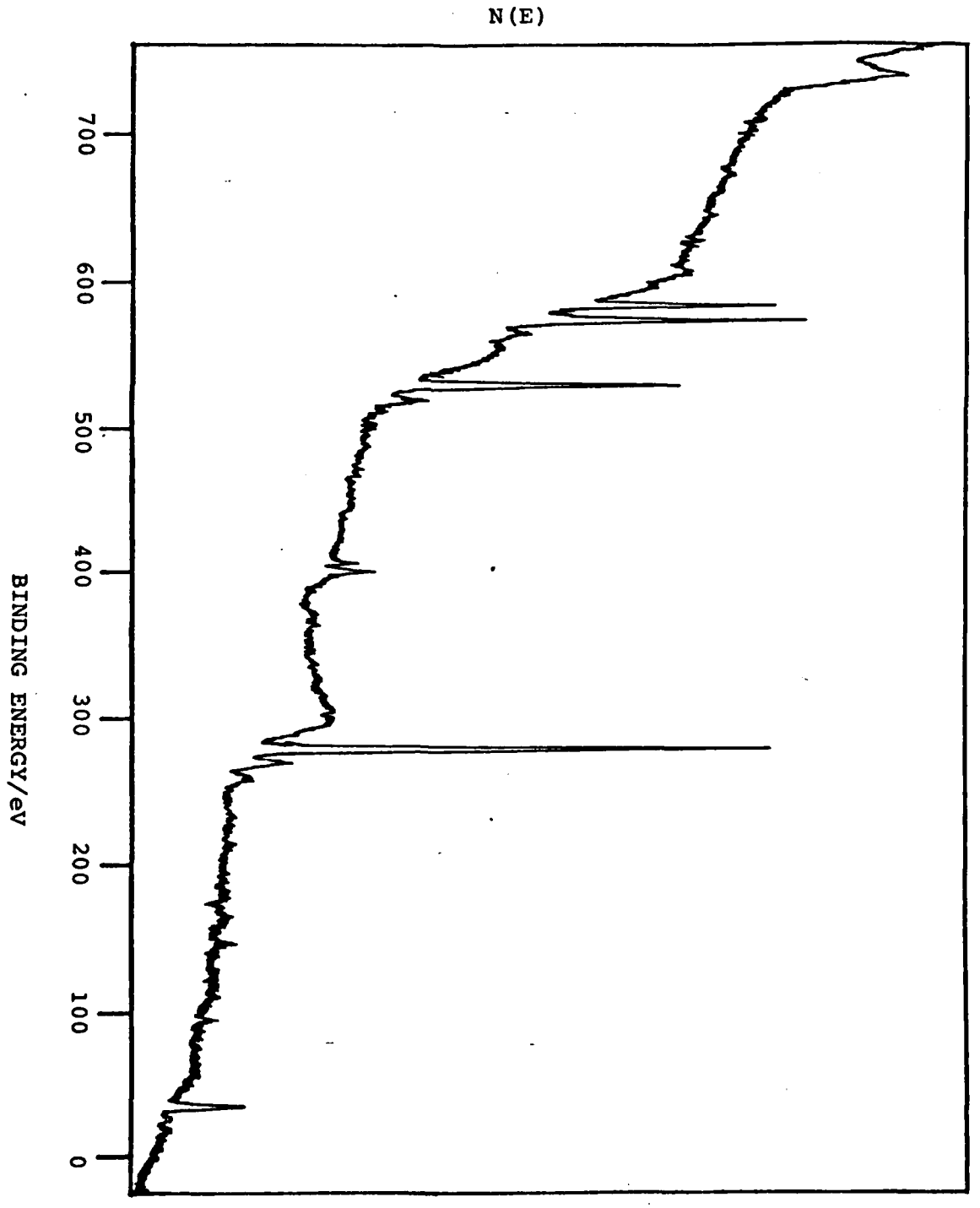

FIG.3.15 a. XPS Spectrum of CdTe surface after etching in Concentrated Nitric acid.
b. XPS Spectrum of the Te_{3d} region.

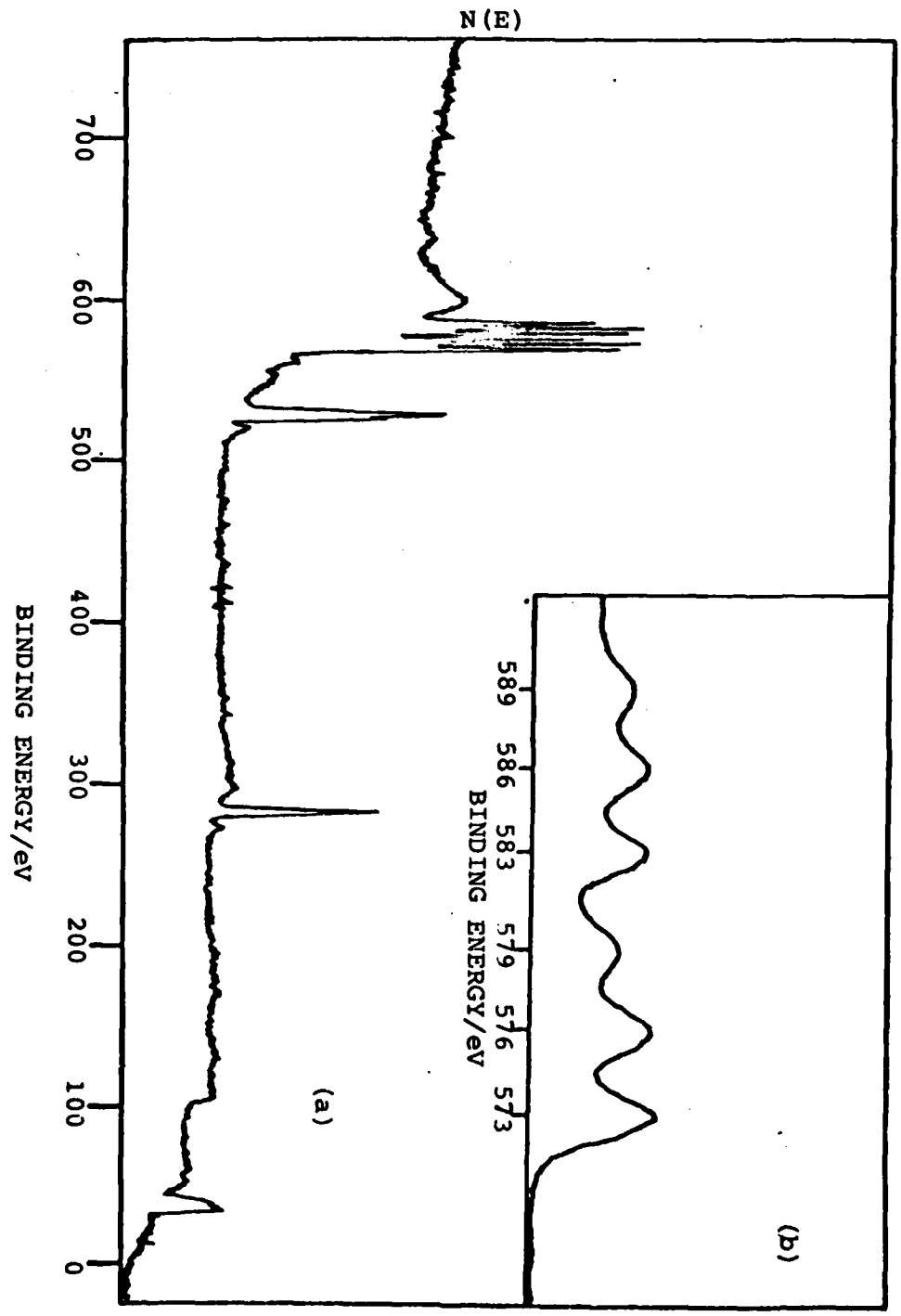

The ratio Cd:Te after heating was measured as 1.1:1 (compared to the air cleaved surface after heating 0.95:1).

AES and UPS have yet to be carried out on this surface.

4. Potassium Bichromate

XPS results of this etched surface proved to be very interesting. A typical spectra is shown in Fig.3.14. Emissions are seen for Te, C and O with an emission from Cd just visible. The Tellurium $3d_{3/2}$ and $3d_{5/2}$ levels appear at Binding energies of 586.5 and 576 eV respectively. These correspond to the Binding energies, as before, of Te in TeO_2. The doublet is unsplit i.e. all the tellurium in the surface layers is in the form of TeO_2. Large emissions are seen for oxygen and carbon. The Cd 3d levels, very prominent in air cleaved, vacuum cleaved and Bromine-Methanol etched surfaces, are barely visible over the probing depth of XPS(20-30Å) i.e. A lot of Cadmium has been removed from the surface.

5. Nitric Acid

A typical XPS spectrum is shown in Fig.3.15a. As can be seen this surface preparation has presented us with a totally new and as it proved to be, unique surface to deal with. No emission lines are seen at all for Cd. C is seen as a prominent singlet, oxygen as a doublet and the Te_{3d} and $_{4d}$ lines as triplets! Fig.3.15b. If we look at the Te $3d_{3/2}$ emission, the first two components at 583 eV and 586.5 eV correspond, as before, to emissions of Te in metallic Tellurium, and Te in TeO_2. The peak at 589 eV is, however, something of a mystery. A splitting of 6 eV from the elemental Te $3d_{3/2}$ position. This splitting is also seen for the Te $3d_{5/2}$ emission and on a smaller scale in the Te 4d emission. The O_{1s} line is split by ~3 eV. Angular resolved XPS studies of this surface indicated a uniform composition of the phases responsible for the three tellurium lines over the probing depth i.e. the relative amplitudes of the various lines did not depend on the angle of electron escape. At first it was thought that the appearance of the tripley split Tellurium and doubly split oxygen was perhaps due to a malfunction in the electronics of the spectrometer. Repeating the experiment in a different spectrometer, with a different crystal, with a different source of Nitric Acid, produced identical results.

6. Ethylene Diamine Tetra Acetic Acid (EDTA)

An XPS spectra for CdTe etched in EDTA is reproduced in Fig.3.16. EDTA has left the surface totally depleted of Cd over the XPS probing depth. Emissions due to Carbon, oxygen and Tellurium are seen. The Te 3d emissions are unsplit and appear at 586.5 and 576 eV. These again correspond to Te being present in the form of TeO_2. Oxygen is prominent on

the surface, but, surprisingly, the carbon presence on the surface is relatively small.

7. Hot Sodium Cyanide

An XPS spectrum is shown in Fig.3.17a. Present in the spectra are emission lines due to Tellurium, Cadmium, Oxygen and carbon. The Te_{3d} lines appear as an unsplit doublet at Binding energies 573 and 583 eV, i.e. Tellurium present on the surface is not oxidised i.e. no TeO_2 or TeO_x ... The Cd 3d lines also appear as an unsplit doublet at Binding energies 405 eV and 412 eV, i.e. no CdO present on the surface. The Cd:Te ratio was measured at 1.6:1. One very interesting feature of this spectrum is the splitting of the Carbon 1_s level, Fig.3.17(b). The splitting was measured as 2.5 eV. This is probably due to the presence on the surface, as well as the ordinary carbon, of carbon in the form of CN-(cyanide). Sodium and Nitrogen emissions, which one would also expect to see if NaCN was present on the surface, would be very weak due to the orbitals being s and p, and would be in the energy range 0-70 eV, where it is possible that weak emissions could be lost in the background noise.

8. PBr_2

An XPS spectrum of the CdTe surface, left by treatment of the surface in "PBr_2" solution, is shown in Fig.3.18. There are extra features in this spectrum which were seen before but only when samples etched in Bromine-Methanol had not been thoroughly rinsed. I refer to the Bromine 3d level emission at 70 eV. Also present in the spectrum are emissions due to Cd, Te, O and C. The Tellurium emissions are split again by 3 eV showing the presence of Te in TeO_2(?) as well as in the form CdTe. The ratio of Te (in unoxidised state): Te in TeO_2 was measured to be about 2:1. The Cadmium peaks are unsplit and form the largest peaks in the spectrum. The ratio Cd:Te (unoxidised) was measured at ~3:1. Oxygen and carbon are both present and both unsplit, although the carbon peak is much smaller than seen in previous surface treatments.

3.4 DISCUSSION

It is obvious from the results presented above that the surface of CdTe is very sensitive to the type of preparation to which it is subjected. Etchants were chosen because previously results had been published of the type of metal contacts made to n-type CdTe with the surface of the CdTe arbitrarily prepared for metal deposition by use of one of the etchants. It is not surprising, therefore, that a large variation in the properties of the metal-CdTe contacts so formed is reported. In a later section the nature of metal contacts to the various CdTe surfaces will be investigated, but here let us consider the different types of

FIG.3.16 XPS Spectrum of CdTe etched in molar EDTA solution.

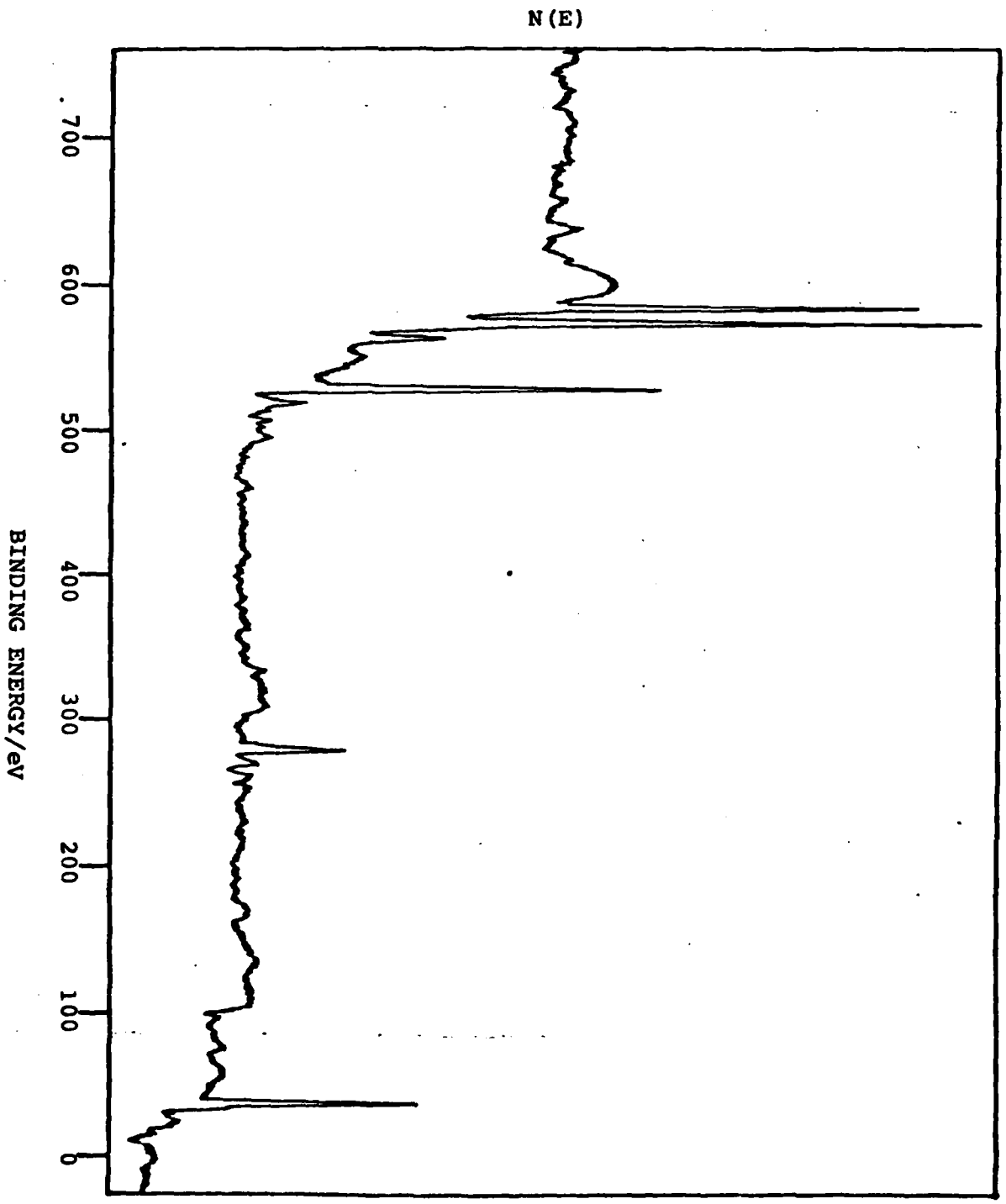

FIG.3.17 a. XPS Spectrum of the CdTe surface etched in boiling NaCN solution for 20 minutes.
b. The Carbon Is region.

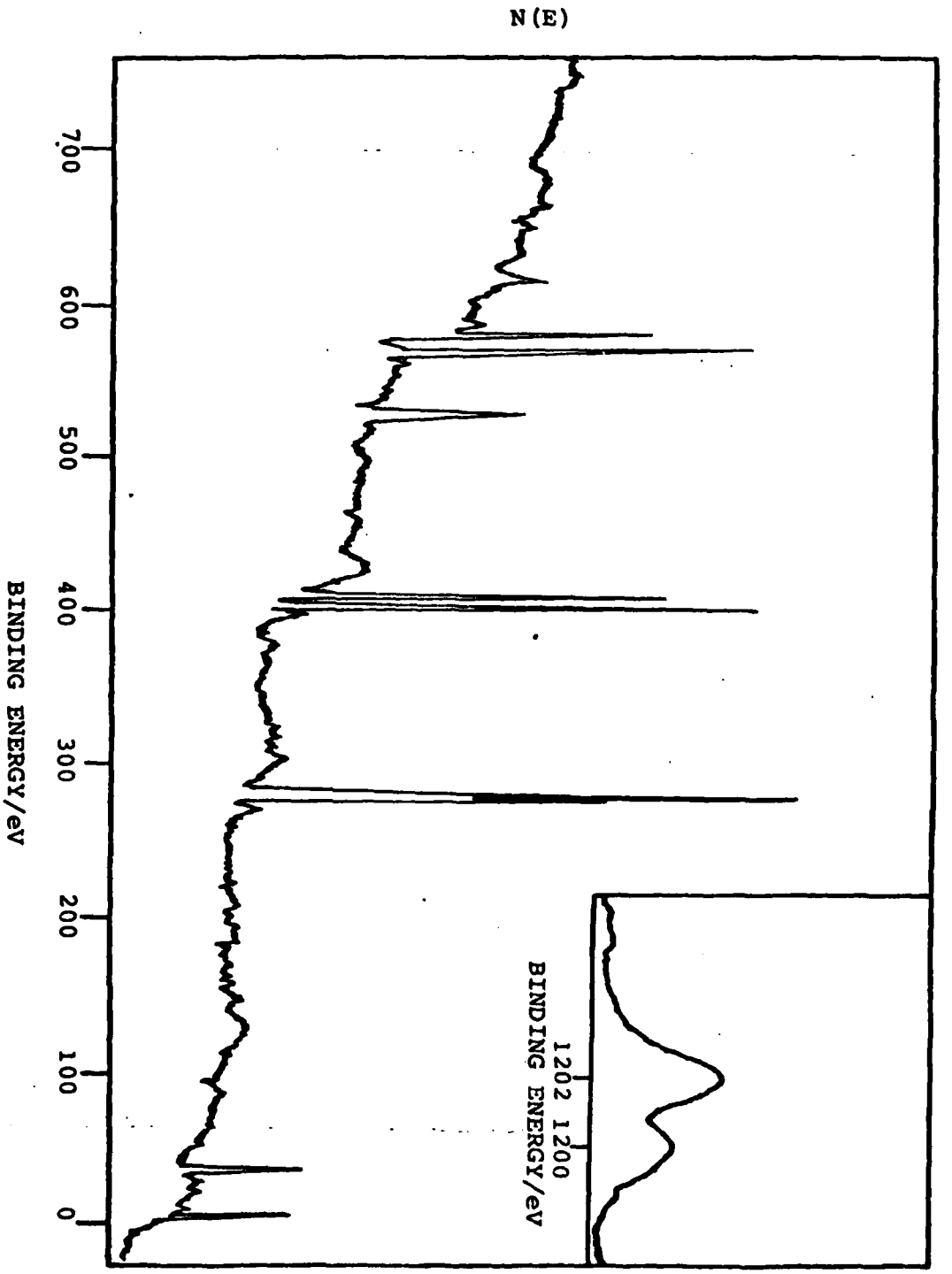

FIG.3.18 XPS Spectrum of the CdTe surface after etching in PBr_2 solution.

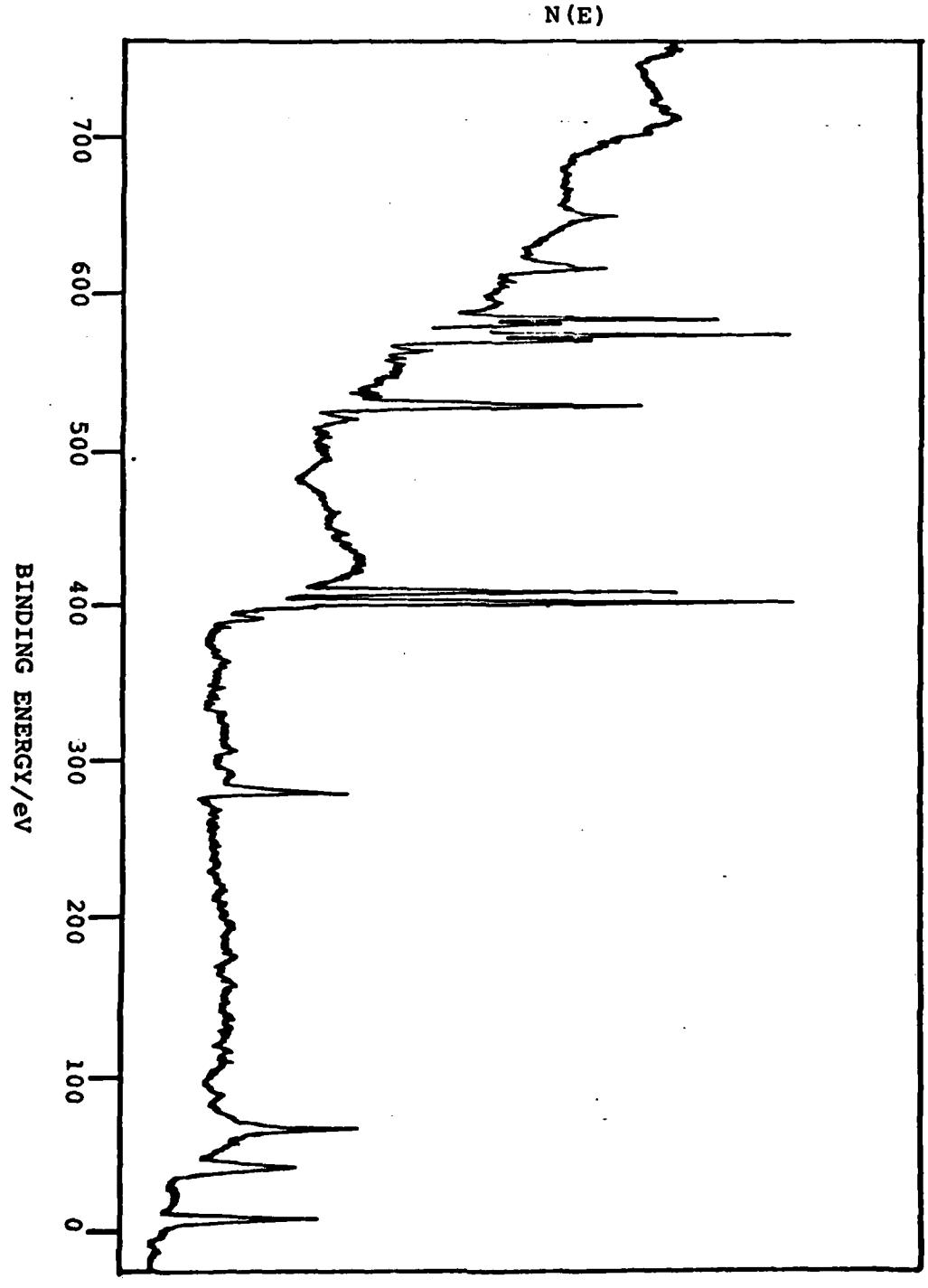

surface presented.

Air cleaved CdTe has a surface rich in Cadmium, with a fair amount of TeO_2 present. Also present on the surface is carbon which appears appreciably in all types of surface preparation with the exception of vacuum cleaved surfaces. In the surface layers the overall Cd:Te ratio is 1:1 but about half of this Te is in the form of TeO_2. Hage Ali et al 1979a reported a ratio of Cd:Te of 1.08, for cleaved sample of CdTe, measured by RBS. On heating the TeO_2 contribution disappears, the oxygen and carbon emissions reduce and the Te, unoxidised, peaks increase till the Cd:Te ratio approaches unity. This could be due to the TeO_2 dissociating and the resultant oxygen being driven off the surface with carbon either as carbon monoxide (CO) or carbon dioxide (CO_2).

Vacuum cleaved CdTe, however, has a totally different surface. There is no TeO_2 on the surface. No oxygen and very little carbon is present.

Etching of the surface generally disturbed the surface to a greater extent than air cleaving. One exception to this generalisation was the etchant Bromine-methanol. This left the surface in a chemical state not dissimilar to the surface left by air cleaving samples i.e. a large presence of TeO_2 on the surface, infact more of surface Tellurium is in the form TeO_2 than in the form of CdTe. There is a slight depletion of Cd from the surface if one considers the Cd : overall Te ratio. If one just considers the Cd:unoxidised Te then a ratio of 1.5:1 is seen. This result is in agreement with the RBS measurements of Hage-Ali et al 1979(a) who reported a value of 1.58 for this ratio on a surface of CdTe etched in Bromine-methanol. Oxygen is very prominent on the surface, as is carbon.

On heating, the level of oxidised Tellurium on the surface reduces and the Cd:Te (unoxidised) approaches unity. There is, however, a large increase in the carbon concentration on the surface. It is possible that the increased carbon presence is a result of "cracking" of any remaining methanol (CH_3OH) molecules left on the surface or organic compounds formed between the methanol and the silver epoxy adhesive used to attack the crystal to the sample holder.

If, after etching in Bromine-methanol, the surface is not very well rinsed it is found that there is residual Bromine on the surface and there is an increase in the Cd concentration compared to the well rinsed surfaces. This could be due to the formation of a cadmium Bromide species. $CdBr_2$ is very soluble in both water and alcohol. The Heat of Reaction (ΔHR) for the reaction of Bromine with CdTe is - 2.32 eV $atom^{-1}$, so one would expect Bromine to react readily with CdTe to form $CdBr_2$. If $CdBr_2$ is formed as a

surface species then it is possible that a thorough rinsing in water or methanol could remove all $CdBr_2$ from the surface, and a bad rinse could leave some $CdBr_2$ on the surface. If this were the case then one might expect to see a splitting in the Cd 3d peaks due to Cd on the surface being in two different chemical environments - $CdBr_2$ and CdTe. No such splitting is seen. This could be due to one of two reasons.

(a) Cd is present on the surface in one form only CdTe.

or

(b) the splitting due to the $CdBr_2$ presence is so small as to be unresolved by the spectrometer.

As yet no information on the binding energies of the Cadmium 3d peaks in $CdBr_2$ is available so we're unable to comment further on this.

This experimental observation is in agreement with results recently published by Hagi-Ali et al (1979a). They found that "Badly rinsed" samples showed a larger surface Cadmium presence than was exhibited by well rinsed samples. Bromine presence was also high. Using various samples they showed that the Cadmium peak height was proportional to the Bromine concentration on the surface. In other words, rinsing the surface of Bromine-methanol etched CdTe removes both Bromine and Cadmium at the same rate. If indeed $CdBr_2$ was present after etching in Bromine-methanol, then this equivalent reduction of Cadmium with Bromine reduction could be explained by removal of $CdBr_2$ from the surface.

The above three surface preparations are the most commonly used when fabrication of CdTe devices has been carried out. They present three quite different surface chemical compositions, as such one would expect different chemical reactions to occur when these surfaces come into contact with other chemicals, such as metals. This is borne out by work presented later on the different electrical behaviours observed when metals were evaporated onto these various surfaces. Some metals produce surface barriers which vary relatively little with the surface. An example of this type of behaviour is seen with Gold which gives good Schottky barriers whether it is evaporated onto air cleaved, vacuum cleaved or Bromine-Methanol etched surfaces. Other metals give good Schottky barriers on one surface but give ohmic contacts when evaporated onto another surface. An example of this is the Aluminium-CdTe contact. On air cleaved CdTe Aluminium gives a good Schottky barrier whereas on vacuum cleaved CdTe an ohmic or zero barrier contact is formed. This observation was noted by TAKEBE et al 1978 who suggested that change in Barrier height associated with the three surfaces was a function of the thickness of the interfacial layers formed by the different surface preparations and/or

the surface state density. This problem will be considered in a later section.

The etchant PBr_2 was unique among the etchants used because it was the only one which left Bromine well attached to the CdTe surface. Even thorough rinsing would not remove Bromine from the surface. The etchant is a satisfactory one from the point of view of maintaining the cadmium level in the surface. Cadmium appears to be in the largest concentration. Tellurium is present in two or more species. The Te emissions are split by ~3 eV. This could be due to Tellurium being in the form of TeO_2, Tellurium Bromide ($TeBr_3$) or both. The Binding energies of the $3d_{5/2}$ level of Te in TeO_2 is given as 576.1 eV and in $TeBr_3$ as 576.2 eV (BAHL et al). Within experimental error of ±0.2 eV it is not possible to say accurately which, or if both, species are present. $TeBr_3$ would appear to be fairly insoluble in cold water and would not be expected to dissolve off. The heat of reaction (ΔH_R) of Bromine with CdTe, in acidic conditions, to form Tellurium Bromide is -1.1 eV $atom^{-1}$. Hence formation of the Te Bromide should occur readily. The possibility of Bromine being present as $CdBr_2$ or $CdBr_2$ $4H_2O$ is very doubtful. These Cadmium Bromides are very soluble in cold water and one would expect the cadmium bromide to dissolve off with rinsing.

Hot sodium Cyanide left the CdTe surface stoichiometry fairly well intact. There is no evidence of oxidised Tellurium on the surface. The Cd:Te ratio was measured as 1.6:1. Oxygen is seen on the surface, coupled with a large carbon presence. The Carbon is present as ordinary surface carbon, and in the form of CN left over from the etching procedure. It would appear that the main reason for the unpopularity of hot Sodium Cyanide as an etchant, only one publication (TOUSKOVA et al 1972), is in the danger associated with the etching procedure. Sodium Cyanide is a very deadly poison. If there is any acid about to get in contact with NaCN, highly poisonous hydrogen cyanide gas could be formed.

The remaining etchants investigated all destroyed the surface stoichiometry one way or another. The etchants used have all been used fairly widely and a large amount of results have been published.

Of these etchants the most commonly used is the Potassium Bichromate etch. Our etching procedure was identical to that of INOUE et al 1962. They proposed the chemistry of the situation thus. Nitric acid attacks cadmium on the surface, leaving a polycrystalline layer of Te, which becomes oxidised, by the oxidising properties of the potassium Bichromate/Nitric acid mixture, to TeO_2. TeO_2 being soluble in acidic solution is then dissolved from the surface. The presence of silver ions, which have a lower ionisation

tendency than cadmium in the solution should mean that any Cadmium left is replaced on the surface by silver ions. The result of this should be a smooth dissolution of the CdTe surface, with traces perhaps of silver on the surface. In practice we find that there is very little Cadmium seen on the surface, a large amount of TeO_2 and no unoxidised Tellurium is seen on the surface. No Silver is on the surface. but carbon is present in large quantities. We therefore suggest a reaction scheme where two reactions occur simultaneously.

1. Reaction of oxidising acidified potassium bichromate with Te to form TeO_2.
2. Reaction of excess acid with the surface Cd, thereby removing Cd from the surface and removing some of the acidity from the etchant.

If this was the case, and the acidity was removed from the etchant then one would expect TeO_2 to be seen on the surface, since TeO_2 is soluble only in acidic solution. The thickness of this TeO_2 layer would be dependant on the amount of acid unreacted with Cd, and the amount of TeO_2 dissolved off by this remaining acid. Silver ions would not be able to get near Cd, lying beneath the TeO_2 and so would remain in solution. If the TeO_2 layer were, say, 20Å thick and the probing depth of the experiment 25Å, then one might see some Cd emissions from Cd sites lying between 20 and 25Å below the surface.

Concentrated Nitric Acid leaves the surface in a chemical state that we found to be unique. The surface is completely depleted of Cadmium, there are large Carbon and Oxygen emissions. In fact oxygen is present in two different chemical environments, shown by the splitting of the O is level by 3 eV in the XPS spectrum. The splittings of the tellurium levels are not so easy to explain, one possibility is that the extra line, 6 eV up from the elemental Te position in the 3d emissions, is due to another oxide or oxygen containing molecule of tellurium such as TeO_3 or Te_2O_5 or $Te(OH)_6$. TeO_3 is unlikely, since the Binding energy of $Te3d_{3/2}$ in TeO_3, measured by BAHL et al, is 587.3 eV. This would cause a splitting of 4.2 eV from the position of $Te3d_{3/2}$ in CdTe. This value of 4.2 eV is 1.8 eV less than the measured splitting and is therefore unlikely to be the cause. In $Te(OH)_6$ the Binding energy is 587.1 eV, a splitting of 3.6 eV therefore $Te(OH)_6$ is unlikely. There is no data available of any other oxides or oxygen containing tellurium compounds. Another possibility is that all the energy levels have shifted with respect to the Fermi energy. If a wide gap oxide is grown on a small gap substrate, and if the Fermi levels are in the middle of the band gaps in both phases, then, in equilibrium all core levels of atoms in the oxide will appear shifted to higher

binding energies. It is difficult to see how the threefold splitting of the tellurium levels observed here could be brought about in this case however without the presence of a second oxide phase. Unfortunately the band gaps of other oxides of Tellurium are not known. Obviously further studies and experimentation will be required to clarify this situation.

The results obtained for the acid etch of CdTe agree generally with those reported by Montgomery 1964 and Zitter 1971. Montgomery reported on a high energy electron diffraction examination of a CdTe surface treated by immersion in Conc. HNO_3, followed by a HNO_3/HF solution. He found the surface to be "an amorphous layer of tellurium which completely obscured the underlying material". He estimated the thickness of this layer to be about 0.5 μM. Zitter concluded, after an investigation using surface Raman spectroscopy, that immersion of CdTe in a HNO_3 solution for 40 mins. produced a poly-crystalline tellurium layer with a thickness of at least 500Å.

Ethylene Diamine tetra acetic acid has the structural formula:

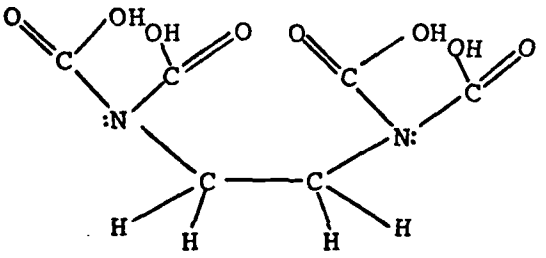

This is an organic acid used largely in the synthesis of large organic molecules. It was used here, however, to see if the surface of CdTe was susceptible to reaction with organic acids as well as mineral acids. It turned out that EDTA also destroyed the surface stoichiometry. The layers are depleted of cadmium over the probing depth of the spectrometer. No unoxidised Te is seen on the surface in fact all the tellurium seen is in the form TeO_2. Carbon is relatively scarce on the surface, but oxygen is very prominent. One could therefore conclude that the CdTe surface is left with a layer of Tellurium oxide on it after etching in EDTA.

3.5 CONCLUSIONS

The various surface preparations employed in this investigation all influence the chemical composition of the CdTe surface. Nitric acid, EDTA and potassium bichromate etches all leave the surface depleted of cadmium over at least some tens of angstroms and should therefore be avoided

when preparing surfaces for device fabrication.

Surface stoichiometry was maintained to a greater or lesser extent using the etchants Bromine-Methanol, PBr_2 and NaCN. Of these NaCN is a very dangerous chemical to work with due to its toxicity, and PBr_2, while maintaining stoichiometry, leaves Bromine on the surface. So use of these two etchants is not really recommended. It appears that for etching of CdTe the best method of preparing a near stoichiometric surface is by etching in Bromine-Methanol, rinsing very well and heating to at least 400°C in UHV. If device fabrication is to be effected on the (110) face of CdTe, the only natural cleavage plane in CdTe, then either an air cleaved surface heated to 400°C in UHV or a vacuum cleaved (10^{-9} torr) surface is recommended. In both of these the surface stoichiometry is maintained and the oxygen and carbon presence on the surface is minimal.

Finally it is noted from our experiments with XPS, UPS, AES etc. on CdTe, that once a clean stoichiometric surface of CdTe has been obtained in UHV then the surface may be maintained in this state in a good vacuum for considerable lengths of time.

METAL CONTACTS TO CADMIUM TELLURIDE

INTRODUCTION

The earliest systematic investigation on metal-semiconductor rectifying systems is generally attributed to BRAUN in 1874 who noted the dependance of total resistance on the polarity of the applied voltage and on the detailed surface conditions. The point contact rectifier, in various forms, found practical applications in 1904. In 1931 WILSON formulated the transport theory of semiconductors based on the band theory of solids. This theory was then applied to metal-semiconductor contacts. In 1938 SCHOTTKY suggested that the potential barrier could arise from stable space charges in the semiconductor alone without the presence of a chemical layer. This gave rise to the model known as the SCHOTTKY BARRIER. Also in 1938 MOTT devised a model for "swept-out" metal-semiconductor contacts, known as MOTT barriers. The basic theory and historical development of metal-semiconductor contacts was summarised by HENISCH in 1957. Because of their importance in D.C. and microwave applications and as tools in the analysis of fundamental physical parameters M-S contacts have been studied extensively. Recently reproducible and near ideal M-S contacts have been fabricated on materials such as Si, Ge, InP etc. Up to now however relatively little work has been devoted to the study of Schottky Barriers formed on CdTe. Since the first paper to appear in 1964 by MEAD and SPITZER improvements in crystal quality, vacuum techniques etc. have led to more interest in the field. Barrier height values for various metal-CdTe contacts have been reported (MEAD, 1966; PARKER and MEAD, 1969; TOUSKOVA and KUZEL, 1976, 1977; PONPON and SIFFERT, 1977; TAKEBE, 1978 etc.). Metals have been evaporated onto both n and p type material, onto etched, cleaved and polished surfaces. It is not surprising therefore in view of the wide variation in surface chemical structure presented by these various surface treatments, that variations in the types of metal-CdTe contacts have been reported.

In this section we report on the formation of metal CdTe Schottky barriers on various CdTe surfaces. We have used various methods to establish Schottky barrier heights e.g. I-V, C-V, UPS. Barrier formation and depth profiling of the metal-CdTe contacts were monitored using XPS, UPS, AES. In particular the contacts formed by the three metals Gold, Silver and Aluminium to vacuum cleaved, air cleaved and Bromine-Methanol etched (110) surfaces are under investigation. Using the results of surface investigations carried out previously, and results of the following series of experiments, we have tried to explain these Schottky Barriers in terms of the defect model of the interface.

4. CURRENT TRANSPORT THROUGH SCHOTTKY BARRIERS

Current transport in metal-semiconductor barriers is mainly due to majority carriers, in contrast to p-n junctions where minority carriers are responsible. Before it can be emitted over a barrier in the metal, an electron must just be transported through the depletion region of the semiconductor. In this process the motion of the electron is determined by the usual mechanisms of diffusion and drift, while the emission process is controlled by the number of block states in the metal which can communicate with states in the semiconductor. These two processes are essentially in series and current flow is determined predominantly by whichever causes the larger resistance.

If barrier thickness is large compared to the mean free path, so that the charge carrier experiences numerous collisions within the barrier region, then this region will have a large resistance and hence current flow will be determined by the diffusion of carriers through the barrier region. This is the basis of the diffusion theory. It could also be postulated that the barrier thickness is so small compared to the mean free path that collisions within the barrier region can be neglected for all practical purposes. Therefore current flow will be limited by the rate at which carriers can be emitted over the barrier. This is the basis of the Diode or Thermionic emission theory. Physically the mean free path should be compared, not with the barrier thickness as a whole, but with the distance within which the potential energy changes by KT near the top of the barrier. This distance is generally smaller than the barrier thickness.

1. Thermionic Emission Theory

The simple isothermionic emission theory was first derived by BETHE in 1942. The theory is derived from three assumptions:-

i. Barrier Height $q\phi_{Bn} > KT$.

ii. Electron collisions within the depletion layer are neglected.

iii. Image force effect is also neglected.

Because of the above assumptions the shape of the barrier profile is immaterial and the current flow is dependant on Barrier Height only. The current density, from semiconductor to metal $J_{S\rightarrow M}$, is given by the standard thermionic emission equation

$$J_{S\rightarrow M} = qn\left(\frac{KT}{2\pi m^*}\right)^{\frac{1}{2}} \exp\left(-\frac{m^* Vox^2}{2KT}\right) \qquad (1)$$

where Vox is the minimum velocity required in the x direction

to surmount the barrier and is given by:-

$$\tfrac{1}{2}M^*Vox^2 = q(V_{bi}-V) \qquad (2)$$

where V_{bi} is a built in potential and V is the applied potential. n, the electron concentration is given by

$$n = N_c\exp\left(-\frac{Ec-Ef}{KT}\right) = 2\left(\frac{2\pi m^*KT}{h^2}\right)^{\frac{3}{2}}\exp\left(\frac{-qVn}{KT}\right) \qquad (3)$$

putting equations 2 and 3 into 1 gives

$$J_{S\to M} = A^*T^2\exp\left(\frac{-q\phi Bn}{KT}\right)\exp\left(\frac{qV}{KT}\right) \qquad (4)$$

$A^* = \frac{4\pi qm^*K^2}{h^3}$ is the Richardson Constant.

As the barrier height for electrons moving from the metal to the semiconductor remains the same the current flowing into the semiconductor is unaffected by the applied voltage. It must therefore be equal to the current flow from the semiconductor into the metal when thermal equilibrium prevails i.e. when v = o in equation 4 then

$$J_{M\to S} = -A^*T^2\exp\left(\frac{-q\phi Bn}{KT}\right) \qquad (5)$$

the total current density J_n is given by the sum of $J_{S\to M}$ and $J_{M\to S}$

i.e. $$J_n = \left[A^*T^2\exp\left(\frac{-q\phi Bn}{KT}\right)\right]\left[\exp\left(\frac{qV}{KT}\right)-1\right]$$

so

$$J_n = J_{ST}\left[\exp\left(\frac{qV}{KT}\right)-1\right] \qquad (6)$$

where $$J_{ST} = A^*T^2\exp\left(\frac{-q\phi Bn}{KT}\right) \qquad (7)$$

= the Saturation Current density.

2. Diffusion Theory

The mechanism of rectification as envisaged in the diffusion theory first proposed by Schottky in 1938 is similar to that of the thermionic emission theory except that the effect of electron collisions within the depletion layer is no longer neglected and that charge carrier mobility remains constant.

As current in the depletion region depends on the local field and the local concentration gradient, calculation of the voltage current relation for n type material must be based on the current density equation

$$J_n = q\left[n(X)\mu E + D_n \frac{\partial n}{\partial x}\right]$$

where D_n is a diffusion constant.

The current voltage relation is calculated from this to be

$$J_n = \left[\frac{q^2 DnNc}{KT}\left(\frac{q(V_{bi}-V)2N_D}{Es}\right)^{\frac{1}{2}} \exp\left(\frac{-q\phi_{Bn}}{KT}\right)\right]\left[\exp\left(\frac{qV}{KT}\right)-1\right] \quad (8)$$

i.e.
$$J_n = J_{SD}\left[\exp\left(\frac{qV}{KT}\right)-1\right] \quad (9)$$

The current density expressions of the diffusion theory, equation 9, and the thermionic emission theory, equation 6, are basically very similar. However the "saturation Current density" J_{SD} for diffusion theory varies more rapidly with voltage compared to the 'saturation Current density' J_{ST} of the thermionic emission theory.

3. Thermionic Emission-Diffusion Theory

Several authors have combined the Diffusion theory and the thermionic emission theories. The most fully developed being that of CROWELL and SZE in 1966. This approach is derived from the boundary condition of a thermionic recombination velocity V_R, near the metal-semiconductor interface. For the case where the Barrier height is large enough that charge density between metal surface and the edge of the depletion layer (W) is essentially that of ionised donors an applied voltage, V, between the metal and semiconductor bulk would give rise to a flow of electrons in the metal. According to Crowell and Sze the current density, J, is given as

$$J = \frac{qNcvR}{1+\frac{V_R}{V_D}} \exp\left[\frac{-q\phi_{Bn}}{KT}\right]\left[\exp\left(\frac{-qV}{KT}\right)-1\right] \quad (10)$$

V_D is an effective diffusion velocity associated with the transport of electrons from the edge of the barrier, W, to the potential energy minimum, and is given by

$$V_D = \left[\int_{X_M}^{W} \frac{\sigma}{nKT}\exp\left[-\frac{q}{KT}(\phi_{Bn}+\psi)dx\right]\right]^{-1}$$

If no electrons, passing from semiconductor to metal, are scattered back into the semiconductor then $v_R = \frac{\bar{v}}{4}$ where $\bar{v}$ is the average thermal velocity of electrons in the semiconductor.

If $v_D \gg v_R$ the pre-exponential term in equation 10 is dominated by v_R and thermionic emission theory most nearly applies.

If $v_D \ll v_R$ then the diffusion process dominates. If image forces are neglected and the electron mobility, μ, were independant of electric field then

$$v_D = \mu E$$

where E is the electric field in the semiconductor near the boundary.

Crowell and Sze derived a complete expression of the current density-voltage characteristics which took into account f_p, the probability of electron emission over the potential maximum, and f_q, the theoretical ratio of total current flow, considering tunnelling and quantum mechanical reflection, to the current flow neglecting these effects i.e.

$$J = J_S\left(e^{\frac{qV}{KT}} - 1\right) \tag{11}$$

where

$$J_S = A^{**}T^2 \exp\left[\frac{-q\phi_{Bn}}{KT}\right] \tag{12}$$

$A^{**} = \dfrac{f_p f_q A^*}{\left(1+f_p f_q \frac{v_R}{v_D}\right)}$ is the effective Richardson Constant.

4.1 SCHOTTKY BARRIER HEIGHT MEASUREMENTS

1. I-V Measurements

(a) Forward Characteristics

From equation (11) one can predict the ideal forward characteristics of a Schottky Barrier Diode. If $V > \frac{3KT}{q}$ then the equation may be rewritten as

$$J = A^{**}T^2 \exp\left[\frac{-q\phi_B}{KT}\right] \exp\left[\frac{q(\Delta\phi+V)}{KT}\right] \tag{12}$$

where ϕ_B is the zero field asymmetric barrier height

A^{**} is the effective Richardson Constant = $\dfrac{4\pi q m^* k^2}{h^3}$

$\Delta\phi$ is the Schottky barrier lowering

M^* is the effective mass of an electron in the semiconductor.

A^{**} and $\Delta\phi$ are functions of applied voltage, so that the forward J-V characteristic is not represented by $J \simeq \exp(\frac{qV}{KT})$ but rather by

$$J \simeq \exp\left(\frac{qV}{nKT}\right)$$

n is the ideality factor and is given by $n = \dfrac{q}{KT} \dfrac{\partial V}{\partial(\ln J)}$

the saturation current is then given by

$$J_s = A^{**}T^2 \exp\left(\frac{-q\phi_B}{KT}\right) \qquad (13)$$

J_s is found experimentally by extrapolating the value of current density to zero voltage. It is seen that from this the Barrier Height can be obtained

i.e. $$\phi_{Bn} = \frac{nKT}{q} \ln\left[\frac{A^{**}T^2}{J_s}\right] \qquad (14)$$

for an ideal barrier the value of n, the ideality factor, is unity. The value of 'n' is easily determined since $\frac{\partial V}{\partial \ln J}$ is the reciprocal of the slope of the graph of lnJ against applied voltage V.

The junction resistance R_j of a metal-semiconductor contact is given by

$$R_j = \frac{\partial V}{\partial I} = \frac{nKT}{q \cdot J \cdot A_j}$$

where A_j is the area of the contact.

If the forward bias is sufficiently high then the junction resistance approaches a constant value. This value is the series resistance, R_s, and is given by

$$R_s = \underbrace{\frac{1}{A_j}\int_{x_1}^{x_2} \rho(x)dx}_{i} + \underbrace{\frac{\rho B}{4r}}_{ii} + \underbrace{R_c}_{iii}$$

Term i is the series resistance of the quasi neutral region; x_1 and x_2 denote the depletion layer edge and the surface layer-susbstrate boundary.

Term ii is the spreading resistance of the metal-semiconductor barrier substrate, with resistivity ρB and circular area of radius r.

Term iii is the resistance due to the ohmic contact with the substrate.

(b) Reverse Characteristics

In the reverse direction the dominant effect is due to Schottky barrier lowering i.e.

$$J_R \simeq J_S \quad \text{if} \quad V_R > \frac{3KT}{q} = A^{**}T^2 \exp\left(\frac{-q\phi_B}{KT}\right) \exp\left(\frac{+q\sqrt{qE/4\pi Eo}}{KT}\right)$$

where $E = \sqrt{\frac{2qN_D}{E_s}\left(V+V_{bi}-\frac{KT}{q}\right)}$

If the barrier height $q\phi_{Bn}$ is reasonably smaller than the band gap such that the depletion layer generation-recombination current is small compared to the Schottky Emission Current then the reverse current will increase gradually with reverse bias.

2. C-V Measurements

The barrier height can be determined by capacitance measurements. When a small A.C. voltage is superimposed on a d.c. reverse bias, charges, of one sign are induced on the metal surface and charges of the opposite sign in the semiconductor by a slight widening of the depletion layer. The space charge layer may be represented by an effective capacitance $C(=\varepsilon/d)$ per unit area. ε is the permittivity of the semiconductor, and d is the depletion layer width. As a larger reverse bias voltage is applied the depletion layer expands as

$$d = \frac{2\varepsilon (V_d-V)^{\frac{1}{2}}}{qN_D}$$

V_d is the diffusion potential, N_D is the dopant density, V is the reverse bias voltage. Consequently the capacitance C decreases

$$C = A\,\frac{qN_D\varepsilon^{\frac{1}{2}}}{2(V_d-V)} \qquad \text{A is sample Area}$$

$$\text{or} \qquad \frac{1}{C^2} = \frac{2}{A^2 q\varepsilon N_D}\cdot(-v) + V_d$$

Hence a plot of $1/C^2$ against reverse bias should be linear with intercept V_i and slope $= 2/A^2 q\varepsilon N_D$. This plot does not however give the barrier height directly, it only gives the diffusion potential $V_d(V_d=V_i+KT/2)$. To this must be added the Fermi Energy V_n. This can be calculated directly from the donor density N_D (N_D is calculated from the slope of the plot).

$$N_D = N_C \exp\left[\frac{-qV_n}{KT}\right]$$

N_C is the density of states in the conduction band and is given by

$$N_C = 2\left[\frac{2\pi M_d eKT}{h^2}\right]^{\frac{3}{2}} Mc$$

where M_c = number of equivalent minima in the conduction band which for CdTe = 1.

M_{de} = density of state effective mass of electrons.

Hence one can now calculate V_n and hence ϕ_{Bn}

$$\text{i.e.} \quad \phi_{Bn} = V_d + V_n$$

$$= V_i + V_n + \frac{KT}{q} - \Delta\phi$$

$$\phi_{Bn} \simeq V_i + V_n + \frac{KT}{q}$$

4.2 EXPERIMENTAL

Metal semiconductor contacts were investigated using several techniques, some applied sequentially to samples in the same UHV system. The experimental investigation really consisted of two types of experiments.

First the magnitude of Schottky barriers were measured using the methods of I-V, C-V and UPS.

Second, formation of Schottky barriers was monitored by looking at the surface using XPS, UPS, AES and LEED, during the fabrication of the barriers.

1. Schottky Barrier Heights measured by Current Transport Properties

(a) Fabrication of Contacts

n Type CdTe crystals grown by the Fast Vertical Bridgman method of crystal growth and doped with Indium were selected for use here. After various experiments it was found that crystals grown from Ingots doped with 2×10^{18} atoms cm^{-3} of In and slow cooled gave best results. Electrical properties were typically of the order:

Resistivity/Ω cm: 10-50

Mobility/$cm^2\ v^{-1}\ s^{-1}$: ~500

Carrier Concentration/cm^{-3}: ~10^{17}

Samples were cleaved and ohmic contacts made to one side of the crystals by evaporating high purity (99.9999%) Indium, from a Molybdenum boat, in a vacuum of 10^{-6} torr. Contacts were then annealed by heating the samples in vacuum to 200°C for 10 minutes. For this purpose an evacuatable quartz furnace was constructed. The CdTe surface onto which metal, M was to be evaporated was then prepared, using one of the surface preparations, air cleaved, vacuum cleaved or etched, described in the previous section. Samples were then placed

in holders and placed inside a UHV system. At this point electrical contact was made to the ohmic contact via an insulated wire from a lead through one of the ports of the UHV chamber. The UHV chamber was then evacuated to $\sim 5\times10^{-10}$ torr and left unbaked. It was found that baking the UHV system at this point produced very inconsistent results probably due to the ohmic contact evaporating off or diffusing through the crystal. Vacuum cleaved surfaces were prepared, immediately prior to metal evaporation, using a specially constructed cleaver placed as close as possible to the metal evaporation port. Metals were generally evaporated from tungsten filaments. A glass tube with a mask, containing several holes of 1 mm diameter, was placed around the filament. Immediately after cleavage the crystal face was manoeuvred in front of the mask and the metal evaporated. Filaments and metal were both outgassed thoroughly prior to evaporation of the metal onto the semiconductor surface. After evaporation I-V and C-V measurements were carried out either in vacuum or air. For measurements carried out in UHV electrical contact was made to the evaporated metal surface by a small manoeuvreable gold probe attached to an insulated lead through. The I-V and C-V measurements were then carried out by attaching the measuring circuits to the two lead throughs.

Measurements made in air were restricted to investigations of metal contacts to air cleaved and etched surfaces. After metals had been evaporated onto these surfaces in UHV the samples were removed and prepared for I-V and C-V measurements as follows: samples were attached to stainless steel base plates and contact made to the ohmic In contact using silver conductive paint. Contact to the top metal electrode was made using a fine gold probe. I-V and C-V measurements were then made in the manner described below.

(b) I-V Circuit

It can be seen that measurement of the forward I-V characteristics of a Schottky diode enables one to calculate the Schottky Barrier Height i.e.

$$\phi_{Bn} = \frac{nKT}{q} \ln\left[\frac{A^{**}T^2}{J_S}\right]$$

If one measures the variation in I, and hence variation in J, the current density, with variance of the d.c. voltage V applied then one can plot lnJ against voltage V. Current density J = Current ÷ Contact area. From this plot one can extrapolate the line to V = O to find J_S the saturation current density. The value of n is obtained from the slope of the line.

Barriers were fabricated, and mounted as described previously. By applying a d.c. voltage (V), supplied from

a battery operated power supply, in the forward direction i.e. Metal→Semiconductor→ohmic contact one gets a current generated. Measurement of this current at different values of V will give the points to enable a lnJ against voltage plot to be drawn. From this plot one can calculate ϕ_{Bn} and 'n' the ideality factor.

In some cases, where higher resistivity (~1000Ωcm) CdTe was used, the problem of the series resistance of the crystal was encountered. This led to non-linear plots in the higher voltage (>0.3v) regions. This was compensated for by estimating the series resistance of the crystal through applying a fairly high voltage. Once the series resistance was known, one could adjust the readings at lower voltages to enable linear plots, due to the surface barrier only, to be obtained.

Experimentally, voltages were measured using a Keithly Electrometer Model No.602. Currents were measured using an AVO multimeter which could measure currents from 1μA to 10.0 amps accurately. The D.C. power supply enabled voltages of up to 10 volts, to be applied.

(c) C-V Circuit

The current through the depletion region of a Schottky diode can be considered as being made up of two components, the Conduction current, J_C, and the displacement current, J_D. The Conduction current J_C can be split into two components J_{C_1}, due to drift and diffusion of electrons injected over the barrier and into the metal, and J_{C_2}, due to the flow of electrons and holes out of the depletion region. J_{C_1} exists even if there is no variation of bias with time and constitutes the reverse current of the diode. J_{C_2} exists only if there is a change in bias. J_{D_1} the displacement current is given by $J_D \simeq E_S \frac{\partial E}{\partial T}$ i.e. the electric field increases with time as the bias increases.

Consider a reverse bias (D.C.) varying sinusoidally being applied to a Schottky diode. J_{C_1} will be in phase with the bias and will be the parallel conductance G_x. J_{C_2} and J_D will be 90^o out of phase and will give rise to the capacitance C_x (although both J_{C_2} and J_D both vary with x, their sum $(J_{C_2}+J_D)$ remains constant).

Hence measurement of the out of phase component will give an indication of C_x, and of the phase component G_x. To see how this is done one must first of all consider what effect applying an a.c. signal to a Schottky diode has.

A Schottky barrier can be thought of as a resistor, R_x, in parallel with a capacitance, C_x. If an a.c. signal is applied to this then the total impedance at frequency ω, may be written as

$$Z_x = \frac{1}{G_x + j\omega C_x}$$

G_x is the sample conductance and is equal to $1/R_x$. Bridge techniques are commonly used to measure C_x or G_x with respect to the frequency. If however one of the components of impedance is much greater than the other i.e. $G_x \gg C_x$ or $C_x \gg G_x$ then the standard bridge techniques break down, as the phase angle becomes either very small or very large. A phase sensitive detection system is therefore used. Fig.4.1 represents a schematic diagram of one such system. If the sample, C_x and R_x, is in series with a standard capacitor C_o, then if a voltage V is applied to the sample a voltage V_o appears across C_o comprising of two components. One In phase with the applied signal and the other in quadrature. From standard a.c. theory the form of these two components of V_o can be written as:

$$V_o(\text{in phase}) = \frac{\omega^2 C_x (C_o + C_x) + G_x^2}{\omega^2 (C_o + C_x) + G_x^2}$$

$$V_o(\text{out of phase}) = \frac{\omega C_o G_x}{\omega^2 (C_o + C_x) + G_x^2}$$

the ratio of these terms is:-

$$\frac{V_o(\text{in phase})}{V_o(\text{out of pnase})} = \frac{\omega^2 C_x (C_o + C_x) + G_x^2}{\omega C_o G_x}$$

since $G_x = \frac{1}{R_x}$ then

$$\frac{V_o(\text{in phase})}{V_o(\text{out of phase})} = \frac{\omega^2 R_x^2 C_x (C_o + C_x) + 1}{\omega C_o R_x}$$

if C_o is chosen such that $C_o \gg C_x$, the sample capacitance, and as $G_x \ll \omega C_o$ then

$$\frac{V_o(\text{in phase})}{V_o(\text{out of phase})} = \omega C_x R_x \qquad (15)$$

This can therefore be used to measure the conductance over a selected frequency range. If a.c. conductivity measurements were to be taken a known resistor and capacitor in parallel would be placed in series with the standard capacitor C_o. The values of the known resistor and capacitors would be chosen to be as close as possible to the resistance and capacitance

of the sample. Care should be taken so that the value of C_o chosen would be at least ten times the capacitance of the sample. A small a.c. field, of the order of 10-20 mV would be applied to the capacitor-resistor combination using a wide range low frequency oscillator. The resulting voltage V_o, appearing across C_o, would be fed into a low noise amplifier and then into a phase sensitive detector. A phase shifter and a reference unit would deal with a reference signal coming straight from the oscillator. The phase shifter, common to both channels, compensates for any stray phase shift of the a.c. signals due to, for example, lead capacitances and the input impedance of the amplifier. The reference unit would give the desired 90^o phase difference between the two detectors. This arrangement meant that while one phase sensitive detector gave readings proportional to V_o (in phase) i.e. proportional to C_x, the other gave readings proportional to V_o(out of phase) i.e. proportional to G_x.

The values of known resistance and capacitance are substituted into equation (15) to give a ratio between the in phase and out of phase voltage components. When the known resistance and capacitance are plugged into the circuit the ratio of in phase and out of phase voltages can be measured and checked against the calculated ratio. Any small discrepancy in the two values can be removed by adjusting the phase shifter on the reference unit. Various values of known resistances and capacitances are used to check that the readings given by the detectors scale in proportion to the change of input resistance and capacitance. When this is the case the system is said to balance. The sample is now plugged into the system and its capacitance obtained by direct comparison with the known standard capacitors. G_x can be calculated from equation (15) by substituting the in phase and out of phase signals, capacity and frequency. To measure Schottky barrier heights we need to know how capacitance and conductance of the samples varies when a reverse d.c. voltage bias is applied. The circuit shown in Fig.4.1 is modified to that shown in Fig.4.2. D.C. and A.C. voltages were fed through separate inputs. The a.c. signal was superimposed on the d.c. level bypassing the a.c. signal through an inductance. A resistor, R, was used in place of C_o with a value equal to or greater than $1/\omega C_o$. It was also necessary that the value of R was much less than the value R_x. This ensured that most of the applied d.c. voltage was dropped across the sample. Instead of using separate phase sensitive detectors, phase shifters etc. we used an ORTHOLOC model 9502 2 phase lock-in amplifier and Vector Voltmeter. Incorporated into this instrument was an ORTEC BROOKDEAL model 5012F variable oscillator. For measurements of Schottky barrier heights on CdTe we used a frequency of $10KH_3$. The measurement technique was similar to the method

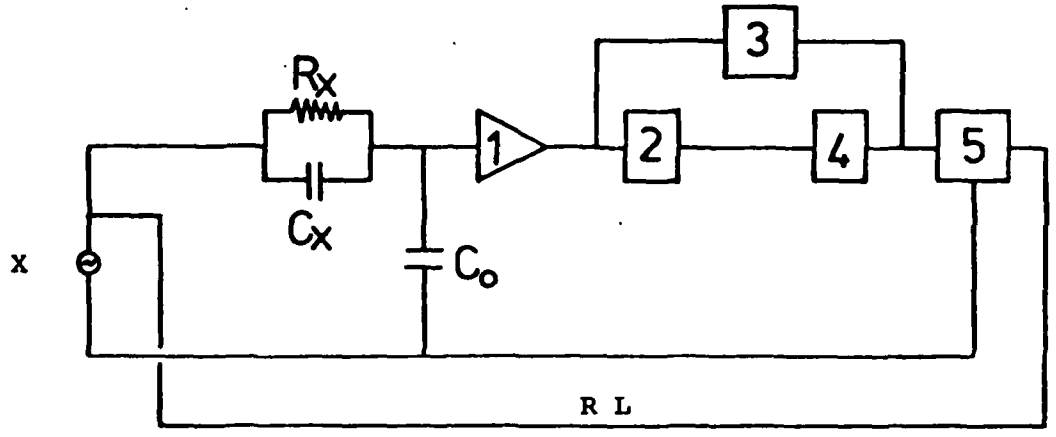

Fig. 4.1 Schematic Diagram of the Phase Sensitive Technique Available to Meansure A.C. Conductivity

(Rx, Cx): Sample: 1. Low Noise Amplifier: 2,3 are Phase Sensititve Detectors: 4,5 are Phase Shifters. X is a low Frequency Oscillator. R L is the Reference Line.

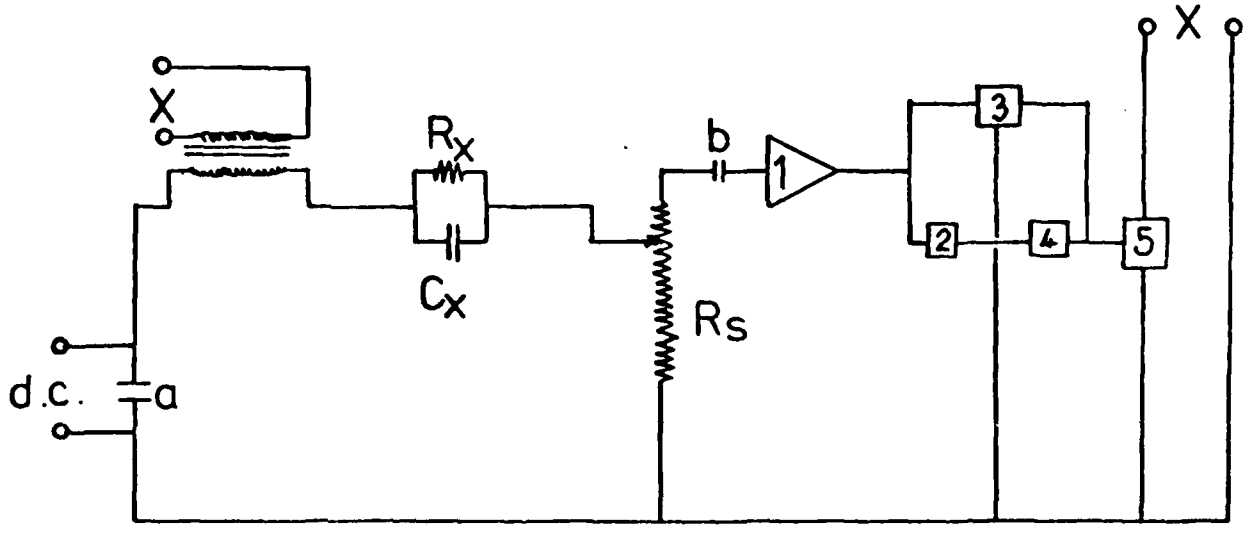

Fig. 4.2 Schematic Diagram Illustrating the Phase Sensitive Technique Employed to Measure Schottky Barrier Heights by the C-V Method.

(Rx, Cx) is the Sample: R_s is a variable resistance to allow variation in Sensitivity: a=4.7μF, b=250μF: 1 is Low Noise Amplifier: 2,3 are Phase sensitive detectors: 4,5 are Phase Shifters: X is the low frequency oscillator.

above. The bridge was balanced using resistors and capacitances of known values. Conductance and capacitance were measured as before by measuring the magnitude of the in phase and out of phase components of voltage, and comparing them with those of standard capacitances and resistors. The applied reverse d.c. bias varied from a simple battery operated power supply. Values of C_x were measured for various values of reverse d.c. bias. A plot of $1/C_x^2$ against reverse bias was made and from this the slope, equal to $2/Aq^2\varepsilon N_D$, and the intercept, equal to V_i were measured. From these values one can calculate N_d, the dopant density, and from this one is able to calculate V_n, the Fermi energy, from the relationship

$$N_d = N_c \exp\left[\frac{-qV_n}{KT}\right]$$

Where N_c is the density of states in the conduction band and is given by

$$N_c = 2\left[\frac{2\pi M_{de} KT}{h^2}\right]^{\frac{3}{2}} M_c$$

for CdTe, N_c was calculated to be 1.31×10^{18} cm^{-3} assuming the following values:

M_{de} = density of state effective mass of electrons = $0.14M_o$

M_c = number of equivalent minimum in the Conduction band and is equal to 1 for CdTe

Knowing V_n, the fermi energy and V_d, the diffusion potential one can calculate the barrier height ϕ_{Bn}. V_d, the diffusion potential is given by:

$$V_d = V_i + \frac{KT}{q}$$

where V_i is the intercept of the $1/C_x^2$ against reverse bias.

Therefore

$$\phi_{Bn} = V_i + V_n + \frac{KT}{q}$$

$$\phi_{Bh} = V_d + V_n$$

2. Schottky Barrier Formation Investigation

The formation of Schottky barriers on various surfaces of n type CdTe was investigated using the techniques of XPS, UPS and AES. These techniques have been reviewed previously. UHV systems 1, 2 and 3 were used in this

investigation. The main change in the UHV systems used for this investigation was the provision of metal evaporation systems. These were of the resistance heated filament type, usually tungsten. Three core tungsten wire was used for evaporation of Aluminium and single core tungsten wire for gold, silver etc. The filaments were made in our laboratory. Prior to loading a filament with metal, for evaporation, the new filament was inserted in a small UHV chamber, electrical connections made to it, and the chamber evacuated. The filament would then be "outgassed" by "flashing" to white heat a few times, till no further outgassing was seen. Metals to be evaporated were in the form of high purity (99.999% pure) wire, where available. Filaments, which had been outgassed, were attached using stainless steel connectors to two insulated lead throughs on a 2¾" flange. Small loops of the metal wire were made and threaded onto the spirally wound filaments. The filaments were then inserted into the UHV chamber, the glass envelope with evaporating mask put in place, the CdTe Crystals introduced to the chamber and the system evacuated to $\sim 10^{-9}$ torr. The filament and metal were outgassed in UHV by slowly melting the metal on the filament. If this was carried out slowly then the vacuum didn't suffer too much and recovered quickly, and the metal would generally form "Blobs" on the bottom of the filament from which evaporation of metal occurred. During this procedure a blank crystal holder was placed over the evaporation mask to prevent contamination of the inner walls of the chamber and the prepared CdTe surface. Evaporation of metal onto the CdTe surface could be controlled in one of two ways.

In the first of these the crystal was put into position at the evaporating mask and a constant current was applied to the filament. The crystal was left in the metal stream for a measured period of time, and then turned out of the metal stream and the current to the filament turned off. The main disadvantages of this system were that filaments tended to burn out quickly, the 'blobs' of metal tended to fall off the filaments and the rate of metal evaporation was not constant. This last observation was due to the fact that as the metal is evaporated from the filament, the load on the filament reduces so, for a constant current, the filament becomes progressively hotter and the rate of evaporation increases.

In the second method a blank crystal holder is put into position in front of the glass evaporation funnel and the filament slowly heated up until metal evaporation occurs. Metal evaporation is increased till a constant pressure reading is achieved. For instance if the base pressure prior to metal evaporation was 5×10^{-10} torr, then an evaporation pressure of, say, 10^{-9} torr was used. The crystal was then quickly turned into the metal stream for a pre-determined

period of time, say 10 seconds, then turned out of the stream and the filament current reduced to zero. The main advantage of this system is that one can be more certain of obtaining a constant number of atoms of metal impinging on the semiconductor surface in consecutive periods of time than with the previous method and therefore plots involving evaporating times will be more meaningful. The main drawback of this system is that it tends to use up the metal on the filament quicker than the previous method, and each evaporation takes longer, since time is spent adjusting the filament current until the correct rate of metal evaporation is achieved. This second evaporation technique was used in UHV system 2 and 3 where XPS and UPS investigations were carried out. The procedure was a continual one of recording a spectrum, moving the sample into a metal stream for evaporation, moving the sample back into the spectrum recording position, recording a spectrum, moving the sample into the metal evaporation stream etc. This was carried out until a thick film of metal had been evaporated onto the crystal surface or until the Cd and Te emissions had disappeared. In UHV system 1 where AES was carried out metal evaporation technique one was used. This was because the metal evaporator was positioned such that one could evaporate a metal onto the sample surface without moving the sample from its AES position.

In all three UHV systems an Ion gun was available so that depth profiles could be made by etching the surface then recording spectra etc.

4.3 RESULTS

A. Vacuum Cleaved CdTe

1. Gold

Gold on vacuum cleaved CdTe produces a Schottky barrier with a barrier height of 0.96 eV. Rectification for these barriers, measured from I-V data, was of the order of 100-200. Values of 'n', the ideality factor, were in the region of 1-1.5, the higher values being attributed, in some cases, to the series resistance of the bulk CdTe. After allowances, for series resistance etc., had been made to the I-V results it was found that good agreement was obtained between I-V and C-V results. Typical C-V and I-V plots are shown in Figs.4.3 and 4.4. respectively.

AES results showed that as gold is evaporated onto the vacuum cleaved (110) surface there is an immediate fall in peak intensities of both Cadmium and Tellurium see Fig.4.5(a). After a period of more evaporation the situation stabilised and a position of equilibrium was reached where the intensities of both the Cadmium and Tellurium peaks remained constant no matter how much gold was evaporated onto the

surface. A similar phenomena was later seen when the experiment was repeated, on a different crystal in a different system, the VG ESCAIII, using XPS, see Fig.4.5(b).

UPS spectra were recorded in UHV system 2, during Schottky barrier formation. The results are shown in Fig.4.6. It is seen that as gold is deposited so that Cadmium 4d levels move towards the Fermi level i.e. the valence bands are bent upwards in the surface region. The magnitude of the bending and hence of the shift in the Cadmium 4d levels gives an indication of the Schottky barrier height. The movement in the 'd' levels after evaporation of a reasonably thick film of gold was measured to be 0.9 eV, which correlates well with I-V and C-V data.

LEED was attempted on the surface after a thick overlayer of metal had been evaporated. The results showed the metal overlayer to be disordered.

2. Silver

Current transport measurements of this system produced results very different to the gold-vacuum cleaved CdTe system. Very low (<0.1 eV) barrier or ohmic contacts were seen when silver was evaporated onto vacuum cleaved CdTe. These observations were checked by evaporating gold contacts and silver contacts side by side onto the same vacuum cleaved (110) surface of CdTe in the same UHV system at the same time and then measuring the Barrier heights by I-V and C-V. In the case where gold produced a barrier of 0.96 eV silver gave very low or ohmic contacts.

UPS showed no overall movement of the cadmium 4d bands either away from or towards the Fermi level, see Fig.4.7. It could therefore be concluded that a zero barrier or ohmic contact was being produced. AES measurements produced a different behaviour pattern to that seen for gold or vacuum cleaved CdTe, see Fig.4.8a. Initially Cadmium and Tellurium intensities reduce, but the rates of reduction are different. Cadmium is lost more quickly than the Tellurium. At large silver coverages there was still evidence of tellurium on the surface.

XPS results produced different results to those presented by AES. XPS showed that Tellurium was lost from the surface region very quickly (see Fig.4.8b). In fact evaporation of a small film of silver caused Tellurium to disappear from the surface. Cadmium remained in the surface layers (25Å) even after evaporation of quite a thick silver film.

LEED showed the Silver layer to be disordered.

3. Aluminium

I-V and C-V measurements showed, like silver on vacuum

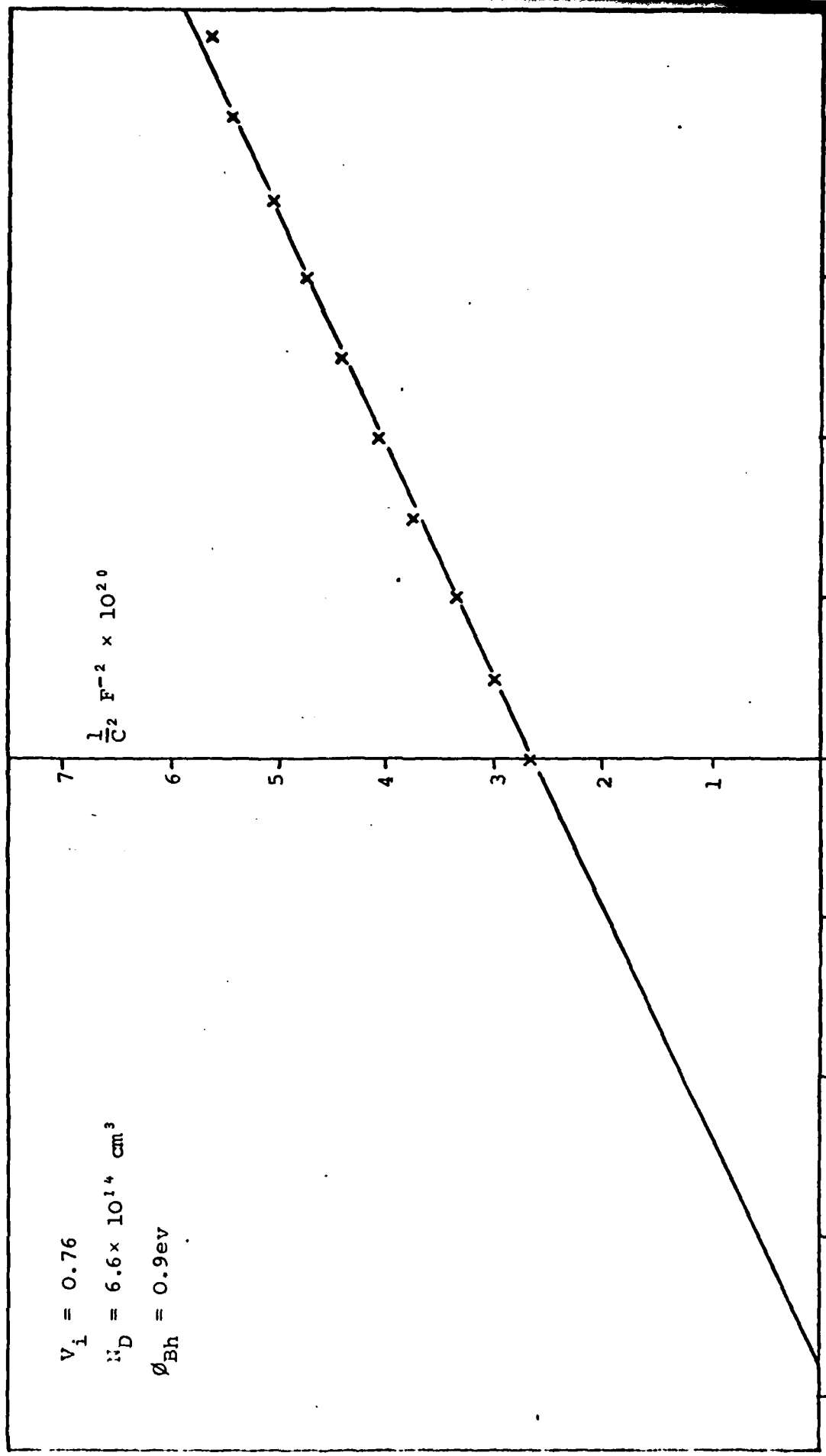

Fig. 4.3 Plot of $\frac{1}{C^2}$ against Reverse Bias for a typical Au - Vacuum cleaved CdTe contact.

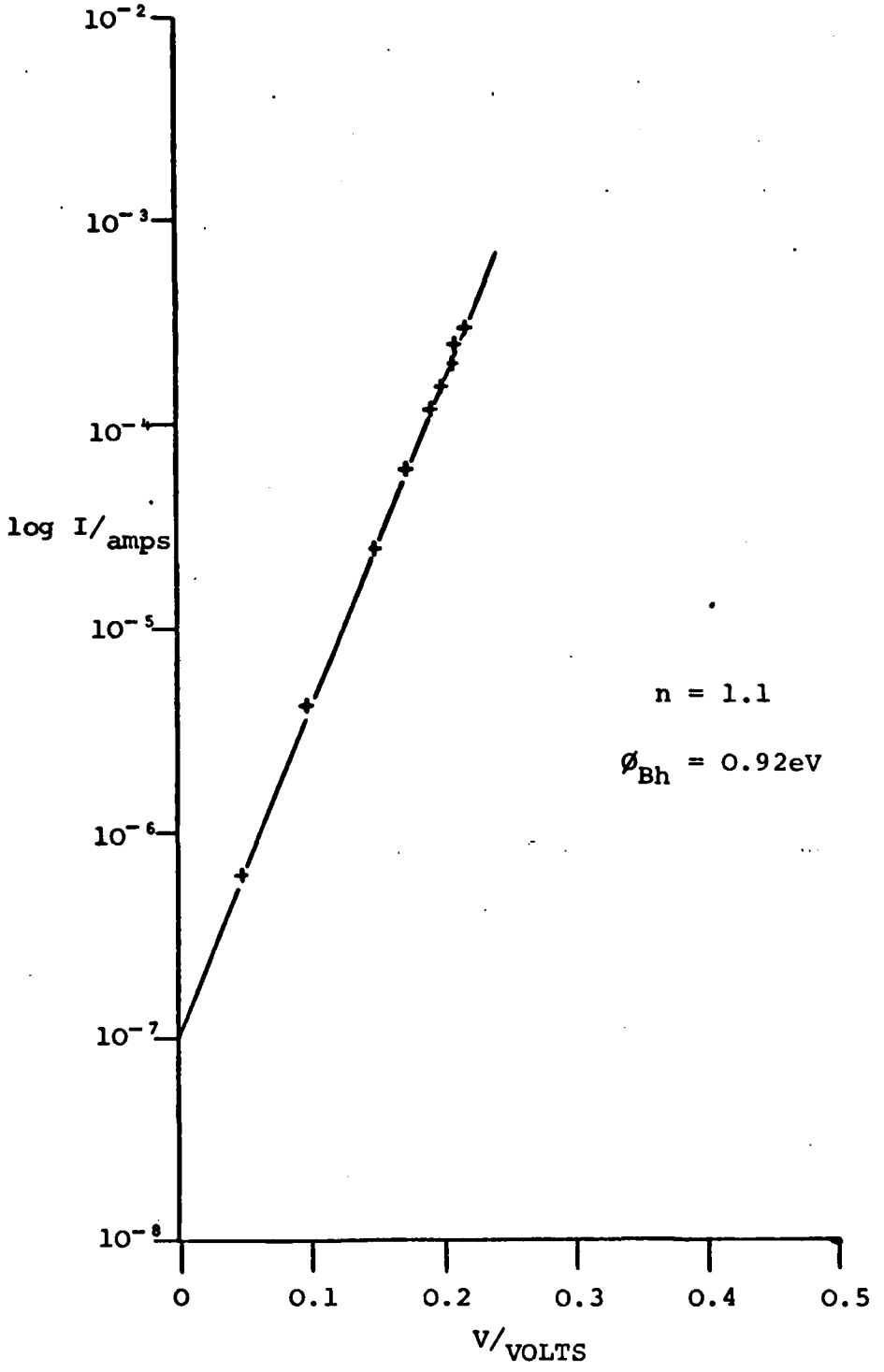

Fig. 4.4 Plot of log I against V for a typical Au-vacuum cleaved CdTe contact.

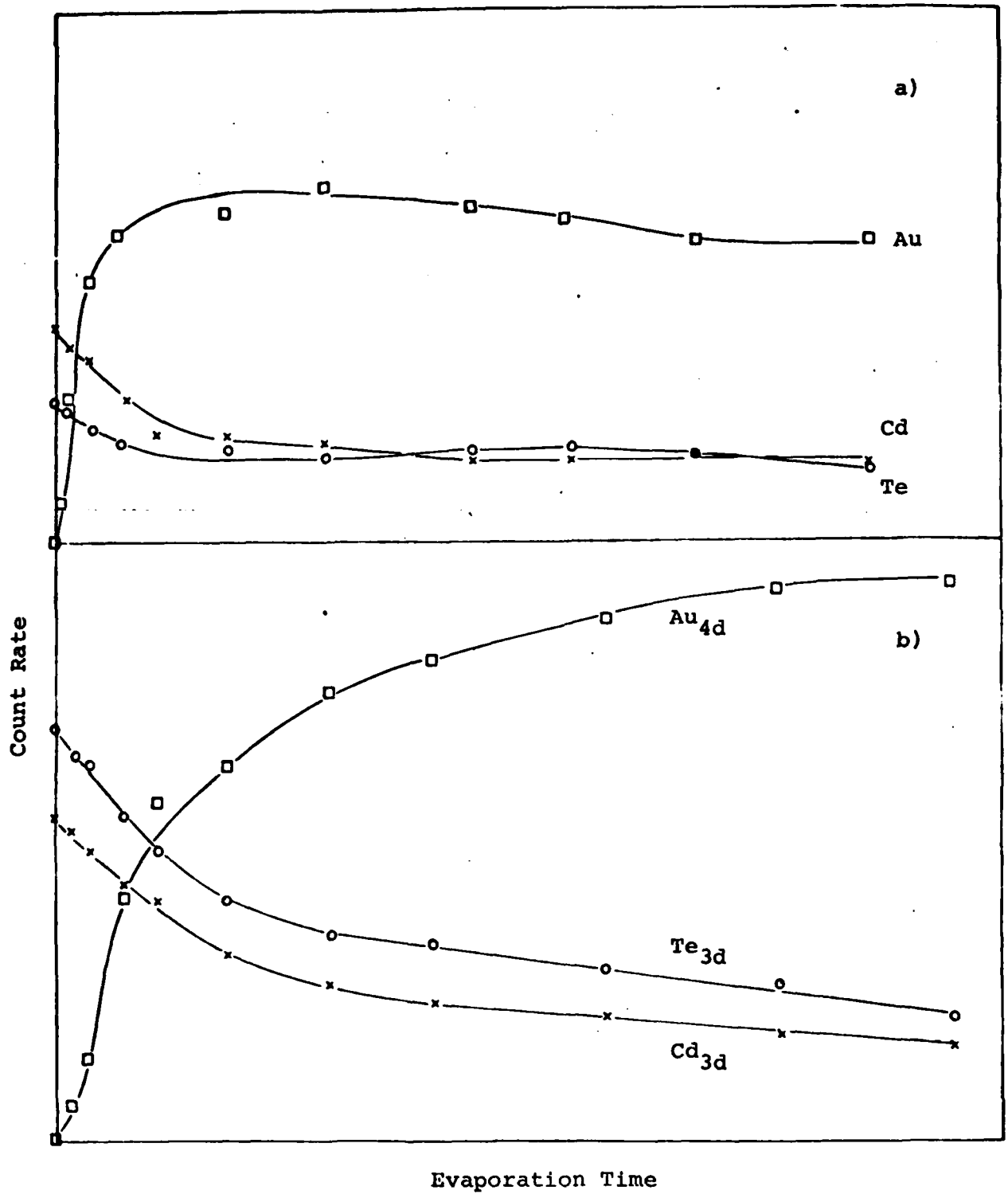

Fig. 4.5 a) AES deposition profile of Au depositing on vacuum cleaved CdTe

b) XPS deposition profile of Au depositing on vacuum cleaved CdTe

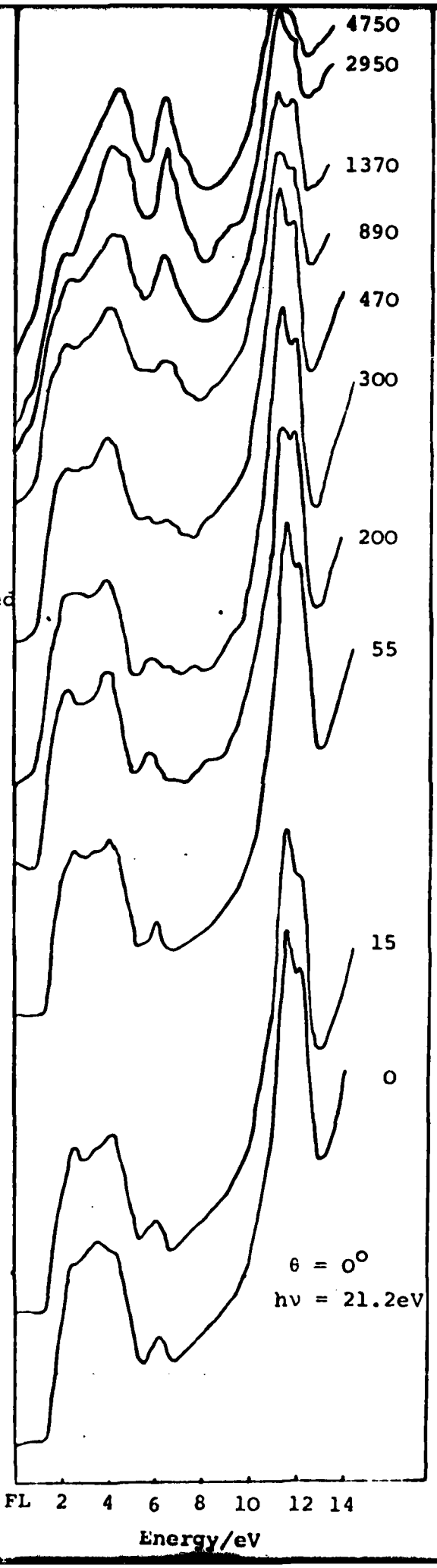

Fig. 4.6 UPS spectra of Au deposited on vacuum cleaved CdTe.

(Evaporation time are in seconds)

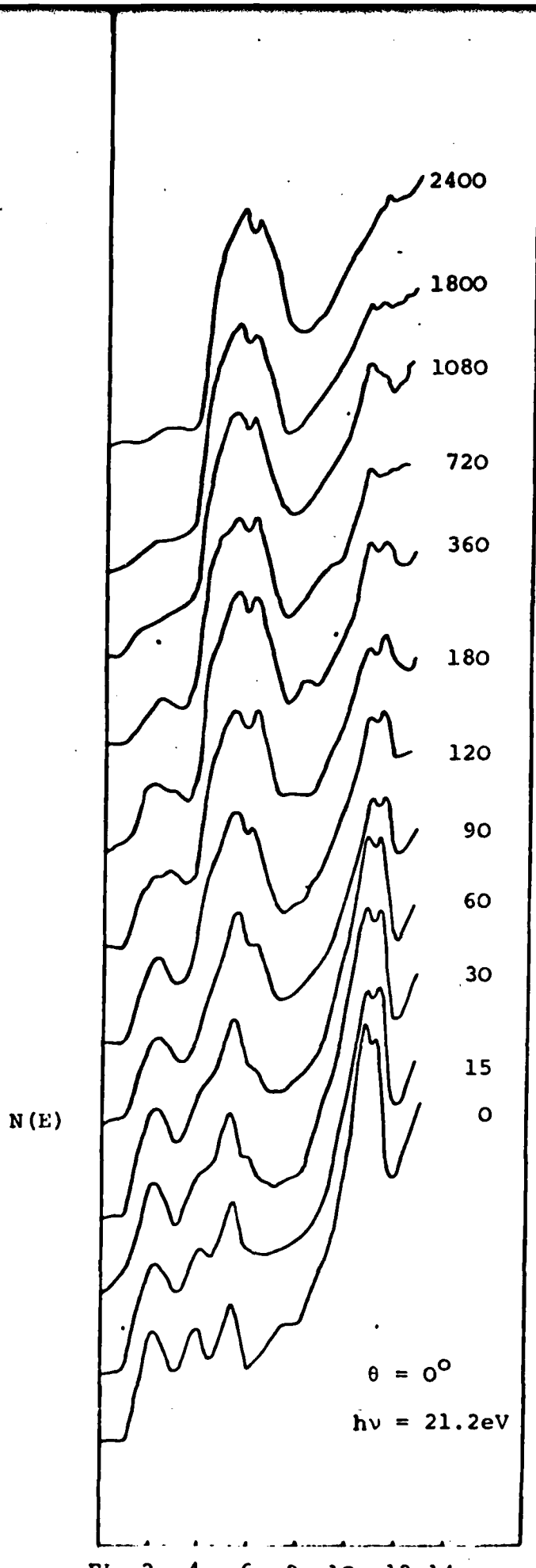

Fig. 4.7 UPS Spectra of Ag deposited on vacuum cleaved CdTe

(Evaporation time are in seconds)

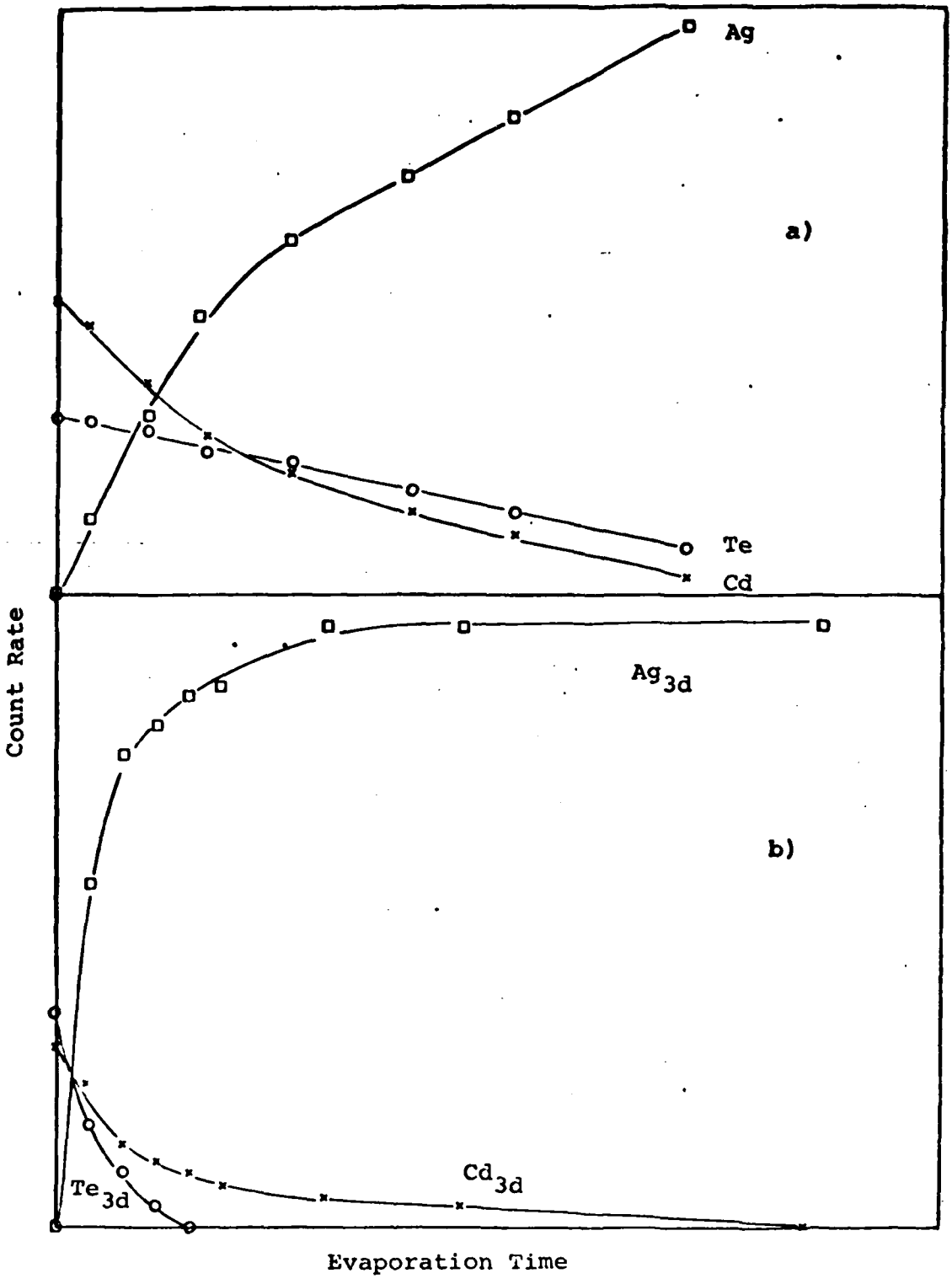

Fig. 4.8 a) AES deposition profile of Ag depositing on vacuum cleaved CdTe

b) XPS deposition profile of Ag depositing on vacuum cleaved CdTe

cleaved CdTe, but unlike gold on vacuum cleaved CdTe, very low barrier or ohmic characteristics. Again to check this observation aluminium contacts were evaporated beside gold contacts on the same vacuum cleaved face of CdTe, in the same UHV system at the same time and the measurements remade. These showed that where Gold gave good Schottky barriers of 0.96 eV, aluminium gave ohmic contact behaviour.

UPS spectra were measured in UHV system 2. The results are presented in Fig.4.9. As can be seen no movement of the Cadmium 'd' bands towards the Fermi level is seen i.e. $\phi_B \simeq 0$. It is noted also that even with large aluminium coverages there is still evidence of cadmium being in the surface layers. This is seen by the small presence of the Cd '4d' bands. It is not possible to say whether Tellurium is present in the surface layers as the positions of the Te levels are enveloped by the aluminium bands.

AES measurements produced a similar result to that obtained for evaporation of silver on V.C. CdTe (see Fig.4.10) i.e. An initial loss of Cadmium and Tellurium with Cadmium being lost more rapidly from the surface than was the case for Tellurium. With large coverages of Aluminium Tellurium is still seen on the surface but Cadmium is lost altogether from the surface.

XPS results again proved to be contradictory. These showed an initial reduction of Cadmium and Tellurium at the same rate. This rate of reduction was fairly slow. At large Aluminium coverages there was still evidence of Cd and Te in the surface layers.

LEED showed the Aluminium overlayer to be disordered.

B. Air-Cleaved CdTe

1. Gold

I-V and C-V measurements on the gold contact to air cleaved CdTe showed the presence of a Schottky Barrier with Barrier height ~ 1.1 eV. Values of n, the ideality factor, were typically in the region 1.0-1.5, with typical rectification of the order 1000-2000. Typical I-V and C-V plots are shown in Figs.4.11 and 4.12 respectively.

AES profiles of the evaporation of gold onto air cleaved CdTe (see Fig.4.13a) proved to be different to the profile of gold evaporated onto vacuum cleaved CdTe. Initially there is a reduction in both Cd and Te as Au is evaporated, but soon Cadmium is lost from the surface. Tellurium remains on the surface even after a thick gold film has been evaporated. XPS produced similar profiles to AES (see Fig. 4.13b). Cd and Te reduce initially at the same rate until Cd disappears altogether and Tellurium is left on the surface even after evaporation of a thick film. UPS was not attempted

due to the EDC of an air cleaved CdTe having so little identifiable structure.

2. Silver

I-V and C-V measurements showed the presence, consistently, of barriers of height ≈0.5 eV. n Values were good i.e. 1.0-1.15 with rectification values typically of the order 50-100. Typical C-V and I-V plots are shown in Figs.4.14 and 4.15.

XPS produced profiles similar to thcse seen for gold on air cleaved CdTe (see Fig.4.16). Cadmium and Tellurium both reduce at about the same rate, as the silver film builds up, until a point is reached where the Cadmium presence reduces to zero. It is then seen that Te remains on the surface even after evaporation of a thick film.

LEED showed the Silver overlayer to be disordered. (AES and UPS have still to be done.)

3. Aluminium

I-V and C-V measurements showed the presence, consistently, of Schottky barriers of height ~0.93 eV. Values of n however were high i.e. 1.5-2.9 but good rectification of the order of 400-500 was seen. Typical I-V and C-V plots are shown in Figs.4.17 and 4.18. AES showed profiles in which Cadmium and Tellurium peaks reduced at about the same rate as Aluminium coverage increased. After a thick film had been evaporated both Cd and Te were seen in the surface layers, although the peak heights were still reducing (see Fig.4.19a). XPS showed a similar behaviour pattern to that seen with AES. (See Fig.4.19b) i.e. As the Aluminium coverage increased so the Cadmium and Tellurium peak intensities reduced. The peak due to TeO_2 also reduces. The TeO_2 peak disappears first followed by the disappearance of both the Cd and Te from the surface layers. At the point where the Cd and Te emissions disappear, the Aluminium peak height has stopped increasing even though more Aluminium is evaporated. This would indicate that here we are seeing an Aluminium film of thickness greater than the XPS probing depth i.e. a film of >25Å has been laiddown.

UPS spectra of Aluminium evaporated on air cleaved CdTe are shown in Fig.4.20. As can be seen, not a lot of information can be gained from the spectra on Schottky barrier formation.

LEED showed the Aluminium overlayer to be disordered.

The Results of the I-V and C-V Barrier Height estimations are presented in Table 4.1, along with the corresponding measurements for InP.

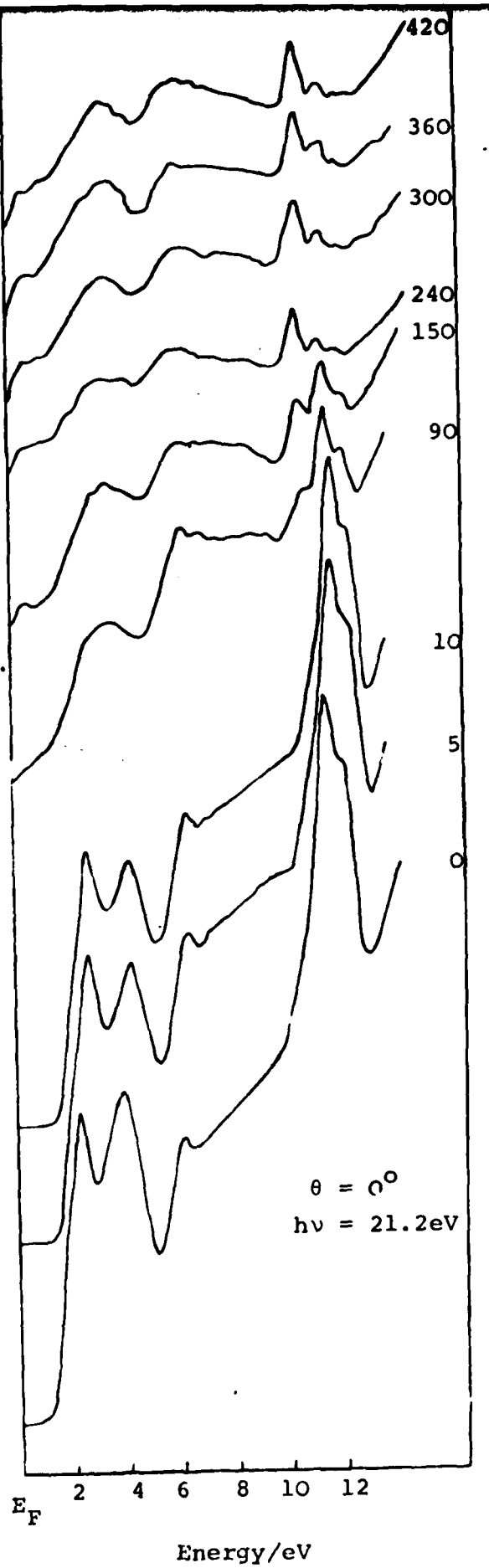

Fig. 4.9 UPS spectra of Al deposited on Vacuum cleaved CdTe

(Evaporation times are in seconds)

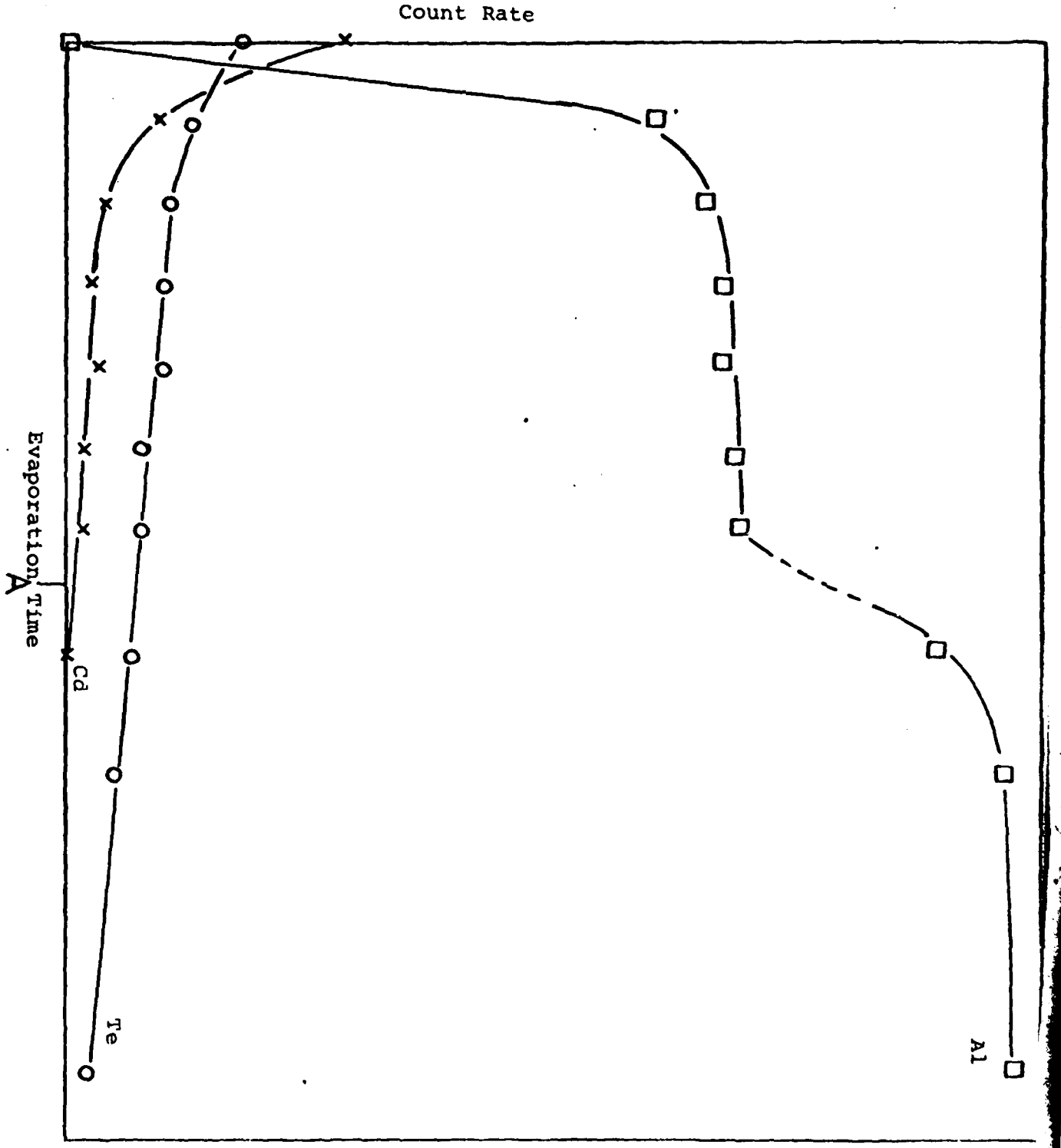

Fig. 4.10 AES deposition profile of Al depositing on Vacuum cleaved CdTe (Evaporation rate increased at 'A')

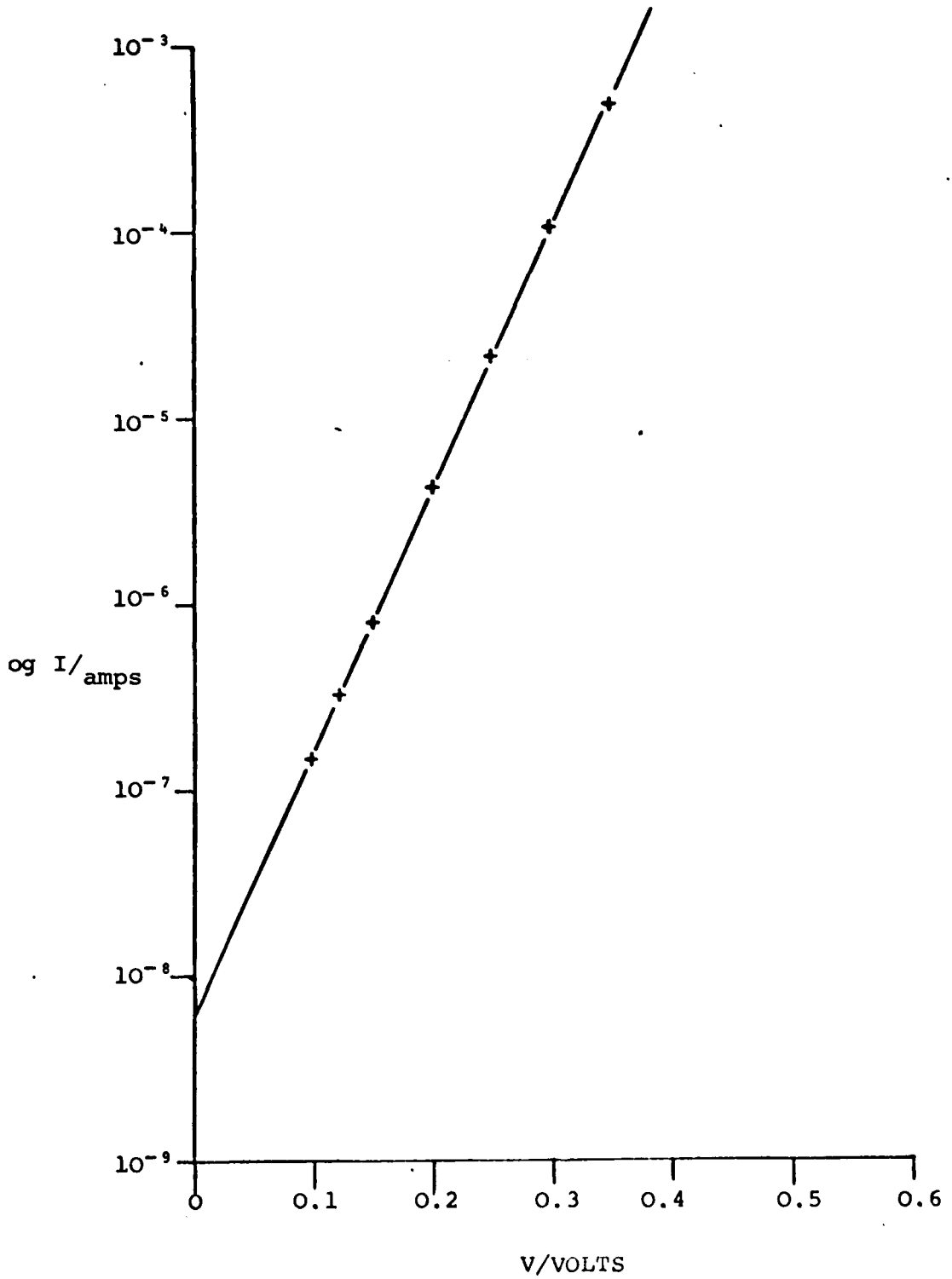

Fig. 4.11 Plot of log I against V for a typical Au-Air cleaved CdTe contact

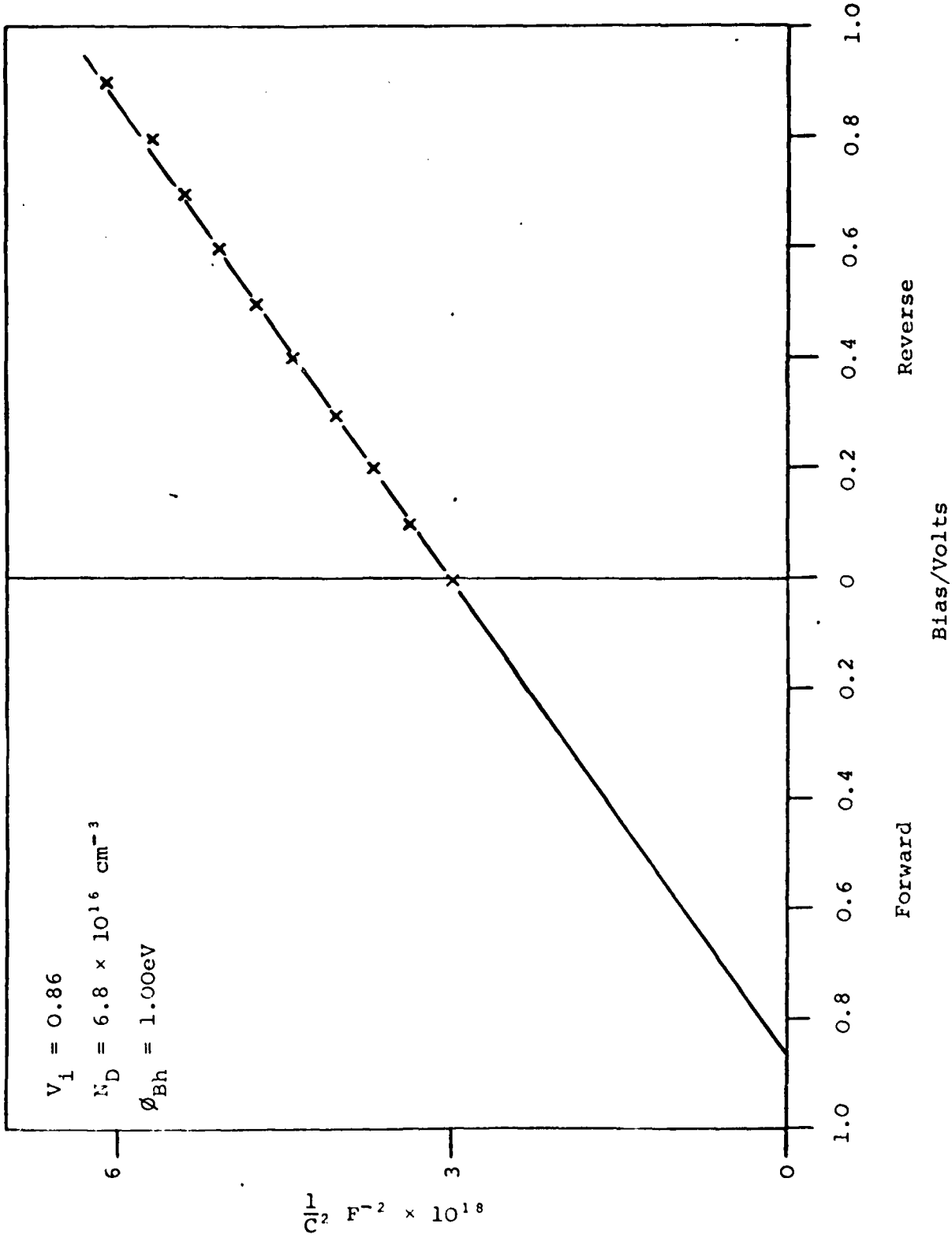

Fig. 4.12 Plot of $\frac{1}{C^2}$ against reverse bias for a typical Au-Air cleaved CdTe contact

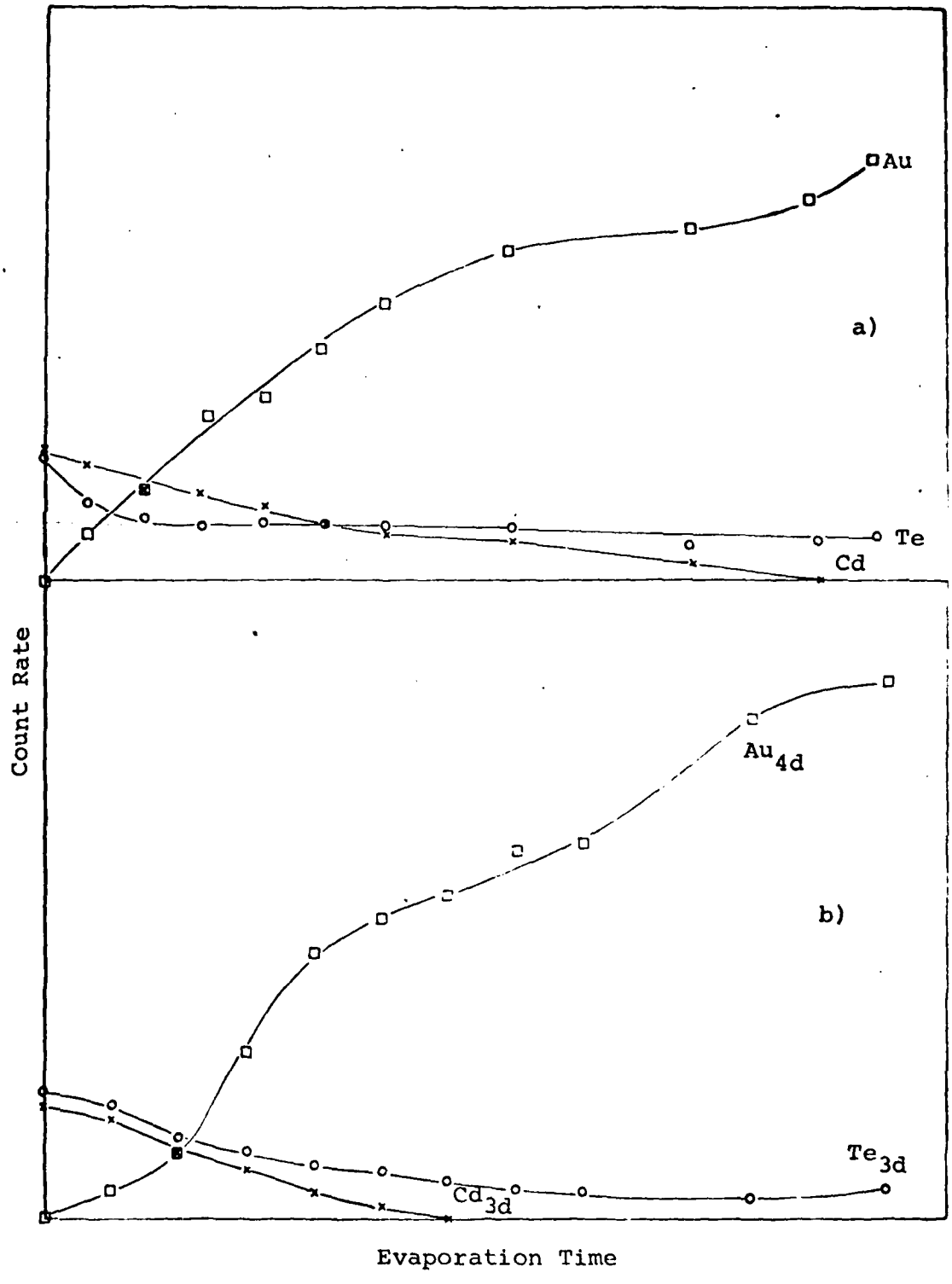

Fig. 4.13 a) AES deposition profile of Au depositing on air cleaved CdTe

b) XPS deposition profile of Au depositing on Vacuum cleaved CdTe

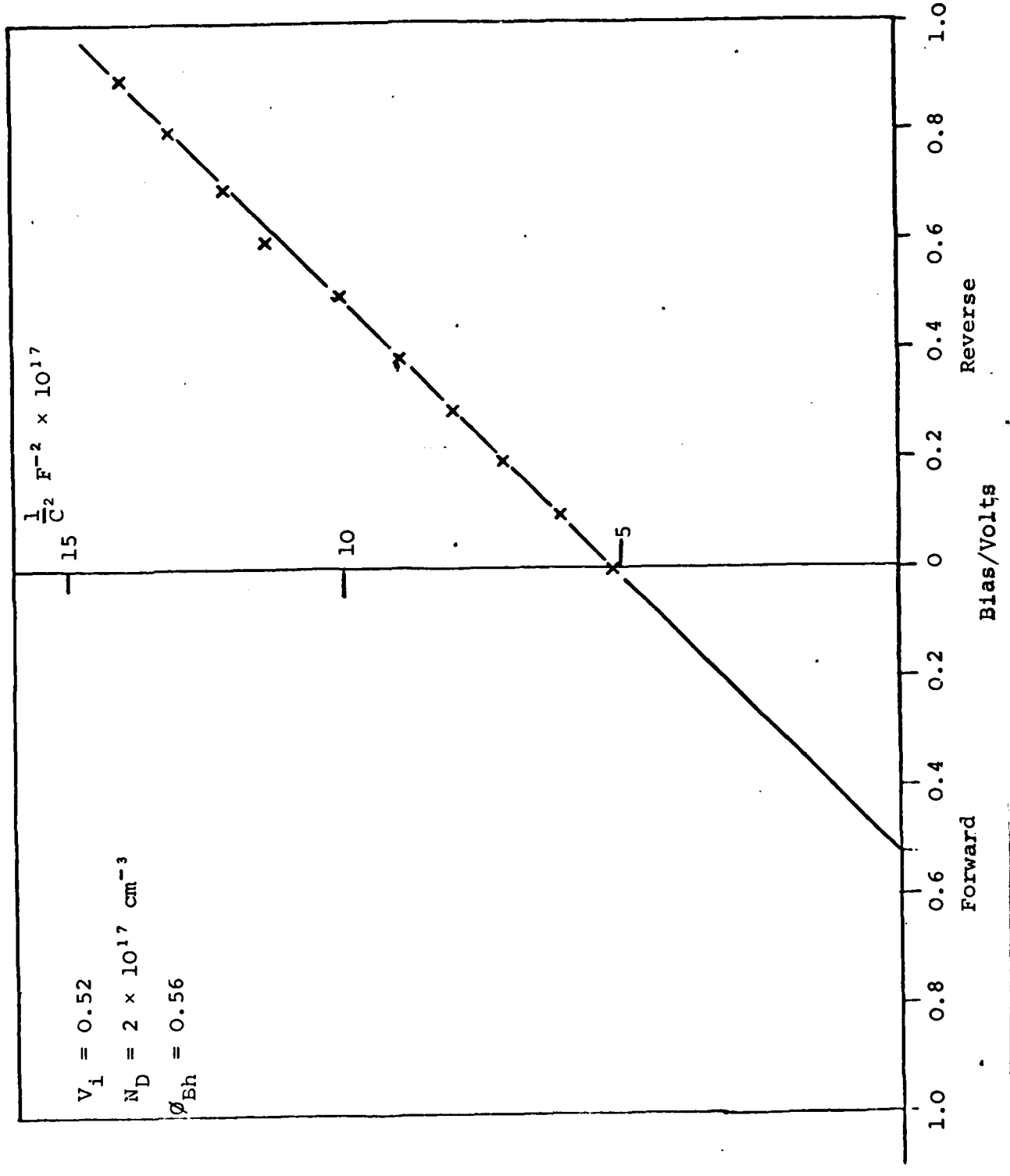

Fig. 4.14 Plot of $\frac{1}{C^2}$ against reverse bias for a typical Ag-Air cleaved CdTe contact.

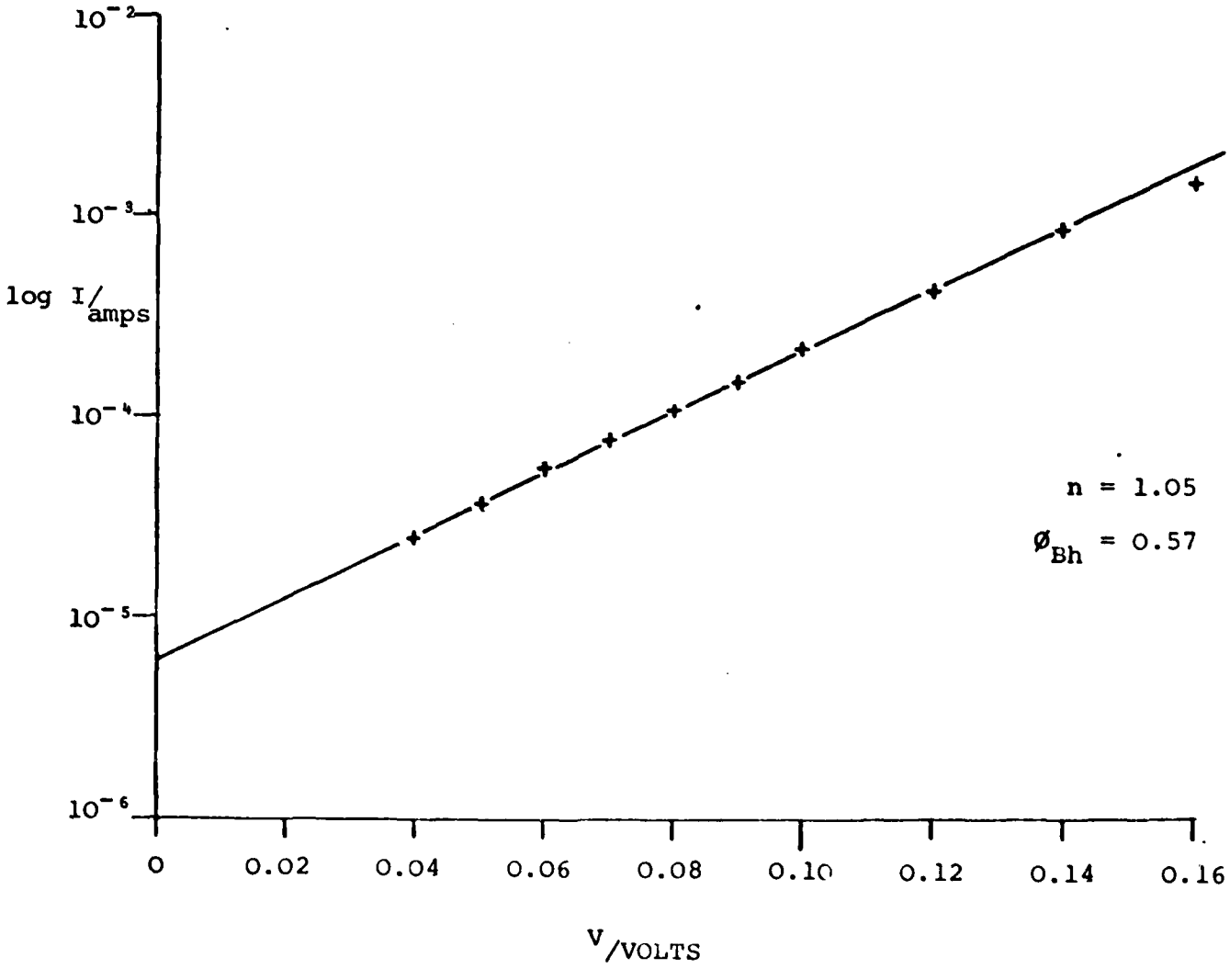

Fig. 4.15 Plot of log I against V for a typical Ag-air cleaved CdTe contact

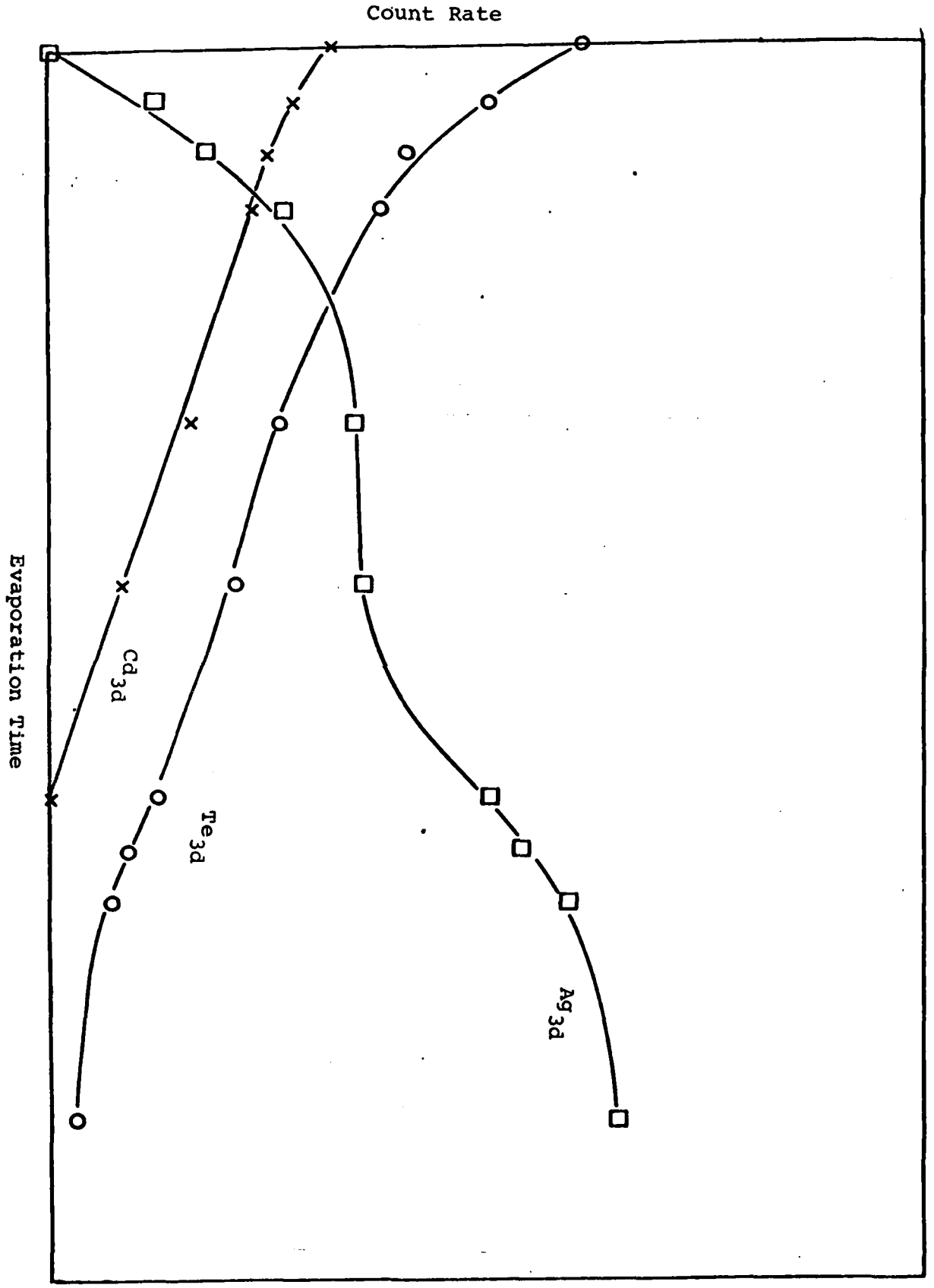

Fig. 4.16 XPS deposition profile for Ag depositing on air cleaved CdTe

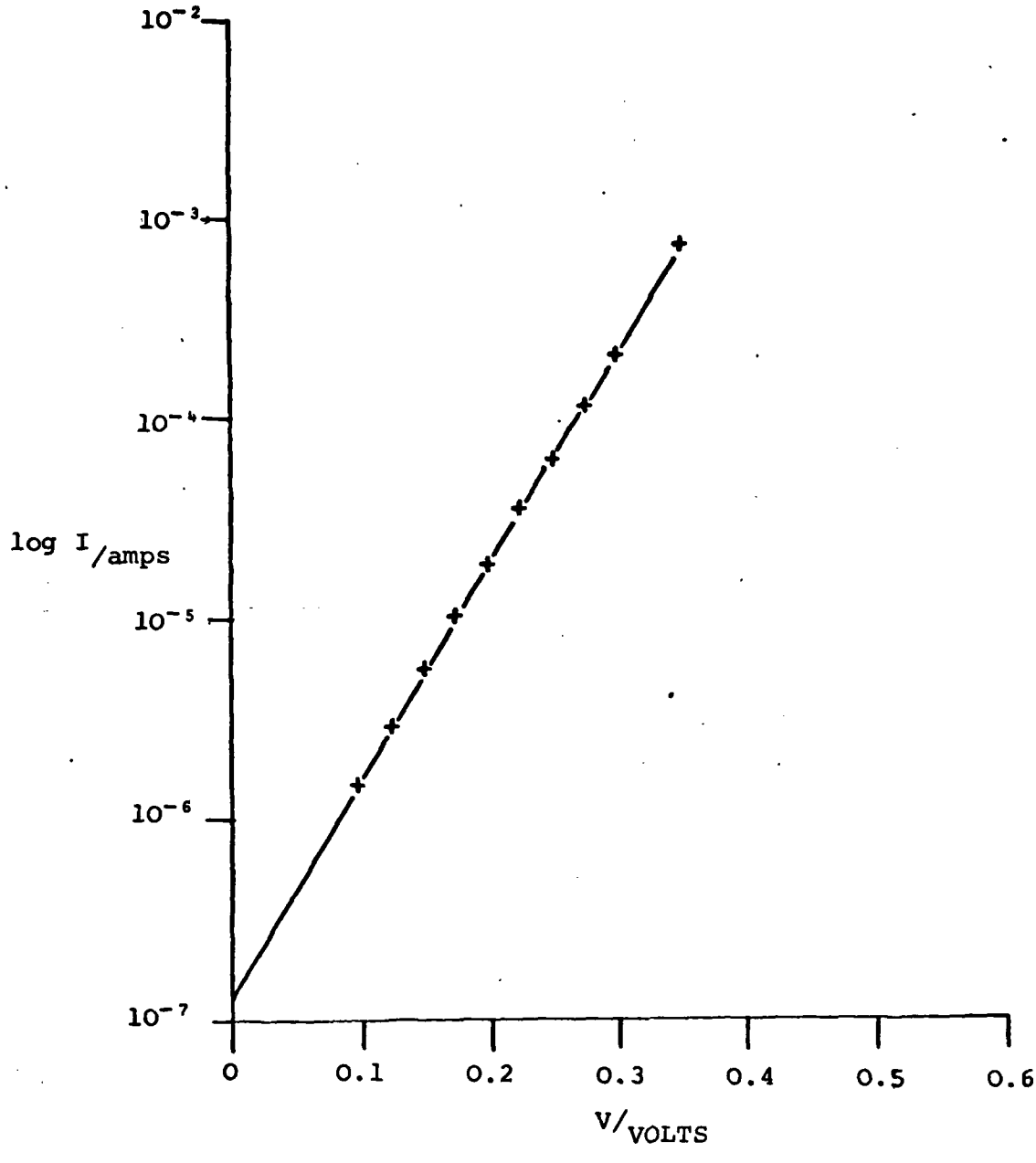

Fig. 4.17 Plot of log I against V for a typical Al-air cleaved CdTe contact

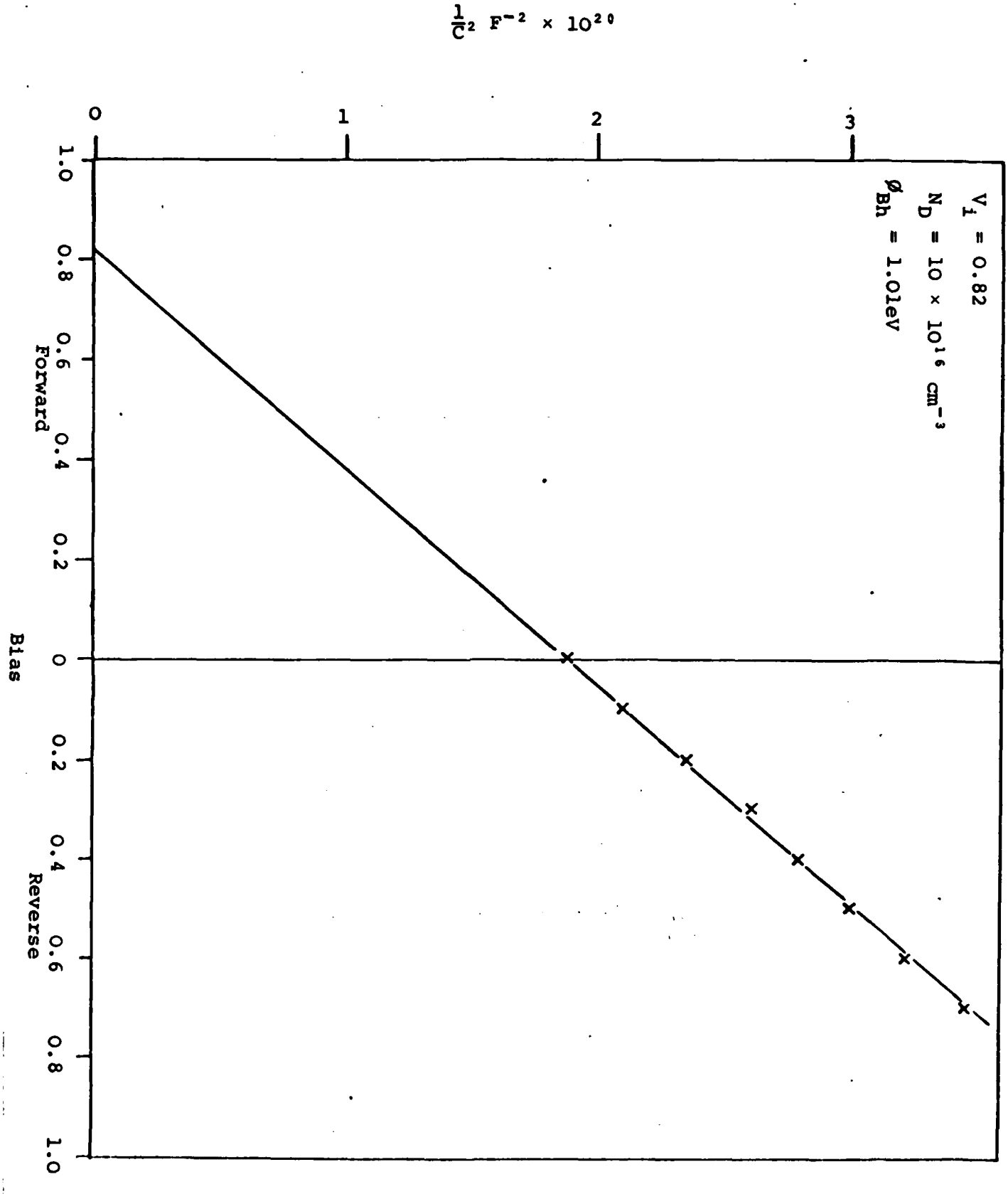

Fig. 4.18 Plot of $\frac{1}{C^2}$ against reverse bias for a typical Al-air cleaved CdTe contact

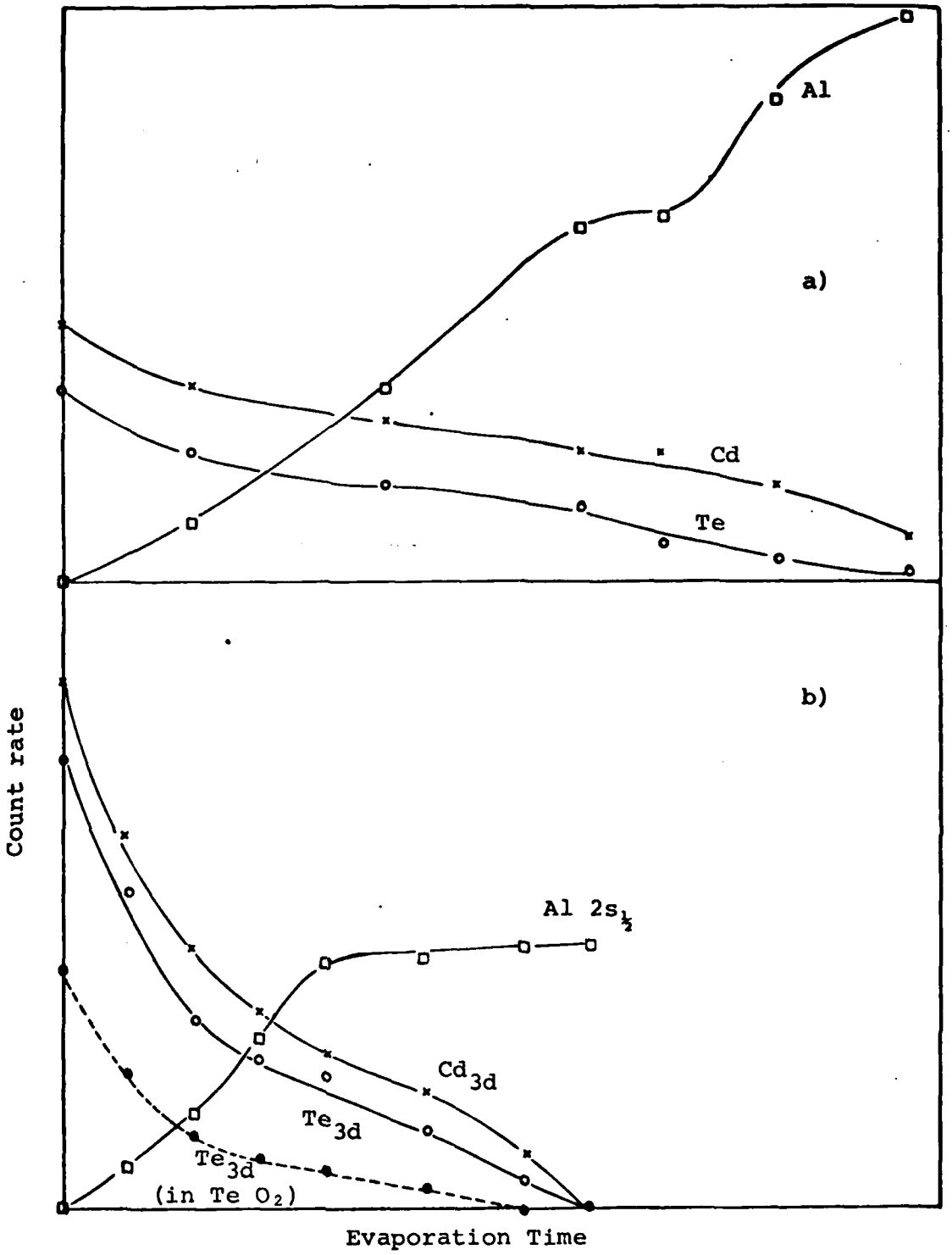

Fig. 4.19 a) AES disposition profile for Al depositing on air cleaved CdTe

b) XPS disposition profile for Al depositing on air cleaved CdTe

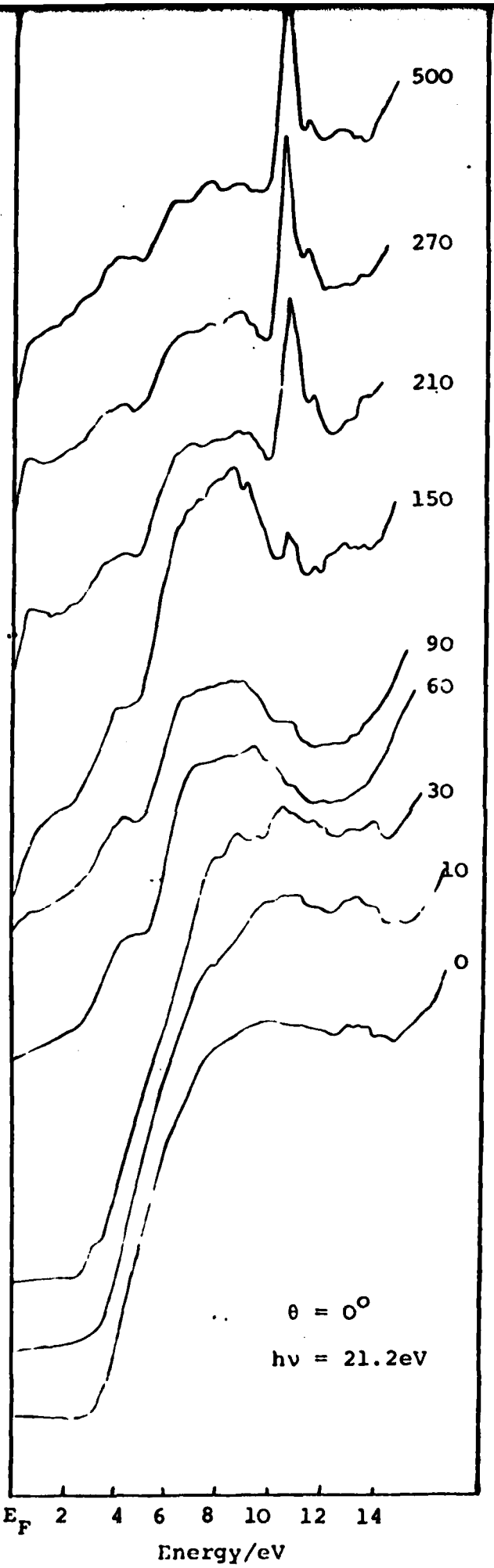

Fig 4.20 UPS spectra of Al deposited on Air cleaved CdTe.

(Evaporation times are in seconds)

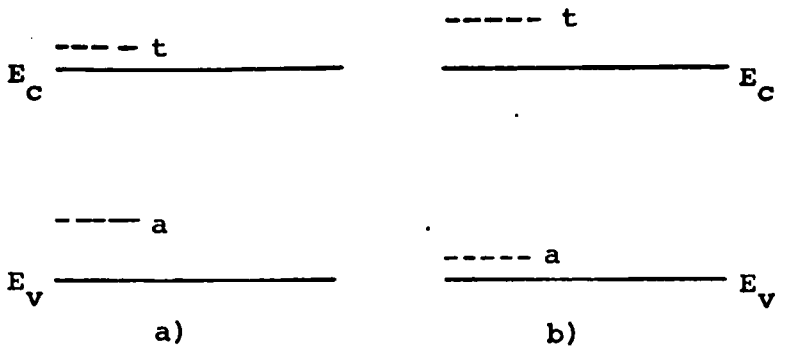

Fig. 4.21 Defect levels (roughly calculated) associated with a) P vacancy in In P b) Te vacancy in CdTe

TABLE 4.1

Barrier Heights measured on air cleaved and vacuum cleaved surfaces of CdTe and InP*

(* InP results from WILLIAMS et al 1977 and 1978)

MATERIAL	METAL	SURFACE	BARRIER HEIGHT/eV
CdTe	Au	VC	0.96
CdTe	Au	AC	1.1
CdTe	Ag	VC	ohmic
CdTe	Ag	AC	0.5
CdTe	Al	VC	ohmic
CdTe	Al	AC	0.93
InP	Au	VC	0.5
InP	Au	AC	ohmic
InP	Au	Br	0.57
InP	Ag	VC	0.45
InP	Ag	AC	0.55
InP	Al	VC	ohmic
InP	Al	AC	0.46

KEY : VC = Vacuum-cleaved

AC = Air cleaved

Br = Bromine-Methanol etched (On Inp gives a thin oxide layer)

4.4. DISCUSSION

Recently the properties of intermediate adsorbed layers at the interface between metals and the semiconducting solids Silicon (Si) and Indium Phosphide (InP) have been the subject of careful investigation (VARMA et al 1977, WILLIAMS et al 1978). For Si the exposure of a clean surface to Chlorine (Cl_2), air, or oxygen (O_2) prior to metal deposition does not lead to major changes in the Schottky Barrier height (ϕ_B). For metals on cleaved InP the situation is entirely different. For example deposition of gold (Au) or Silver (Ag) contacts onto atomically clean cleaved InP surfaces yields Schottky Barriers of height ~0.5 eV whereas Aluminium (Al) gave zero barrier, ohmic behaviour. If, however, a clean InP surface is exposed to Cl_2, air or O_2 prior to metal deposition then zero barrier, ohmic contacts are obtained at room temperature. These results and those of others (ANDREWS and PHILLIPS 1975, BRILLSON 1978) suggest that chemical reaction between the metal or gas and the outermost atomic layer of the semiconductor can often dominate the electronic nature associated with the interface formed, casting some doubt on the usefulness of most conventional theories of intimate contact (see, for example, a review by RHODERICK 1978). It is clear that in order to verify the generality of these suggestions a study of interfaces formed between several metals and a range of semiconductors is desirable.

In the series of experiments, described above, we have looked at the influence of the surface layers on the electronic nature of metal contacts to CdTe. The series of experiments is by no means complete, but already it is possible to see trends in the changes of Schottky Barrier heights with changes in metals and surfaces. If we consider the three metals Au, Ag and Al, then on air cleaved CdTe, they all produce Schottky Barriers of height ranging from ~0.5 eV for Ag to ~1.1 eV for Au. On the vacuum cleaved surface only Au produces a Schottky Barrier (0.96 eV). Ag and Al both show zero barrier, ohmic behaviour. Our evaluation of the Schottky Barrier height of Al on vacuum cleaved CdTe agrees with the findings of TAKEBE et al 1978, but not with those of MEAD and SPITZER 1964 who reported a Barrier height of 0.76 eV. In both of these experiments, however, the vacuum was ~10^{-7} torr during cleavage and some surface contamination may have occurred.

Our LEED experiments show that on deposition of thick films the three metals Au, Ag and Al all form disordered layers on CdTe. AES and XPS deposition profiles have shown that the interfaces formed are not atomically abrupt and that there is considerable intermixing between the metals and the CdTe. Low energy electron beams have dramatic effects on the CdTe surface, disordering it without altering the chemical

composition, and on the interfaces formed with metals.

It is of interest to question the origin of these effects introduced by the interfacial layers on CdTe, and to examine the reasons for the different behaviour compared to Si and InP.

Several theoretical models have been proposed to explain the formation of Schottky Barriers. Some assume that new metal induced states are formed at the interface (LOUIE and COHEN 1976), but in the absence of detailed calculations it is not clear whether this model would account for the data presented here. Other models consider the tunnelling of metal wave functions into the semiconductor (HEINE 1965, CROWELL 1974), so that the effective metal surface is inside the semiconductor. Provided an oxide thickness is thin enough for electrons to tunnel through, then it is possible to account for the insensitivity of Au-InP barriers to thin intermediate layers. However the same arguments would suggest a similar insensitivity of the Al-CdTe interface to the same intermediate layers, contrary to observations.

For many metal-semiconductor systems it is becoming increasingly clear that the chemical reactivity of the metal contact has an important bearing on the Schottky barrier development (ANDREWS and PHILLIPS 1975, BRILLSON 1978). This is certainly the case for metals such as Al on InP (WILLIAMS et al 1978). In the present case we have considered the heats of Reaction (ΔH_R) of Au, Ag and Al with Tellurium to yield the most stable Telluride. The value for Au is not known, but is likely to be similar to that for Ag i.e. ~0.5 eV atom^{-1}. For Al the value is -0.51 eV atom^{-1}, so that compound formation is likely for Al on clean CdTe. It could be argued that the Schottky Barriers for Au, Ag and Al are related to metal work function (ϕ_m). (ϕ_m(Au) = 5.2eV, ϕ_m(Ag) = 4.26eV, ϕ_m(Al) = 4.28eV.) It is therefore suggested that Al leads to an ohmic contact with clean CdTe following a chemical reaction across the interface. The exact mechanism involved however is not completely clear. There is strong evidence that in similar cases such as Al on InP the Schottky Barrier is controlled by defects such as Phosphorous vacancies (MONTGOMERY et al 1979, SPICER et al 1979) which form shallow donor levels near the surface. It has been suggested that for the Al-InP case the fermi level is pinned near the conduction band by the phosphorous vacancies. The calculated levels 'a' and 't' are shown in Fig.4.21. The level 'a' has two electrons and 't' just one (three electrons from the excess Indium). For CdTe which is more ionic a rough calculation shows that the 't' level is up in the conduction band and is empty (due to there being only two valence electrons in Cd). If the 'a' level still remains deep in the gap then Tellurium vacancies will pin the Fermi level in CdTe and then Schottky

Barrier can then change with change in metal work function. However it is still necessary to calculate a range of defect levels including the Cd vacancy near the surface. The assumption that a defect model is responsible for the ohmic nature of the Al-CdTe interface immediately makes clear the role of the oxide layer present on air cleaved samples. The oxide has the effect of spatially separating the Al and the CdTe thus preventing chemical reaction and the resulting formation of electron donating defects.

4.5 CONCLUSION

In conclusion, therefore, we see that difference in electronic behaviour of the interfaces formed between CdTe and the metals Au, Ag and Al are more easily understood in terms of the chemical and metallurgical microstructure of the interface than in terms of more conventional theories. Further more intermediate thin surface layers can have drastic effects on the electronic nature of the metal-CdTe contact.

PUBLICATIONS RESULTING FROM THIS WORK

1. Surface Layers on Cadmium Telluride - M. H. Patterson and R. H. Williams, J. Phys. D. 11 (1978) L.83.

2. The Influence of The Surface on The Electronic Nature of Gold and Aluminium Contacts to Cadmium Telluride - R. R. Varma, M. H. Patterson and R. H. Williams, J. Phys. D. 12 (1979) L71.

3. Angle Resolved Photoemission Studies of Gold, Silver and Aluminium on Clean Cleaved Cadmium Telluride - T. Humphreys, R. H. Williams and M. H. Patterson - manuscript in preparation for submission to J. Phys. C.

4. Metal Contacts to Clean and Oxidised Cadmium Telluride and Indium Phosphide Surfaces - T. Humphreys, M. H. Patterson and R. H. Williams - paper to be presented at the 7th Annual Conference of Physics of Compound Semiconductor Interfaces at Estes Park, Colorado January 29-31 1980.

Literature Cited

Agrinskaya, N.V. and Matveev, O.A., 1977. Rev. de Phys. Appl. 12, 235.

Akadeva, E.N., Matveev, O.A., Rud Yu.V. and Ryvkin, S.M. 1966 Sov. Phys. Tech. Phys. 36, 1146.

Akobirova, A.T., Maslova, L.V., Matveev, O.A., Khusainov, A.Ku. 1975. Sov. Phys. Semicond. 8, 1103.

Akutagawa, W., and Zanio, K. 1971. J. Cryst. Gr. 11, 191.

Allemand, R., Bouteilleur, P., Laval, M., 1977. Rev. de Phys. Appl. 12, 365.

Andrews, J.M. and Phillips, J.C. 1975. Phys. Rev. Letts. 35 56.

Appel, J. and Lautz, G. 1954. Physica XX, 110.

Aven, M. and Swank, R.K. 1966. "Ohmic contacts to Semiconductors". ed. Schwartz - electrochem Soc. N.Y. U.S.A.

Bahl, M.K., Watson, R.L. and Irgolic, K.J. 1977. J. Chem. Phys. 66, 5526.

Basov, N.G. 1960. J. Phys. Soc. Jpn. 21, 277.

Bell, R.O., Hemmat, N. and Wald, F. 1970. Phys. Stat Sol(a) 1, 375.

Bernard, J., Lancon, R., Paparodijis, C. and Rodot, M. 1966. Rev. de. Phys. Appl. 1, 211.

Bethe, H.A., 1942. "Theory of Boundary Layer Crystal Rectifiers". M.I.T. Radiation Lab. report no. 43-12.

Bodaĸov, Yu.A., Lomakina, G.A., Naumov, G.P., Maslakovets, Yu.P. 1960. Sov. Phys. Sol. St. 2, 49.

Bosjen, J., Rossing, N., Soeberg, O., Vadstrups. 1977. Rev. de Phys. Appl. 12, 361.

Boltaks, B.I., Konorov, P. and Matveev, O.A. 1955. Z. Tekh. Fiz. 25, 2329.

Braun, F. 1874. Ann. Physik. Chem. 153, 556.

Briggs, D. 1977. "Handbook of X-ray and UV Photoelectron spectroscopy". ed. D. Briggs. pub. Heyden & Son, London.

Brillson, L. 1978. Phys. Rev. Letts. 40, 260.

Brooks. 1955. "Advances in Electronics and electron Physics". ed. Morton. pub. Academic, vol. 7, 85.

Brundle, C.R. 1972. "Defect and Surface Properties of Solids". ed. Roberts and Thomas. Specialist Report of the Chem. Soc., London. Vol. 1.

Brundle, C.R. 1974. J. Vac. Sci. Technol. 11, 212.

Brundle, C.R. and Baker, A.D. 1977. "Electron Spectroscopy, Theory, Techniques and Applications". vol. 1, 2 & 3 - Academic.

Cabrera, N. and Coleman, R.V. 1963. "The Art and Science of Growing Crystals". page 3. ed. Gilman. pub. Wiley & Son, N.Y.

Calvert, G. 1962. Chem. Abstr. 57, 106886.

Cardona, M. and Ley. L. 1978. "Photo-emission in Solids" parts I and II. pub. Springer-Verlag.

Chang, C.C. 1974. "Characterisation of Solid Surfaces". p. 509. eds. Kane and Larabee. pub. Plenum.

Chapnin, V.A. 1968. Sov. Phys. Semicond. 2, 212.

Conwell and Weiskopf. 1950. Phys. Rev. 77, 388.

Cornet, A., Siffert, P. and Coche, A. 1970. Appl. Phys. Letts. 17, 432.

Crowell, C.R. 1974. J. Vacuum Sci. and Technol. 11, 951.

Crowell, C.R. and Sze, S.M. 1966. Sol. St. Electron. 9, 1035.

Cusano, D.A. 1962. I.R.E. Transactions Ed-9, 504.

Debye and Conwell. 1954. Phys. Rev. 93, 693.

de Nobel, D. 1959. Phillips. Res. Rpts. 14, 361 and 430.

de Nobel, D. and Kroeger, F.A. 1959. U.S. Patent no. 3,033,791. May 1962.

Deutsch, T.F. 1975. J. Electron Mat. 4, 663.

Ebina, A., Asano, K. and Takahaski, T. 1979. Surf. Sci. 86, 803.

Entine, G., Garcia, D.A. and Tow, D.E. 1977. Rev. de Phys. Appl. 12, 355.

Fabre, M. 1888. Ann. Chem. Phys. 14, 110.

Farrell, R., Entine, G., Wilson, F. and Wald, F.V. 1974. J. Electron Mat. 3, 155.

Feurbacher, B. and Willis, R.F. 1976. J. Phys. C. Sol. St. Phys. 9, 169.

Foyt, A.G. and McWhorter, A.L. 1966. IEEE Transactions. Ed-13, 79.

Frerichs, R. 1946. Naturwiss, 387.

Frerichs, R. 1947. Phys. Rev. 72, 594.

Frerichs, R. and Warminsky, R. 1946. Naturwiss 33, 25.

Gaarenstrom, S.N., Winograd, N. 1977. J. Chem. Phys. 67, 3500.

Gabas, I. and Tousek, J. 1977. Phys. Stat. Sol(a) 43, 351.

Gallon, T.E. and Mathew, J.A.D. 1972. Phys. Technol. 3, 31.

Gu, J., Kitihara, T., Sakaguchi, T. 1973. Jpn. J. Appl. Phys. 12, 1460.

Gu, J., Kitihara, T., Fujita, S., Sakaguchi, T. 1975. Jpn. J. Appl. Phys. 14, 499.

Hage-Ali, M., Stuck, R., Saxena, A.N., Siffert, P. 1979(a) Appl. Phys. 19, 25.

Hage-Ali, M., Stuck. R., Scharager, C., Siffert, P. 1979(b) IEEE Trans. NS-26, 281.

Heine, V. 1965. Phys. Rev. A. 138, 1689.

Henisch, H.K. 1957. "Rectifying Semiconductor Contacts". Clarendon Press.

Inove, M., Teramoto, I., Takayanagi, S. 1962. J. Appl. Phys. 33, 2578.

Jenny, D.A. and Bube, R.H. 1954. Phys. Rev. 96, 1190.

Johnson, C.J., Shermang, H. and Weil, R. 1969. Appl. Opt. 8, 1667.

Karpenov, P., Kasherininov, P.G., Matveev, O.A. 1970. Sov. Phys. Semicond. 4, 794.

Kaufman, L., Gamsu, G., Savoca, C.L., Swann, S. 1977. Rev. de Phys. Appl. 12, 369.

Kottke, M. 1971. Rev. Sci Instrum. 42, 1235.

Kroeger, F.A. and de Nobel, D. 1955. J. Electron. 1, 190.

Kyle, N.R. 1971. J. electrochem. Soc. 118, 1790.

Lebrun, J. 1970. Conf. Record of the 8th IEEE Photovoltaic Specialist Conference, p. 33, (IEEE, N.Y.).

Lomakina, G.A., Vodakov, Iu.A., Naumov, G.P., Maslakovets, M.P. 1957. Sov. Phys. Tech. Phys. 2, 1477.

Lorenz, M.R. and Blum, S.E. 1966. J. electrochem. Soc. 113, 559.

Lorenz, M.R. and Halstead, R.E. 1963. J. electrochem. Soc. 110, 343.

Louie, S.G. and Cohen, M.L. 1976. Phys. Rev. B. 13, 2461.

Lynch, R.T. 1962. J. Appl. Phys. 33, 1009.

Mandel, G. and Morehead, F.F. 1964. Appl. Phys. Letts. 4, 143.

Mayer, J.W. 1967. J. Appl. Phys. 38, 296.

Mayer, J.W. 1968. Ch. 5 in "Semiconductor Devices" ed. Bertolini and Coche - (Wiley).

Mazurkevich, Yu.S., Pamfilov, A.V., Marusyak, R.A., Kostyuk, L.S., Pakhmova, E.P. 1971. - Katal-Katal. 7, 88.

Mead, C.A. and Spitzer, W.G. 1964. Phys. Rev. 134, A713.

Meiling, G.S. and Leombruno, R. 1968. J. Cr. Growth ¼, 300.

Metz, E.P.A., Miller, R.C. and Mazelsky, R. 1962. J. Appl. Phys. 33, 2016.

Mitchell, K.A.R. 1973. Contemp. Physics 14, 251.

Montgomery, H.C. 1964. Sol. St. Electron 7, 147.

Montgomery, V., Varma, R.R., Williams, R.H. and Srivastava, G.P. 1979. J. Phys. C. Sol. St. Phys. 12.

Morehead, F.F. 1966. J. Appl. Phys. 37, 3487.

Morikawa, K., Yamaka, E. 1968. Jpn. J. Appl. Phys. 7, 243.

Mott, N.F. 1938. Proc. Cambridge. Phil. Soc. 34, 568.

Mullin, J.B. and Straughan, B.W. 1977. Rev. de Phys. Appl. 12, 105.

Nitsch, R. and Richman, D. 1962. Z. Electrochem. 66, 709.

Nygren, S.F. 1973. J. Cr. Growth 19, 21.

Pamfilov, A.V., Mazurkevich, Yu.S., Makhlya, S.Yu. 1967. Ukr. Khim. Zh. 33, 435.

Paorici, C., Attolini, G., Pelosi, C. and Zuccalli, G. 1973. J. Cr. Growth 18, 289.

Paorici, C., Pelosi, C., Attolini, G. and Zuccalli, G. 1974. J. Cr. Growth 21, 227.

Paorici, C., Attolini, G., Pelosi, C. and Zuccalli, G. 1975. J. Cr. Growth 28, 358.

Paorici, C. and Pelosi, C. 1977. Rev. de Phys. Appl. 12, 155.

Parker, G.H. and Mead, C.A. 1969. Phys. Rev. 184, 780.

Pendry, J.B. 1974. "Low Energy Electron Diffraction" - Academic Press.

Ponpon, J.P. and Siffert, P. 1977. Rev. de Phys. Appl. 12, 427.

Ray, B. 1969. II-VI Compounds - Pergamon Press.

Rhoderick, E.H. 1978. "Metal-Semiconductor Contacts". (Oxford-Clarendon Press).

Riviere, J.C. 1972. Contemp. Phys. 14, 513.

Rodot, M. 1977. Rev. de Phys. Appl. 12, 411.

Schottky, W. 1938. Naturwiss. 26, 843.

Shwarz, E. 1948. Nature. 162, 614.

Siffert, P., Hage-Ali, M., Stuck, R., Cornet, A. 1977. Rev. de Phys. Appl. 12, 335.

Spicer, W.E., Lindan, I., Pianetta, P., Chye, P.W. and Garner, C.M. 1979. Thin Sol. Films. 56, 1.

Strauss, A.J. 1971. Proc. Int. Conf. on CdTe. Strasbourg 1971.

Strauss, A.J. 1977. Rev. de Phys. Appl. 12, 167.

Taguchi, T., Shirafuj, J., Inuishi, Y., 1977. Rev. de Phys. Appl. 12, 117.

Takebe, T., Saraie, J., Tanaka, T. 1978. Phys. Stat. Sol(a). 47, 123.

Teramoto, I. 1963. Phil. Mag. 8, 357.

Tibbals, C.A. 1909. J. An. Chem. Soc. 31, 902.

Touskova, J. and Kuzel, R. 1972. Phys. Stat. Sol(a) 10, 91.

Touskova, J. and Kuzel, R. 1973. Phys. Stat. Sol(a) 15, 257.

Triboulet, R. 1977. Rev. de Phys. Appl. 12, 123.

Triboulet, R. and Marfaing, Y. 1973. J. electrochem. Soc. 120, 1260.

Van Atta, L.B., Picus, G.S., Yariv, A. 1968. Appl. Phys. Letts. 12, 84.

Vanderkerkof, J. 1971. Proc. Int. Conf. on CdTe - Strasbourg. pub. Siffert and Cornet.

Varma, R.R., McKinley, A., Williams, R.H. and Higginbotham, I.G. 1977. J. Phys. D.: Appl. Phys. 10, L171.

Vavilov, V.S. and Nolle, E.L. 1966. Sov. Phys. Sol. State 8, 421.

Vogel, J., Ullman, J., Entine, G. 1977. Rev. de Phys. Appl. 12, 375.

Williams, R.H., Montgomery, V., Varma, R.R. and McKinley, A. 1977. J. Phys. D.:Appl. Phys. 10, L253-6.

Williams, R.H., Montgomery, V. and Varma, R.R. 1978. J. Phys. C. Sol. St. Phys. 11, L735.

Wilson, A.H. 1931. Proc. Roy. Soc. A. 133, 458.

Yamada, S. 1960. J. Phys. Soc. Jpn. 15, 1940.

Yamada, S. 1962. J. Phys. Soc. Jpn. 17, 645.

Zitter, R.N. 1971. Surf. Sci. 28, 335.

Zitter, R.N. and Chavda, D.L. 1975. J. Appl. Phys. 46, 1405.

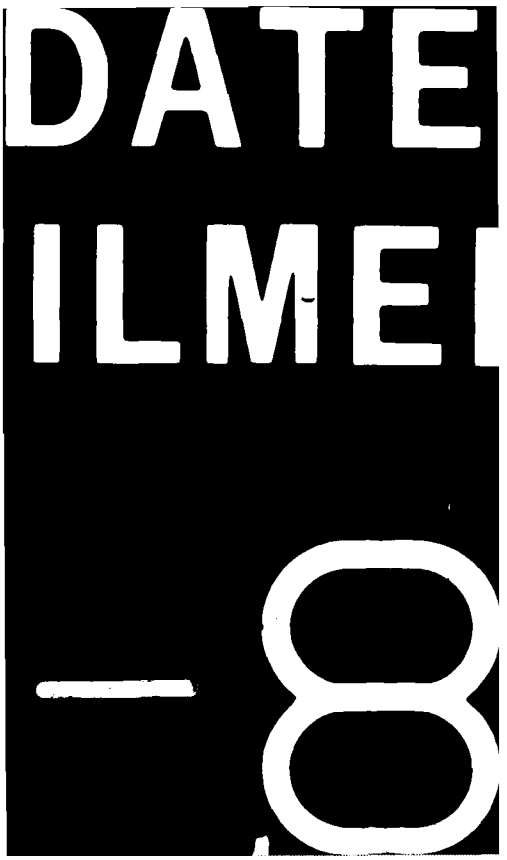
DATE
ILME
8